INFORMATION TO USERS

While the most advanced technology has been used to photograph and reproduce this manuscript, the quality of the reproduction is heavily dependent upon the quality of the material submitted. For example:

- Manuscript pages may have indistinct print. In such cases, the best available copy has been filmed.

- Manuscripts may not always be complete. In such cases, a note will indicate that it is not possible to obtain missing pages.

- Copyrighted material may have been removed from the manuscript. In such cases, a note will indicate the deletion.

Oversize materials (e.g., maps, drawings, and charts) are photographed by sectioning the original, beginning at the upper left-hand corner and continuing from left to right in equal sections with small overlaps. Each oversize page is also filmed as one exposure and is available, for an additional charge, as a standard 35mm slide or as a 17"x 23" black and white photographic print.

Most photographs reproduce acceptably on positive microfilm or microfiche but lack the clarity on xerographic copies made from the microfilm. For an additional charge, 35mm slides of 6"x 9" black and white photographic prints are available for any photographs or illustrations that cannot be reproduced satisfactorily by xerography.

Zhou, Ru Ling

SOLITONS INDUCED BY BOUNDARY CONDITIONS

City University of New York PH.D. 1987

SOLITONS INDUCED BY BOUNDARY CONDITIONS

By

Ru Ling Zhou

A dissertation submitted to the Graduate
Faculty in Physics in partial fulfillment
of the requirements for
the degree of Doctor of Philosophy,
The City University of New York

1987

This manuscript has been read and accepted for the Graduate Faculty in Physics in satisfaction of the dissertation requirement for the degree of Doctor of Philosophy.

1/29/87
Date

Rodney L. Varley
Co-Chairman of Examining Committee

1/29/87
Date

Executive Officer

Chia Kun Chu (Co-Chairman)

Arnold H. Kritz

Richard Churchill

Guido Sandri

Supervisory Committee

The City University of New York

Abstract

SOLITONS INDUCED BY BOUNDARY CONDITIONS

by

Ru Ling Zhou

Adviser: Professors Chia Kun Chu, Rodney Varley

Although soliton phenomena have attracted wide attention since 1965, there are still not enough efforts paid to mixed boundary-initial value problems which are important in real physical cases. The main purpose of this thesis is to study carefully the various boundary induced solitons under different initial conditions.

We start with three sets of nonlinear equations: KdV equation and Boussinesq equation (for water); two fluid equations for the cold ion plasma.

We have been interested in four types of problems involved with water solitons: excitation by different time-dependent boundary conditions under different initial conditions; head-on and over-taking collisions; reflection at a wall and the excitation by pure initial conditions. For KdV equation, only cases one and four are conducted. The results from two fully non-linear KdV and Boussinesq equations are compared, and agree extremely well.

In both set of equations, for the constant boundary but finite (nonzero) unperturbed water level, the ratio between the disturbed amplitude and the unperturbed water level plays

the key role in determining the soliton maturing time. When this ratio is small, new solitons take a long time to mature; results of [23] are hold at the opposite extremes. Dealing with various time-dependent boundary conditions, the ratio between the soliton maturing period and the time-scale of boundary controls the envelope of solitons induced. A random boundary for KdV equation (unperturbed water level approaches zero) can also induce a series of solitons as a constant boundary does. This is a very striking result.

The Boussinesq equation permits soliton head-on collisions and reflections, studied the first time. The results from take-over collision agree with KdV results.

The numerical schemes used are up to fourth order accurate in x and second order accurate in t. For the KdV equation, the schemes from [23] are adopted.

For the ion acoustic plasma, we have derived a set of Boussinesq-type equations from the standard two fluid equations for the ion acoustic plasma. It theoretically proves the essential nature of the solitary wave solutions of the cold-ion plasma. The ion acoustic solitons are also obtained by prescribing a potential ϕ_0 at one grid point. A part of these results had been presented in the 1984 APS Plasma Physics Division Meeting and the IMACS 1985 World Congress.

Acknowledgments

I am deeply grateful to Professor Rodney Varley, my advisor, from whom I have learned much. He not only taught me various courses and led me the way to research but also gave me important lessons about the United States. I value highly his advice of all kinds and treasure his friendship.

My sincere thanks go to Professor C. K. Chu, my supervisor for this work, who has guided and encouraged me through all these years.

In the spring semester of 1984, I registered at Caltech as a special graduate student under Prof. Theodore Yao-Tsu Wu. During that period, I finished most of the work about the ion acoustic soliton and benefited very much from Professor Wu and his group. I take this opportunity to thank them.

Special thanks are due Mrs. Lorraine Varley for her warm friendship and great assistance and advice in all affairs.

My deepest appreciation goes to my dear parents and sons who have encouraged me to go abroad for advanced study and have sacrificed much since I left.

I gratefully acknowledge financial support from the Department of Physics and Astronomy of Hunter College, Prof. Wu's research group at Caltech and the Research Foundation of CUNY through a grant awarded to Prof. Varley (the work was published elsewhere). The CCNY Physics Department and the Columbia University Department of Civil Engineering provided me generously with their computing facilities.

Contents

I. Introduction 1

II. Shallow water solitons 14

1. Korteweg and de Vries equation 14

1.1). Physical model and boundary-initial conditions 14

1.2). Numerical schemes 19

A). The case for $\zeta_0 = 0$ 19

B). The case for $\zeta_0 \neq 0$ 19

2. Boussinesq equation and its soliton solutions 19

2.1). Physical model 19

2.2). Consideration of characteristics 22

2.3). Initial and boundary conditions 24

A). Pure initial excitation 26

B). Soliton collisions and reflection 27

C). Soliton induced by boundary condition 32

2.4). Numerical schemes 33

A). Schemes for interior points 33

B). Difference approximation for boundary 36

3. Relationship between Boussinesq and KdV equations 41

4. Computational results 44

4.1). Some important results from KdV equation 45

4.2). Results from Boussinesq equation 50

4.2.1). Results of initial excitation 51

4.2.2). Soliton collision 55

4.2.3). Soliton reflection at left boundary 62

4.2.4). Boundary induced soliton in Boussinesq equation 64

4.3). Comparison between the results of Boussinesq and KdV equations 68

5. Few comments on the numerical schemes 70

III. Ion acoustic solitons 77

1. Physical model and derivation of Boussinesq-type equation 77

1.1). Two fluid equations and ion acoustic waves 77

1.2). Ion acoustic solitons and Boussinesq equation 83

1.3). Physical model for boundary induced soliton 87

2. Numerical methods and results 90

IV. Conclusion 94

Figures 96

References 166

Figure captions

Figure captions

The typical parameters for the following figures are chosen as $\beta = 0.000484$, the unperturbed water level $h_0 = 1.0$ and the unperturbed water speed $u_0 = 0.0$ for Boussinesq equation and correspondingly, $\varepsilon = 0.00898$, unperturbed water level $\zeta_0 = 1.0$ for KdV equation; the grids are set up as $\Delta x = 1/40$, $\Delta t = 1/600$ for both equations; the forth order scheme is chosen as our main numerical scheme. A half sine function and a single narrow hump are chosen to be the two types of initial conditions, no matter how big the amplitudes they have, the half sine function covers 20 grid points and the width of the single hump is very close to that of soliton. The figures below typically show the distributions of the total water depth h in Boussinesq equation.

Any information different from above will be indicated specifically.

1.1 ---------- 96
Soliton induced by an initial excitation from KdV equation (1.4). The initial function is a half sine function over $\zeta_0 = 1.0$ whose amplitude = 0.75.

1.1.1 Solitons at t = 1.0 .

1.1.2 Solitons at t = 3.0 .

1.1.3 Solitons in terms of fluctuation η obtained through transformation (2.72) and (2.73), $\alpha = 0.5$. t = 1.0 .

1.1.4 same as Fig. 1.1.3, but t = 3.0 .

1.2 ---------- 98
Calculating directly from (2.71), solitons in terms of fluctuation η are induced by the initial condition, which is equivalent to the initial function used in Fig. 1.1, the amplitude of this half sine function now is 1.0 . The unperturbed water level $\eta_0 = 0.0$ while $\alpha = 0.5$.

1.2.1 Solitons at t = 1.0. This is identical with Fig. 1.1.3.

1.2.2 Solitons at t = 3.0. This is identical with Fig. 1.1.4.

1.3 ---------- 99
Solitons induced from KdV equation by periodic

boundary condition: $\zeta_b = 0.5\{1 + 0.5 \cos(t)\}$.
$\zeta_0 = 0.0$. The numerical scheme is adopted from [23].

1.3.1 Solitons at t = 6.0.

1.3.2 Solitons at t = 8.0.

1.3.3 Solitons at t = 10.0.

1.3.4 Solitons at t = 14.0.

1.4 ---------- 101
Solitons induced by the random boundary function in KdV equation. The expectation of this random function equals 0.5. $\zeta_0 = 0.0$. The numerical scheme is adopted from [23].

1.4.1 Solitons formed by random boundary condition which changes at every time step. t = 1.0.

1.4.2 Same as Fig.1.4.1, t = 10.0.

1.4.3 Solitons formed by random boundary function whose random value is held every 5 time steps. t = 1.0.

1.4.4 Same as Fig. 1.4.3, t = 10.

1.4.5 Solitons formed by random boundary function whose random value is held every 10 time steps. t = 1.0.

1.4.6 Same as Fig. 1.4.5, t = 10.0.

1.4.7 Solitons induced by a steady boundary $\zeta_b = 0.5$ which is the expectation value of the random function used above. t = 0.25.

1.4.8 Same as Fig. 1.4.6, t = 6.0.

1.5 ---------- 105
Results taken from [23]: $\varepsilon = 0.022$, $\zeta_0 = 0.0$.

1.5.1 Solitons formed from the fixed boundary condition $\zeta_b = 1.0$ at t = 2.5.

1.5.2 Profile of collisionless shock for $\upsilon = 2.0$. t = 4.9.

1.6 ---------- 107
Solitons formed from KdV equation by the fixed boundary $\zeta_b = 1.75$ while $\zeta_0 = 1.0$ and $\varepsilon = 0.022$. Second order scheme is used.

1.6.1 Solitons at t = 1.0 .

1.6.2 Solitons at t = 2.0 .

1.6.3 Solitons at t = 4.0 .

1.6.4 Solitons at t = 6.0 .

1.6.5 Solitons at t = 8.0 .

1.7 ---------- 110
Solitons induced from KdV equation by the fixed boundary $\zeta_b = 0.75$ while $\zeta_0 = 0.5$ and $\varepsilon = 0.022$. Second order scheme is used.

1.7.1 Solitons at t = 2.0 .

1.7.2 Solitons at t = 4.0 .

1.7.3 Solitons at t = 6.0 .

1.7.4 Solitons at t = 8.0 .

1.8 ---------- 112
Solitons induced by the fixed boundary $\zeta_b = 1.15$ in KdV equation.

1.8.1 Solitons from KdV equation at t = 1.0. Comparable with Fig. 5.1.1.

1.8.2 Solitons from KdV equation at t = 3.0. Comparable with Fig. 5.1.2.

2.1 ---------- 113
Solitons induced by an initial condition which is a half sine function. $\beta = 0.000484$ is fixed.

2.1.1 Amplitude of initial hump is 0.25. Solitons at t = 1.0.

2.1.2 Amplitude of initial hump is 0.25. Solitons in h at t = 6.0.

2.1.3 Amplitude of initial hump is 0.50. Solitons in h at t = 1.0.

2.1.4 Amplitude of initial hump is 0.50. Solitons in h at t = 4.0.

2.1.5 Amplitude of initial hump is 0.75. Solitons in h at t = 1.0.

2.1.6 Amplitude of initial hump is 0.75. Solitons in h at t = 4.0.

2.1.7 Amplitude of initial hump is 1.00. Solitons in h at t = 1.0.

2.1.8 Amplitude of initial hump is 1.00. Solitons in h at t = 4.0.

2.1.9 Amplitude of initial hump is 1.25. Solitons in h at t = 1.0.

2.1.10 Amplitude of initial hump is 1.25. Solitons in h at t = 4.0.

2.1.11 Amplitude of initial hump is 1.25. Solitons in u at t = 4.0.

2.2 ---------- 119
Solitons induced by an initial condition which is a half sine function. Amplitude of initial hump is fixed at 0.5.

2.2.1 β = 0.0000, solitons at t = 1.0.
2.2.2 β = 0.0000, solitons at t = 4.0.
2.2.3 β = 0.0001, solitons at t = 1.0.
2.2.4 β = 0.0001, solitons at t = 4.0.
2.2.5 β = 0.0003, solitons at t = 1.0.
2.2.6 β = 0.0003, solitons at t = 1.0.
2.2.7 β = 0.0007, solitons at t = 1.0.
2.2.8 β = 0.0007, solitons at t = 4.0.

2.3 ---------- 123
Solitons induced by an initial excitation which is a single hump of amplitude 0.82 .

2.3.1 β = 0.0001, soliton at t = 1.0 .
2.3.2 β = 0.0001, soliton at t = 3.0 .
2.3.3 β = 0.0003, soliton at t = 1.0 .
2.3.4 β = 0.0003, soliton at t = 3.0 .
2.3.5 β = 0.0004, soliton at t = 1.0 .
2.3.6 β = 0.0004, soliton at t = 3.0 .
2.3.7 β = 0.000484, soliton at t = 1.0 .
2.3.8 β = 0.000484, soliton at t = 3.0 .

3.1 ---------- 127
Process of two single soliton head-on collision.

Peaks of initial humps are 0.58 and 0.82 and they are 100 grid points apart.

3.1.1 Solitons at t = 0.5 before collision.

3.1.2 Solitons just collided and have not totally split yet, t = 1.0.

3.1.3 At t = 1.5, collision is over and two solitons propagate in opposite directions.

3.2 ---------- 129
Process of two single identical soliton head-on collision. Peaks of initial humps are 0.58 and they are 100 grid points apart.

3.2.1 Solitons at t = 0.5 before collision.

3.2.2 Two solitons are overlapping. t = 1.0.

3.2.3 After collision, solitons at t = 1.5.

3.3 ---------- 131
Head-on collisions of series solitons induced by two identical initial half sine humps which are 300 grid points apart and their amplitudes are 0.5.

3.3.1 Solitons in h at t = 0.5 before collisions.

3.3.2 Solitons in h at t = 2.5 before collisions.

3.3.3 Solitons in u at t = 2.5 before collisions.

3.3.4 Solitons in h at t = 3.0 during collisions.

3.3.5 Solitons in u at t = 3.0 during collisions.

3.3.6 Solitons in h at t = 3.5 during collisions.

3.3.7 Solitons in u at t = 3.5 during collisions.

3.3.8 Solitons in h at t = 4.0 during collisions.

3.3.9 Solitons in h at t = 4.5 after collisions.

3.3.10 Solitons in h at t = 7.0 after collisions.

3.4 ---------- 137
Head-on collisions of series solitons induced by two initial half sine humps which are 220 grid points apart and their amplitudes are differed by factor 10: 0.05 and 0.5 . h_0 = 0.5 .

3.4.1 Two initial humps: half sine shape, amplitudes are 0.05 and 0.5; each covers 20 grid points; they are 220 grid points apart.

3.4.2 Solitons in h at t = 2.0 before collision.

3.4.3 Solitons in u at t = 2.0 before collision.

3.4.4 Solitons in h at t = 3.0 during collision.

3.4.5 Solitons in u at t = 3.0 during collision.

3.4.6 Solitons in h at t = 4.0 during collision.

3.4.7 Solitons in u at t = 4.0 during collision.

3.4.8 Solitons in h at t = 5.0 after collision.

3.4.9 Solitons in u at t = 5.0 after collision.

3.5 ---------- 142
Collision of two solitons traveling in the same direction. Amplitudes of each initial humps are 0.27 and 0.82. Two humps are 20 grid points apart.

3.5.1 Two solitons traveling in the left direction at t = 0.5.

3.5.2 Fast moving soliton just catches up the slow moving one. t = 1.0 .

3.5.3 Two solitons are overlapping. t = 1.5 .

3.5.4 Two solitons are leaving each other. t = 2.0 .

3.5.5 Two solitons separate totally. t = 2.5 .

4.1 ---------- 145
Process of single soliton reflection at left boundary. Soliton amplitude is 0.94 , it is induced by a narrow single hump of amplitude 0.82 .

4.1.1 Soliton traveling to the left. t = 2.0 .

4.1.2 Soliton traveling to the left. t = 3.0 .

4.1.3 Soliton just reflected from the left boundary at t = 3.5 .

4.1.4 After reflection, soliton is traveling to the right. t = 10.0.

4.2 ---------- 147
Process of two soliton reflection at left boundary.

Soliton amplitudes are 0.14 and 0.056 . They are induced by a half sine function of amplitude 0.1 .

4.2.1 Solitons traveling to the left at t = 4.0.

4.2.2 Leading soliton reflected and collides with the second left going soliton. t = 5.0 .

4.2.3 All two solitons had reflected and propagate toward the right. t = 6.0 .

4.2.4 Solitons traveling to the right. t = 13.0. After reflection, noise has been brought in.

5.1 ---------- 149
Solitons induced by preset fixed boundary h_b = 1.1 .

5.1.1 Solitons at t = 1.0 in domain x = 0.0 to 4.0 .

5.1.2 Solitons at t = 3.0 in domain x = 0.0 to 4.0 .

5.1.3 Solitons at t = 4.0 .

5.1.4 Solitons at t = 12.0

5.1.5 Solitons at t = 18.0 .

5.2 ---------- 152
Solitons induced by preset fixed boundary h_b = 1.5.

5.2.1 Solitons at t = 4.0

5.2.2 Solitons at t = 14.0 .

5.3 ---------- 153
Solitons induced by periodic boundary condition. Boundary $h_b(t)$ is changed as a series of half sine functions whose amplitude is 0.05 and the period is 0.5 . This series of half sine functions is placed over the unperturbed water level h_0 = 0.5 .

5.3.1 At t = 1, solitons just start to form.

5.3.2 Three sets of solitons come out but only the first set is getting mature, t = 3.0 .

5.3.3 At t = 5, the first set of solitons are fully matured, so as the leading soliton in the second set; the latter is gradually catching up the shortest soliton in the first set.

5.3.4 Solitons at t = 6.0, the matured solitons start to line up according to their amplitudes.

5.4 ---------- 155
Solitons induced by one complete sine oscillation then followed by a fixed boundary. The period and amplitude of this sine function are 0.5 and 0.05 . The time averageof the boundary function is $h_b(t)$ = 0.55 which is also the fixed boundary value. h_0 = 0.5.

5.4.1 Solitons at t = 1.0. First two solitons are formed from the oscillation boundary.

5.4.2 Solitons at t = 2.0 . soliton from fixed boundary is starting to catch up the one from oscillating boundary.

5.4.3 Solitons at t = 3.0 .

5.4.4 Solitons at t = 6.0 . The leading soliton from fixed boundary passes the shortest soliton in front completely.

5.4.5 Solitons at t = 10.0 .

5.4.6 Solitons at t = 16.0 .

6.1 ---------- 158
Solitons induced by the initial excitation in Boussinesq equation. A half sine function is chosen to be the initial condition. Its amplitude is 0.1 .

6.1.1 At t = 1.0, solitons are just start to form.

6.1.2 Solitons at t = 3.0. They are not fully split yet.

6.2 ---------- 159
Solitons induced by initial excitation in KdV equation. An half sine function is chosen as the initial condition. Its amplitude is 0.15 . Figs. 6.2.1 to 6.2.2 are almost identical with Figs. 6.1.1 and 6.1.2, respectively.

6.2.1 At t = 1.0, solitons are just start to form.

6.2.2 Solitons at t = 3.0. They are not fully split yet.

7.1 ---------- 160
ε is taken as zero, solitons still can be induced by an initial excitation from KdV equation. Initial function is a half sine function of amplitude 1.0 . ζ_0 =0.0 and second order leap-frog scheme is used.

7.1.1 Solitons at t = 1.0 .

7.1.2 Solitons at t = 4.0 .

7.2 ---------- 161
ε is taken as zero, solitons still can be induced by a boundary excitation from KdV equation. $\zeta_b = 1.0$. $\zeta_0 = 0.0$ and second order leap-frog scheme is used.

7.2.1 Solitons at t = 1.0.

7.2.2 Solitons at t = 4.0.

7.3 ---------- 162
ε is taken as zero, if the numerical scheme for $\zeta\zeta_x$ is chosen according to (2.79), solitons can be induced by an initial excitation from KdV equation, but they can not last long. A half sine function of amplitude 1.0, is chosen to be the initial function. $\zeta_0 = 0.0$ and second order scheme is used.

7.3.1 Solitons at t = 1.0.

7.3.2 Solitons at t = 2.0. Soon after this moment, the calculation blows away.

7.4 ---------- 163
KdV solitons induced by the initial half sine function whose amplitude is 0.75 . Second order scheme is used.

7.4.1 Solitons at t = 1.0.

7.4.2 Solitons at t = 3.0 are already fully formed.

7.5 ---------- 164
KdV solitons induced by the initial half sine function whose amplitude is 0.75 . Forth order scheme is used. This set of figures is identical with Figs. 1.1.1 and 1.1.2 unless this is in a little smaller domain.

7.5.1 Solitons at t = 1.0 .

7.5.2 Solitons at t = 3.0 are already fully formed.

8.1 ---------- 165
Ion acoustic soliton formed from a prescribed $\phi_0 = 0.05$ at x = 0 . A small artificial viscosity $\nu = 0.4$ has been added around the grid (four points on each side of the grid) in numerical scheme. $u_0 = 0.4$. The scheme is set up as

$\Delta x = 0.6$ and $\Delta t = 0.1$.

8.1.1 Potential distribution $\phi(x)$ at 600 time steps.

8.1.2 Velocity distribution $u(x)$ at 600 time steps.

I. Introduction

There have been many papers on solitons since 1960's and the history is well documented. We briefly summarize it for completeness.

In 1834, the British scientist J. S. Russell observed a very interesting phenomenon in the Glasgow canal at Edinburgh. He saw that when a boat towed by a pair of horses stopped suddenly, a mass of water in front of the boat ran away with a constant speed without changing the form of "round, smooth and well defined heap of water". He reported this discovery of the "great wave of translation" to the British Association for the Advancement of Science in 1844 [1]. That was the first report on the solitary wave as is known nowadays.

J. S. Russell also did a series of experiments and got the first empirical formula for solitary waves --- the relationship between its velocity and amplitude.

$$c^2 = g\ (\ h_0 + a\ )$$

where a --- amplitude of the disturbance of the water

h_0 --- height of the undisturbed water.

c --- steady velocity of the wave.

This describes the basic character of solitary waves --- the

taller the disturbance, the faster it runs; but this equation is now known to be the (nonlinear) small amplitude wave speed; the real solitary wave speed is somewhat greater than the value determined above.

Boussinesq (1871) [2] formulated the equation of nonlinear shallow water wave in an inviscid imcompressible fluid, from which Russell's empirical formula for c was deduced in the usual elementary fashion. He also showed essentially that the height of disturbance above the mean level h_0 was given by

$$\zeta(x,t) = a \operatorname{sech}^2 \left(\frac{x - ct}{w} \right) \qquad \text{----------} \qquad (1.1)$$

$$w^2 = \frac{4 h_0^2 (h_0 + a)}{3 a} \qquad \text{----------} \qquad (1.2)$$

here w denotes the width of soliton and the rest of the notations adopted are the same as above. Similar work was done by Rayleigh (1876) [3] independently.

In 1895, Korteweg and de Vries [4] developed these theories and derived an equation governing the one-dimentional motion of weakly nonlinear long waves propagating in a single direction:

$$\frac{\partial \zeta}{\partial t} = \frac{3}{2}\sqrt{\frac{g}{h_0}}\left(\zeta\frac{\partial \zeta}{\partial x} + \frac{2}{3}\alpha\frac{d\zeta}{\partial x} + \frac{1}{3}\sigma\frac{\partial^3\zeta}{\partial x^3}\right)$$

---------- (1. 3)

where α --- small arbitrary constant.

$$\sigma = \frac{1}{3}h_0^3 - \frac{Th_0}{g\rho}$$

T --- surface tension of the liquid.

ρ --- density of the liquid.

This equation is known as Korteweg de Vries (KdV) equation today.

But these fascinating phenomena started to attract wide attention of scientists only after the famous work of Zabusky and Kruskal in 1965 [5]. They observed the unusual nonlinear interaction among "solitary wave pulses" propagating in nonlinear dispersive media. These phenomena were observed in numerical solution of the KdV equation which has a common form as

$$\frac{\partial \zeta}{\partial t} + \zeta\frac{\partial \zeta}{\partial x} + \varepsilon^2\frac{\partial^3\zeta}{\partial x^3} = 0$$

---------- (1. 4)

with periodic initial conditions.

They found that shortly after interaction, each wave reappears unaffected in size and shape, hence possessing

particle like nature, and they coined the name "soliton" for such waves. In other words, solitons "pass through" one another without losing their identities.

In these nonlinear physical processes, interacting localized pulses do not scatter irreversibly, in contrast to nearly all other nonlinear interactions. This is a very important discovery. Soon after this, Gardner, Greene, Kruskal and Miura in a series of papers (such as [6]) obtained the exact solutions of the KdV equation by inventing the ingenious inverse-scattering method. This is one of the few exact solutions that could be obtained for nonlinear equations. The work became a major achievement in twentieth century mathematics.

Since then, a series of advances have been made in mathematical methods for treating these problems, such as the Lax method [7], Bäcklund transfomation, Painlevé properties etc.(see for example, Drazin, P. D., Solitons. Cambridge University Press, 1985), and besides the KdV equation, a number of equations which have soliton properties have been examined. The typical ones include:

Modified KdV equation [8]

$$\frac{\partial u}{\partial t} + 6\,u^2\frac{\partial u}{\partial x} + \frac{\partial^3 u}{\partial x^3} = 0 \qquad \text{---------- (1. 5)}$$

General modified KdV equation [8]

$$\frac{\partial u}{\partial t} + (n+1)(n+2)\, u^n \frac{\partial u}{\partial x} + \frac{\partial^3 u}{\partial x^3} = 0 \qquad n = 1,2,\ldots\ldots$$

---------- (1. 6)

Cubic Schrödinger equation [9]

$$i \frac{\partial u}{\partial t} + \frac{\partial^2 u}{\partial x^2} + |u|^2 u = 0 \qquad (1.\ 7)$$

Nonlinear Klein-Gordon equation [10,11]

$$\frac{1}{c^2} \frac{\partial^2 u}{\partial t^2} = \nabla^2 u - \frac{d\ V(u)}{du}$$

---------- (1. 8)

Nonlinear sine-Gordon equation

$$\frac{1}{c^2} \frac{\partial^2 u}{\partial t^2} - \frac{\partial^2 u}{\partial x^2} + \sin u = 0 \qquad (1 - D)$$

---------- (1. 9)

Boussinesq-type of equations [12]

$$u_{tt} = 3\, u_{4x} - 12\, (u^2)_{xx}$$

---------- (1.10.1)

or

$$u_t = -3\, v_x$$

$$v_t = -u_{3x} + 8\, u u_x$$

---------- (1.10.2)

or [13]

$$\frac{\partial u}{\partial t} = - \frac{\partial v}{\partial x}$$

$$\frac{\partial v}{\partial t} = - \frac{\partial}{\partial x} (u + 6u^2 + u_{xx})$$

---------- (1.11)

Solitary wave in elastic medium [14]

$$\frac{\partial^2 u}{\partial t^2} = \frac{\partial^2 u}{\partial x^2} + \frac{\partial u}{\partial x} \frac{\partial^2 u}{\partial x^2} + \frac{\partial^4 u}{\partial x^4}$$

---------- (1.12)

DABO equation [15]

$$\frac{\partial u}{\partial t} + u \frac{\partial u}{\partial x} + \frac{\partial^2 \mathbf{H}(u)}{\partial x^2} = 0$$

---------- (1.13)

where the Hilbert transformation is

$$\mathbf{H}(u) = \frac{1}{\pi} \mathbf{P} \int_{-\infty}^{\infty} \frac{u(y, t)}{y - x} dy$$

P --- Cauchy principal part of integral

Kadomtsev-Petviashvili equation --- 2-dimensional equation [16].

$$\{ u_t - 6 uu_x + u_{3x} \}_x + 3 u_{yy} = 0$$

---------- (1.14)

So solitons are not only a subject for mathematicians, but already have widely attracted the attention of scientists in all areas: for example, fluid dynamics, plasma physics, optics, oceanography, solid state physics, particle physics, and so on.

A conference on soliton and coherent structure dedicated to Kruskal's 60th birthday was held at Santa Barbara CA in January 1985 [17]. The proceedings consist of the newest summary and review of recent research in this area.

In plasma physics, ion acoustic solitons were first proposed by Sagdeev in 1966 [18]. He theoretically analyzed the ion acoustic solitons in a plasma with finite electron temperature and zero ion temperature (cold ion plasma), and pointed out that the soliton has a hyperbolic-secant-squared shape with Mach numbers between 1. and 1.6 . In 1966, Washimi and Taniuti [19] obtained the KdV equation from the standard two fluid equations of a cold ion plasma under the small but finite amplitude approximation. In 1972, Sakanaka [20] worked out the ion acoustic solitons for a warm ion plasma under initial excitations. He used both fluid and the Vlasov equations, and obtained similar results. The ion acoustic soliton stimulated from a initial hump in the potential was also observed in experiment [21] in 1970.

Wu and his group have worked on water solitons for many years [22]. Their main interests are in solitons stimulated by

various surface pressure or moving objects. Their numerical studies start with Boussinesq-type equations, and they also do the experiments in their small water tank. This work strongly influenced us. Our ion acoustic soliton work (details below) was aimed at finding the counterpart of their run-away soliton induced by a boat, but we did not arrive at a conclusive result.

As mentioned above, all of the numerical works have been devoted to the initial value problem. No comparable attention has been given to the mixed boundary-initial value problem. Actually, in real physical situations, the boundaries not only can not be avoided, but usually are the sources of excitation of the waves. Large number of physical problems indeed lead to mathematical models of mixed boundary-initial problems, such as the launching of solitary wave in a shallow water channel, excitation of ion acoustic solitons in plasma etc..

Chu et al [23] were one of the first groups that worked in this direction. They presented some important results obtained from ordinary KdV equation: solitons can be induced by boundary excitation, and they determined the relationship between the amplitude and velocity of solitons and the boundary values. They also considered the influence of the existence of dissipation (KdV- Burgers equation). But the solitons discussed are only induced by a fixed boundary under zero unperturbed water level and travel only in one direction.

Bona et al have also done a similar work [24].

The main emphasis of this thesis is to carefully study the influence of various boundary effects on solitons. Since we start with Bousinesq-type equations, we are able to further discuss soliton propagation in both directions and the related problems, such as soliton collisions and reflections. The work done in this thesis will be presented from two aspects: shallow water solitons (in section II.) and ion acoustic solitons (in section III.)

For shallow water solitons, we not only expand Chu's work on KdV equation, but also start a new series of studies based on the Boussinesq equation.

Working on the KdV equation, we let boundary values change at two different time scales: a cosine function with the period 2π and a random function that is changed at the rate of few time steps (1 ~ 10) 1/600 . After the Santa Barbara Conference, Tabor suggested to try the random boundary for KdV equation to see if some chaotic behavior or soliton turbulence will appear. The most striking result we obtained is that the random boundary produces a train of solitons just as a fixed value boundary does; while the envelopes of solitons induced by the cosine boundary is strongly influenced by the shape of the boundary. That means, if the time scale of boundary variation is much longer than the soliton mature time, the amplitude of soliton is strongly influenced by the

shape of boundary; in contrast, the random boundary almost has no random effect (compared with a steady boundary) on solitons although we expected a chaotic behavior to appear. The soliton is an integrated effect, and it is a very stable object. This is an obvious conclusion and this result is truly astonishing.

Our main work is done on the Boussinesq equation. Any arbitrary initial hump will produce symmetrically propagating solitons. When the width of initial hump is comparable to that of the soliton, a single soliton is formed: the bigger the β, the greater the width and the smaller the amplitude (due to mass conservation). If the width of the initial hump is much bigger than that of the soliton, then a number of solitons are formed.

We also study the collisions of solitons traveling either in the same or in the opposite directions. We found that for head-on collisions, no matter what amplitudes the pair of solitons have, when they collide, they simply overlap and the joint maximum amplitude is much bigger than the sum of the original amplitudes. Then they pass through each other and split totally into their original shapes, unchanged by the collision. For collisions between solitons traveling in the same direction, the ratio between the two colliding solitons plays an important role: if the ratio ~ 3 , the solitons overlap, but their joint amplitude soon gets to a value which is much lower than the amplitude sum of two original solitons;

if the rario ~ 1.5 , while solitons collide, they exchange their positions instead of overlapping. The results of collision of solitons traveling in the same direction are similar to that from KdV equation. The theoretical criterion was given by Lax [7].

The results of soliton reflection at a boundary are naturally similar with the head-on collision of two identical solitons. But in our calculations, when the soliton hits the left boundary, the maximum amplitude at this boundary is lower than the maximum joint amplitude of the head-on collision and the reflected soliton cannot quite restore to its original amplitude. That means it lost some energy. This result is not surprising. The reason is due to the approximate characteristic method used in this thesis, in other words, our numerical scheme is not perfect for the solitons getting close to the boundary area.

To induce solitons by mixed boundary and initial conditions from Boussinesq equation is still our main interest. For the finite water depth, we try several functions as our boundary conditions, such as a fixed value, a series of half sine function and a combination of one complete cosine function followed by a fixed value boundary etc.. The soliton maturing processes in these cases are completely different from that in [23]. The solitons we obtained superficially look like collisionless shock from [23] very much, but they are not

shocks. The difference is due to that we have used finite initial water depths instead of zero. When we go back to the KdV equation, we have the same results by letting the initial water depth be finite. This proves that the ratio between the perturbation amplitude and the unperturbed water level dominates the maturing period of soliton in the boundary inducing soliton cases. If the ratio is small, it takes a long time to make solitons mature. In contrast, if this ratio is approaching infinity as that in [23], solitons mature soon after they are born. So, the case of [23] actually is the extreme limit of zero total water depth. This limit cannot be handled in our treatment of the Boussinesq equation, and is not physically realistic.

In this thesis, two main efforts were made in the plasma physics. We still worked in the cold-ion plasma: finite electron temperature and zero ion temperature, and we start from the standard two fluid equations. Since the two fluid equations do not restrict the directions of the propagation of waves obtained under various situations, there should be a connection between these two fluid equations and Boussinesq-type equations. We have indeed obtained a set of Boussinesq-type equations from these two fluid equations analytically, assuming that the difference between the number densities of ions and electrons is very small. The idea of boundary induced soliton is also applied in the cold ion plasma situation. The

ion acoustic soliton formed from a fixed potential grid is obtained numerically. The example, such as, a satellite flys through the solar wind, will lead to this type of models, because satellites usually carry small electric potentials which are different from solar wind potential. These physical ideas and results are exhibited in III. Most of the above results had also been presented in the APS plasma physics division meeting held at Boston in 1984 and IMACS 1985 World Congress.

In the conclusion, we summarize and emphasize again the major original contributions made in this thesis.

Zabusky and Kruskal's famous work [5] was stimulated by physical problems but solved by numerical method, then followed the inverse-scattering transformation. This is a very good classic example of how computational results may lead to the development of new mathematics, much as experimental physics leads to new theories.

There are no theories yet to explain the numerical results of Chu' or ours. We are looking forward to the appearance of such new theories, and hope that this thesis will help stimulate them.

II. Shallow water solitons

We first present the soliton solutions obtained from the KdV equation, then from the Boussinesq equations.

1. Korteweg and de Vries equation.

1.1). Physical model and boundary-initial conditions

If the propagation of the soliton is restricted in one direction from the beginning, the KdV equation is commonly used. It has various forms, but usually it is written as

$$\frac{\partial \zeta}{\partial t} + \zeta \frac{\partial \zeta}{\partial x} + \varepsilon^2 \frac{\partial^3 \zeta}{\partial x^3} = 0 \qquad \text{---------- (1. 4)}$$

for the right going and positive hump ($\zeta > 0$) soliton, ε is a small parameter which was chosen as 0.022 in Zabusky and Kruskal [5] and Chu et al [23].

In this equation, $\zeta\zeta_x$ is the nonlinear term and ζ_{xxx} is the dispersive term. Through balance between these two terms, a soliton will be formed. We limit our discussion in a one dimensional domain (0, L). The unperturbed variable ζ_0 can be

chosen to be equal either zero or a constant.

For the purely initial excitation problem, the initial condition is put as:

$\zeta(x,0)$ = arbitrary function with a localized hump over ζ_0

The exact solution of the initial excitation problem by the inverse scattering method is well known nowadays to be a series of solitons. Each soliton looks like:

$$\zeta(x,t) = A\,\mathrm{sech}^2\left(\frac{X - X_0}{\Delta}\right) \qquad X = x - ct$$

---------- (2. 1)

$$c = \frac{A}{3}$$

---------- (2. 2)

$$\Delta = \frac{\varepsilon}{\sqrt{\frac{A}{12}}} = \frac{2\,\varepsilon}{\sqrt{c}}$$

---------- (2. 3)

where A, c and Δ are the amplitude, the speed and the width of the soliton, $\zeta_0 = 0$.

Chu et al [23] is devoted to the case of solitons induced by the mixed boundary-initial conditions. Their boundary conditions for the KdV equation are set up in the following

way. Considering the linearized equation of (1.4)

$$\frac{\partial \zeta}{\partial t} + a \frac{\partial \zeta}{\partial x} + \varepsilon^2 \frac{\partial^3 \zeta}{\partial x^3} = 0 \qquad \text{---------- (2. 4)}$$

where a = constant (> 0), the number of boundary conditions needed is determined by the uniqueness of the solution of (2.4) given by an energy inequality:

$$\begin{aligned} \frac{d}{dt} \int_0^L \frac{1}{2} \zeta^2 \, dx = \; & a \frac{1}{2} \zeta^2(0) - a \frac{1}{2} \zeta^2(L) \\ & + \varepsilon^2 \zeta \frac{\partial^2 \zeta(0)}{\partial x^2} - \varepsilon^2 \zeta \frac{\partial^2 \zeta(L)}{\partial x^2} \\ & - \varepsilon \frac{1}{2} \left(\frac{\partial \zeta(0)}{\partial x} \right)^2 + \varepsilon \frac{1}{2} \left(\frac{\partial \zeta(L)}{\partial x} \right)^2 \\ \leq 0 \qquad & \text{---------- (2. 5)} \end{aligned}$$

from which follows that:

$\zeta(0,t)$ at $x = 0$ (2. 6)

$\zeta(0,t)$, $\zeta_x(L,t)$, at $x = L$ (2. 7)

should be prescribed. The basic idea of this energy method is the following: We consider ζ_1 and ζ_2 , two solutions to (2.4)

satisfying the same initial and boundary conditions at t=0 and x = 0 and L . Let $\zeta = \zeta_1 - \zeta_2$, then ζ should also satisfy the equation (2.4) and the homogenious boundary and initial conditions. Multiplying (2.4) by ζ , then integrating it over finite x domain (0 to L), we obtain the equality (2.5). If ζ_1 and ζ_2 are given according to (2.6) and (2.7), then the three positive terms on the right hand side of (2.5) vanish for the ζ (difference between the two solutions). In other words, (2.5) holds. But since the integral is a square function integrated, it is ≥ 0. By the initial conditions, this integral is zero at t = 0 . And since (2.5) requires that it decreases or remains constant, so, this integral remains zero all the time, or $\zeta \equiv 0$ all the time. This proves the uniqueness of the solution to equation (2.4) and the initial and boundary conditions. In summary, in order to have this unique solution, the boundary conditions have to be posed as (2.6) and (2.7).

We have only concentrated on the left boundary for the sake of simplicity, and assume that the waves will never pass through the right boundary, so the far away right boundary conditions are simply taken as

$$\zeta(L,t) = \zeta_0 \qquad (2.8)$$

$$\zeta_x(L,t) = 0 \qquad (2.9)$$

and it is our main interest to see what the results will be if

the different left boundary conditions are prescribed.

In Chu's paper, they concluded that " a non-oscillating, steady, long pulse at boundary $\zeta(0,t) = \zeta_b$ (where ζ_b is a constant) will produce a train of identical solitons ". The amplitude and the speed of these solitons are given by:

$$A = 2\,\zeta_b \tag{2.10}$$

$$c = \frac{A}{3} = \frac{2}{3}\,\zeta_b \tag{2.11}$$

A second soliton is "born" just when the first one is about fully mature.

They also considered the KdV-Burgers equation:

$$\frac{\partial \zeta}{\partial t} + \zeta \frac{\partial \zeta}{\partial x} + \varepsilon^2 \frac{\partial^3 \zeta}{\partial x^3} - \upsilon \frac{\partial^2 \zeta}{\partial x^2} = 0 \tag{2.12}$$

where $\upsilon > 0$ and saw how the collisionless shock was formed due to the existence of the dissipation.

They did not work on the time-varying boundary conditions and the non-zero initial data. These points are our concerns and will be addressed in this thesis.

1.2). Numerical schemes.

A). The case for $\zeta_0 = 0$

In order to compare the results with Chu's, we simply adopt their numerical schemes, i. e., the ordinary second order leap-frog scheme for the interior points and a special boundary scheme which is up to fourth order accurate in x and second order accurate in t.

B). The case for $\zeta_0 \neq 0$

Since this is closer to the results from Boussinesq equations, we have used the special schemes for the interior points and the boundary area which are the same as described in section 2.4) for the Boussinesq equation. These schemes are up to fourth order accurate in x and second order accurate in t.

2. Boussinesq equation and its soliton solutions

2.1). Physical model

We consider a one dimensional inviscid incompressible

fluid (water) in a constant gravitational field. The density of the fluid remains constant.

We start from the one-dimensional Boussinesq equation [25]:

$$\frac{\partial h}{\partial t} + \frac{\partial (hu)}{\partial x} = 0$$

$$\frac{\partial u}{\partial t} + u \frac{\partial u}{\partial x} + g \frac{\partial h}{\partial x} + \frac{1}{3} c_0^2 h_0 \frac{\partial^3 h}{\partial x^3} = 0$$

---------- (2.13)

where

h --- total water depth

g --- acceleration of gravity

c_0 --- the speed of long wavelength shallow water wave

$$c_0 = \sqrt{gh_0}$$

h_0 --- total depth of unperturbed water

These equations are derived from the basic fluid equations and boundary conditions [26] (continuity and momentum equations; irrotational fluid conditions; dynamic and kinematic surface conditions and the horizontal bottom condition) under the one - dimensional shallow water approximation.

We choose the quantities: l_0 = characteristic length of

problem or shallow water wavelength, h_0 , c_0 and $t_0 = l_0/c_0$ as our standard quantities to normalize the Boussinesq equation, the equations then become

$$\frac{\partial h^*}{\partial t^*} + \frac{\partial (h^* u^*)}{\partial x^*} = 0 \qquad \text{---------- (2.14)}$$

$$\frac{\partial u^*}{\partial t^*} + u^* \frac{\partial u^*}{\partial x^*} + \frac{\partial h^*}{\partial x^*} + \frac{1}{3} \beta \frac{\partial^3 h^*}{\partial (x^*)^3} = 0 \qquad \text{---------- (2.15)}$$

in which * indicates the dimensionless variables and β is an important shallow water wave parameter defined as

$$\beta = \left(\frac{h_0}{l_0} \right)^2 \qquad \text{---------- (2.16)}$$

Henceforth, the notation * is omitted, but all quantities used now are understood to be dimensionless.

In this set of equations, the term uu_x plays the dominant nonlinear role among the other nonlinear terms and the term h_{xxx} is the dispersive term. The soliton is formed, if these two effects (nonlinear and dispersive) balance each other. As same as for KdV equation, an important conservation law for the Boussinesq equation also exists. It is written as

$$\frac{\partial hu}{\partial t} + \frac{\partial}{\partial x}\{hu^2 + \frac{1}{2}h^2 + \frac{1}{3}\beta[h\frac{\partial^2 h}{\partial x^2} - \frac{1}{2}(\frac{\partial h}{\partial x})^2]\} = 0 \qquad (2.17)$$

The physical meaning of the quantity " hu " is volume flux. This equation is obtained by multiplying (2.15) by h, then combining with (2.14).

2.2). Consideration of characteristics

We know from the theory of partial differential equations that the characteristics of a set of equations are determined by the highest order derivative terms. We also know that when the coefficients of the higher order derivative terms are small, and the lower order derivative terms form a hyperbolic system, then the solution is essentially waves with speeds predicted by the lower order system, the dissipative or dispersive effects of the higher order derivative terms modifying the wave structure appropriately. For the hyperbolic system, the characteristic theory is well established. Since, unlike the case of the KdV equation, we do not have (and cannot obtain) a uniqueness theorem to guide our choice of boundary conditions, we simply treat the boundary as if the dispersive term is absent. Fortunately, the coefficient β in

front of the term h_{xxx} is indeed very small (order ~ 0 to 10^{-4}), we can assume that the term βh_{xxx} is not important in determining the characteristics of the equations, although it is very important in forming the solitons. Then, we neglect this third derivative term and find the characteristics of the Euler equations:

$$\frac{\partial h}{\partial t} + \frac{\partial (hu)}{\partial x} = 0$$

$$\frac{\partial u}{\partial t} + u \frac{\partial u}{\partial x} + \frac{\partial h}{\partial x} = 0$$

---------- (2.18)

which are the normal shallow water equations (without dissipation or dispersion). This is a hyperbolic system and the characteristic velocities are

$$v_l = \left(\frac{dx}{dt} \right)_l = u(x,t) - \sqrt{h(x,t)}$$

---------- (2.19)

$$v_r = \left(\frac{dx}{dt} \right)_r = u(x,t) + \sqrt{h(x,t)}$$

---------- (2.20)

The Riemann invariants along the corresponding characteristics are:

$$R_l = G(x,t) = u(x,t) - 2\sqrt{h(x,t)} \qquad (2.21)$$

$$R_r = F(x,t) = u(x,t) + 2\sqrt{h(x,t)} \qquad (2.22)$$

This set of equations (2.18) is the lowest order approximation to the Boussinesq equations ((2.14) - (2.15)). In the following calculation, we will use their characteristics to approximate the exact characteristics of the Boussinesq equations. This assumption of treating the characteristics has proved to be successful in our following numerical calculations.

2.3). Initial and boundary conditions

For hyperbolic systems, the number of the boundary conditions for the partial differential equations is determined by the number of the characteristics entering the domain in question. If the differential equations contain higher order derivative terms, the characteristics are determined by these highest order terms. In principle, the number of boundary conditions for them cannot simply be found by such counting. It is also not quite clear that how should

we determine the exact boundary conditions for these higher order differential equations. So we have to find an approximation for these boundary conditions in order to continue.

As indicated above, our region is confined in $0 \leq x \leq L$, by neglecting the highest order derivative term in the Boussinesq equations, the equations became a hyperbolic system (2.18) from which we found a pair of characteristics which are considered as the approximation to the exact characteristics of the original equations. We hope that the number of boundary conditions for this hyperbolic system could be used as an approximation number for our Boussinesq system. In other words, now, at each boundary, only one characteristic enters the domain, so only one variable out of $h(x,t)$ and $u(x,t)$ should be preset at each boundary, the other will be determined by the suitable Riemann invariant. Since the KdV equation is derived from the Boussinesq equations by restricting the wave to propagate in one direction, they are essentially consistent. When we look back into the boundary conditions for KdV equation ((2.6) - (2.7)), they are also consistent with the boundary conditions we assumed for the Boussinesq equations. So, in the following calculations, we have used these boundary conditions, and the numerical results indicate that this is reasonable.

Since the two boundaries are symmetrical, without losing

generality, we just concentrate on one boundary $x = 0$ and choose L to be big enough, so the solitary waves will never pass through the right boundary. In other words, if the notations h_0 and u_0 are used for the unperturbed total water depth and the speed of unperturbed water, we just leave the right boundary conditions to be the unperturbed water conditions:

$$h(L,0) = h_0 \tag{2.23}$$

$$u(L,0) = u_0 \tag{2.24}$$

where usually $h_0 = 1.0$ and $u_0 = 0$ is chosen through the whole paper assuming the water is at rest at the beginning. Otherwise, u_0 is taken as an arbitrary constant by special indication.

The concrete boundary and initial conditions should be given separately according to the different physical situations. We will show them through three aspects below.

A). Pure initial excitation

As is well known, it is a main property of the Boussinesq equations that the solitons formed from them can symmetrically propagate in two directions. Any initial perturbations will

lead to these solitons propagating.

An arbitrarily localized hump in h over h_0 is given as the initial condition $h(x,0)$. For example, we choose the half sine function as the hump whose amplitude and width are adjustable, since its width is much bigger than soliton's, few solitons with different amplitudes are formed; or we can choose a hump whose width is similar to soliton's, then a single soliton will be produced, and so on.

For the purely initial excitation problem, how solitons are formed from an arbitrary localized hump that is our main interest, so the boundary conditions are not that important and they are simply chosen in advance like:

$$h(0,t) = h(L,t) = h_0 \tag{2.25}$$

then velocities at both boundaries are followed as:

$$u(0,t) = u(L,0) = u_0 \tag{2.26}$$

assuming that the soliton will never pass through both boundaries.

B). Soliton collisions and reflection

In the problems like collisions between solitons (which travel either in the same or in the opposite directions) or soliton reflection, to control the direction of soliton propagation is crucial.

When $h(x,0)$ is given in advance, we achieve this by choosing the initial condition $u(x,0)$ through the suitable Riemann invariant, i. e., the initial velocity $u(x,0)$ should be determined by the condition that the Riemann invariant along the opposing characteristics should be zero or a constant. For example, if we assume that the soliton is restricted in propagating to the right direction, the Riemann invariant $G(x,t)$ at $t = 0$ along the left going characteristic should be zero or a constant C, i.e.,

$$G(x,0) = u(x,0) - 2\sqrt{h(x,0)}$$
$$= 0 \qquad \text{----------} \quad (2.27)$$

$$\text{or} \quad = -2\sqrt{h_0}$$
$$\text{----------} \quad (2.28)$$

if u_0 is chosen as zero. So $u(x,0)$ is determined correspondingly as

$$u(x,0) = 2\sqrt{h(x,0)}$$
$$\text{----------} \quad (2.29)$$

$$\text{or} \quad = 2\sqrt{h(x,0)} - 2\sqrt{h_0}$$
$$\text{----------} \quad (2.30)$$

and vice verse: if the soliton propagates to the left direction, the Riemann invariant $F(x,t)$ at $t = 0$ along the

right going characteristics should be zero or a constant C , that is,

$$F(x,0) = u(x,0) + 2\sqrt{h(x,0)}$$

$$= 0 \qquad \text{----------} \quad (2.31)$$

$$\text{or} \quad = 2\sqrt{h_0}$$

$$\text{----------} \quad (2.32)$$

if u_0 is taken as zero, and $u(x,0)$ is determined as

$$u(x,0) = -2\sqrt{h(x,0)}$$

$$\text{----------} \quad (2.33)$$

$$\text{or} \quad = -2\sqrt{h(x,0)} + 2\sqrt{h_0}$$

$$\text{----------} \quad (2.34)$$

For the collision of solitons propagating in the same direction, that two arbitrary localized humps over the unperturbed water level h_0 is given as the initial condition for $h(x,0)$. $u(x,0)$ is determined as pointed out in ((2.29); (2.30)) or ((2.33); (2.34)) according to the propagation direction of soliton chosen.

When discussing the soliton head-on collisions, we split the space into left and right two parts in order to prepare solitons propagating in opposite directions. The principle of

forming solitons is identical as above. For clarity, we summarize these initial conditions as follows: the initial total water depths

$h_l(x_l, 0)$ = containing an arbitrary hump over h_0 in the left part of the domain

and

$h_r(x_r, 0)$ = containing an arbitrary hump over h_0 in the right part of the domain

are given in advance, the initial velocities are then as:

$$u_l(x_l, 0) = 2\sqrt{h_l(x_l,0)} - 2\sqrt{h_0} \qquad \text{----------} \quad (2.35)$$

$$u_r(x_r, 0) = -2\sqrt{h_r(x_r,0)} + 2\sqrt{h_0} \quad . \qquad \text{----------} \quad (2.36)$$

In the collision problem, we assume the domain to be big enough so the solitons will never pass through the boundaries. The boundary conditions for $h(x,t)$ and $u(x,t)$ are chosen to be the same as the unperturbed water conditions given in part A) as (2.25) and (2.26).

Since the two boundaries in question are symmetrical, for soliton reflection problems, we only need to treat one

boundary with great care, such as we choose the left one, i. e., we only consider left going solitons to reflect at the left boundary assuming that the reflected soliton will never pass the right boundary. A few key points of setting the initial and boundary conditions are:

a). For the initial conditions, we follow the spirit mentioned above: since (2.32) should be satisfied, while an arbitrary localized hump over h_0 in h is given in advance, $u(x,0)$ is determined from (2.34) correspondingly.

b). At the left boundary, the velocity $u(0,t)$ is given in advance and $h(0,t)$ is determined from the Riemann invariant $G(x,t)$ along the left going characteristic afterwards. That is:

$$u(0,t) = u_b = 0 \qquad (2.37)$$

is given previously. $h(0,t)$ is determined by

$$h(0,t) = 0.25 \{ u(0,t) - G(0,t) \}^2 \qquad (2.38)$$

since the Riemann invariant along the left going characteristic should be chosen as

$$G(0,t) = u(0,t) - 2\sqrt{h(0,t)} \qquad (2.39)$$

The way we choose the boundary condition here is similar

to the situation of ordinary water wave reflection: at the boundary, the velocity is usually chosen as zero and the pressure will be doubled automatically and cannot be prescribed.

C). Soliton induced by boundary condition

In this case, the soliton is induced either by the fixed or time-dependent boundary conditions. The $h(0,t)$ should be prescribed, such as a fixed constant ($> h_0$), a cosine function or a random functions etc.. The time average value of these functions are related with the unperturbed water level h_0 as

$$\overline{h(0,t)} = h_0 + \Delta h \qquad (2.40)$$

where Δh is the amplitude of the perturbation and the bar means the time average.

Since the Riemann invariant $G(0,t)$ along the left going characteristic should be zero or a constant C, the velocity at left boundary should be taken as

$$u(0,t) = 2\sqrt{h(0,t)} - 2\sqrt{h_0} \qquad (2.41)$$

The soliton is not induced by the initial conditions in this case, so the initial conditions are the unperturbed water height and the speed:

$$h(x,0) = h_0 \qquad (2.42)$$

$$u(x,0) = u_0 \qquad (2.43)$$

2.4). Numerical Schemes

A). Schemes for interior points

As usual, we have adopted the notation $F_j^n = F((j-1)\Delta x, n\Delta t)$ representing any function of u, h or hu. The leap-frog scheme is used as our main numerical scheme. For the function F and its derivatives, the difference approximation for the interior points in the domain are written as follows:

$$F_x = \frac{2}{3}\frac{F_{j+1}^n - F_{j-1}^n}{\Delta x} - \frac{1}{12}\frac{F_{j+2}^n - F_{j-2}^n}{\Delta x} \qquad (2.44)$$

$$FF_x = \frac{F_{j-1}^n + F_j^n + F_{j+1}^n}{3}\,\frac{2}{3}\frac{F_{j+1}^n - F_{j-1}^n}{\Delta x} - \frac{1}{12}F_j^n\frac{F_{j+2}^n - F_{j-2}^n}{\Delta x} \qquad (2.45)$$

$$F_{3x} = \frac{F_{j+2}^n - 2F_{j+1}^n + 2F_{j-1}^n - F_{j-2}^n}{2\Delta x^3} \qquad (2.46)$$

$$F_t = \frac{F_j^{n+1} - F_j^{n-1}}{2\,\Delta t}$$

---------- (2.47)

The function F in the term FF_x is written in the usual way to conserve the square sum Σu_j^2 and thereby suppress the nonlinear instability.

It is quite clear that when the whole equation is written at the point A = ((j-1)Δx, nΔt) (it will be abbreviated as (j, n) in following), as shown below,

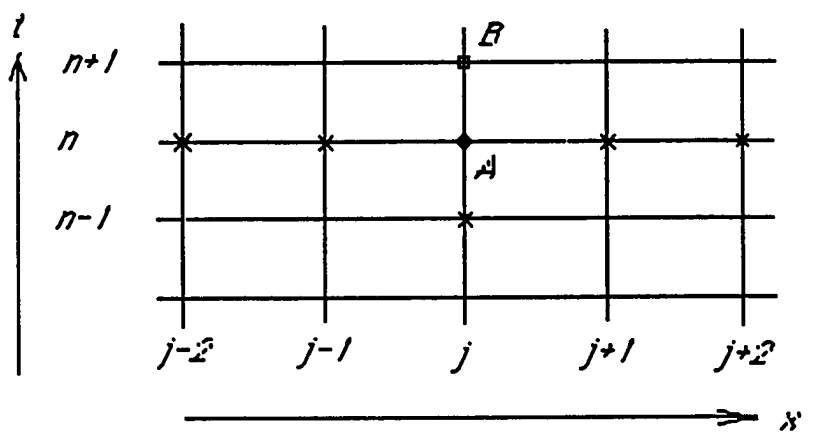

Grids for interior points

five points (j-2, n), (j-1, n), (j+1, n), (j+2, n) and (j, n-1) are needed in order to calculate the unknown point B = (j, n+1) .

The points at row next to the left boundary $x = 0$ deserve special treatment because, as indicated above, two rows of data left to the second row are needed but only one row data are available.

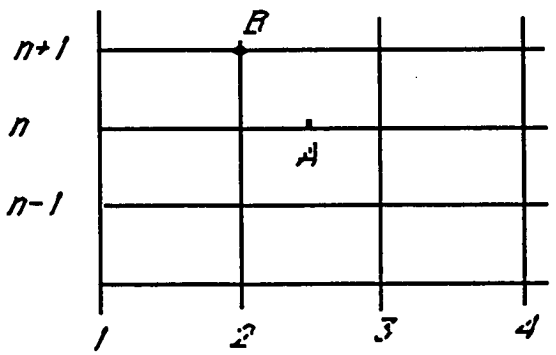

Grids close to boundary area

In order to calculate the points $F_2^{n+1} = F(\Delta x, (n+1)\Delta t)$ at the second row exhibited above, i. e., the values at point B , the whole equation is written at point A .

The difference schemes for function F and its derivatives at row 2 are as follows:

$$F = \frac{1}{8} \{4.5 \ (F_2^n + F_3^n) - 0.5 \ (F_1^n + F_4^n) \}$$

---------- (2.48)

$$F_x = \frac{1}{24} \{ 27 \frac{F_3^n + F_2^n}{\Delta x} - \frac{F_4^n - F_1^n}{\Delta x} \}$$

---------- (2.49)

$$F_{3x} = \frac{F_4^n - 3\,F_3^n + 3\,F_2^n - F_1^n}{\Delta x^3}$$

---------- (2.50)

$$F_t = \frac{1}{16\,\Delta t}\{\,4.5\,[(\,F_2^{n+1} + F_3^{n+1}\,) - (\,F_2^{n-1} + F_3^{n-1}\,)]$$

$$- 0.5\,[(\,F_4^{n+1} + F_1^{n+1}\,) - (\,F_4^{n-1} + F_1^{n-1}\,)]\}$$

---------- (2.51)

we emphasize again that $F(\Delta x, (n+1)\Delta t)$ are the unknown variables to be found.

The whole numerical schemes are kept up to fourth order accurate (except term F_{xxx} which keeps second order accurate) in x and 2nd order accurate in t.

B). Difference approximation for boundary

As pointed out above, for the boundary conditions, among h and u, only one of them should be given in advance, the other is determined by the suitable Riemann invariant along the corresponding characteristic. Since these approximated characteristics might not be a constant any more, how to work out a difference approximation of these characteristics becomes important.

In the problem that soliton is mainly induced by left boundary condition, that is the mixed boundary-initial value problem, all the left going waves should be killed, then, purely right going waves will be left in the domain. In this case, the characteristics are straight lines (constant), so we prescribe the boundary and initial conditions of the total water depth h as:

$$h_1^n = h_b(n) \qquad n = 2,3,\ldots\ldots$$

---------- (2.52)

$$h_j^1 = h_0 = \text{constant} \qquad j = 2,3,\ldots\ldots,N$$

---------- (2.53)

where

$$\overline{h_b} = h_0 + \Delta h$$

---------- (2.54)

and $h_b(n)$ is the difference form of the arbitrary function $h_b(t)$. By the requirement of the Riemann invariant $G(x,t) = 0$ or C which in the discrete form is as:

$$G_j^n = u_j^n - 2\sqrt{h_j^n}$$

$$= 0$$

$$\text{or} \quad = -2\sqrt{h_0}$$

---------- (2.55)

then the boundary and initial conditions of velocity u(x,t) are determined as:

If G = 0,

$$u_1^n = 2\sqrt{h_1^n} = 2\sqrt{h_b(n)} \qquad \text{---------- (2.56)}$$

$$u_j^1 = 2\sqrt{h_j^1} = 2\sqrt{h_0} \qquad \text{---------- (2.57)}$$

If $G = -2\sqrt{h_0}$,

$$u_1^n = 2\sqrt{h_1^n} - 2\sqrt{h_0}$$

$$= 2\sqrt{h_b(n)} - 2\sqrt{h_0} \qquad \text{---------- (2.58)}$$

$$u_j^1 = 0 \qquad \text{---------- (2.59)}$$

where $n > 1$ is integer and $j = 2,3,4,\ldots\ldots,N$.

For the problem of left going soliton reflected at left boundary, as boundary condition, $u(0,t) = 0$ is given in advance and $h(0,t)$ is determined by the condition that the Riemann invariants along left going characteristics should be zero.

The approximated characteristics of the Boussinesq

equation generally are not constants any more. In order to determine the $h(0,t)$, the local characteristics method should be used and is described below.

In this local characteristic method, the characteristics locally are considered as the straight lines, as shown below. According to (2.37) and (2.38), the boundary value of $u(0,t+\Delta t)$ is given in advance, the boundary value of $h(0,t+\Delta t)$ then is determined by

$$h(0,t+\Delta t) = 0.25 \{u(0,t+\Delta t) - G(0,t+\Delta t)\}^2 \qquad (2.60)$$

To try to get Riemann invariant G at time level $t+\Delta t$ is our main aim now. When the time marches from t to $t+\Delta t$ (i.e. from t_A to t_D), the Riemann invariant $G(x,t)$ is assumed to be a constant, so $G(D) = G(B)$. The Riemann invariants $G(A)$ and $G(C)$ at points A and C are calculated from the values of h and u at time level t on the grid points A and C . The $G(B)$ is determined by the linear interpolation of $G(A)$ and $G(C)$.

Let

$$\mu = \frac{AB}{AC} = \frac{AB}{\Delta x} = \frac{G(B) - G(A)}{G(C) - G(A)} \qquad (2.61)$$

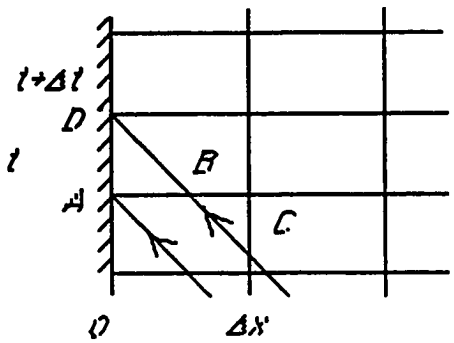

Characteristics locally are considered

as straight lines

then finally

$$G(B) = (1 - \mu)\, G(A) + \mu\, G(C)$$

$$G(D) = G(B)$$

---------- (2.62)

We now summarize the initial and boundary conditions in the following. As the initial conditions,

h_j^n = a function containing a localized hump over h_0

is given in advance, then velocity is determined by

$$u_j^1 = -2\sqrt{h_j^1} \qquad \text{if } F = 0$$

$$\text{or} \quad = -2\sqrt{h_j^1} + 2\sqrt{h_0} \qquad \text{if } F = 2\sqrt{h_0}$$

---------- (2.63)

where j = 2,3,.....,N. The boundary conditions are prescribed as:

$$u_1^n = 0 \qquad \text{---------- (2.64)}$$

$$h_1^n = 0.25 \{ u_1^n - G_1^n \}^2 \qquad \text{---------- (2.65)}$$

where n > 1 is integer.

3. Relationship between Boussinesq and KdV equations

If η is used to denote the dimensionless quantity of the fluctuation of the shallow water perturbation, the Boussinesq equation can also be expressed in η as follows:

$$\frac{\partial \eta}{\partial t} + \frac{\partial v}{\partial x} + \alpha \frac{\partial (v\eta)}{\partial x} = 0$$

$$\frac{\partial v}{\partial t} + \alpha v \frac{\partial v}{\partial x} + \frac{\partial \eta}{\partial x} + \frac{1}{3} \beta \frac{\partial^3 \eta}{\partial x^3} = 0 \qquad \text{---------- (2.66)}$$

where η is normalized according to the amplitude of the shallow water wave a and the important parameter α in these equations is defined as

$$\alpha = \frac{a}{h_0}$$

Obviously, the Boussinesq equations expressed in both forms of the total water depth h and the fluctuation ζ are related. The transformation between them is done through the following relation:

$$h = 1 + \alpha\eta \qquad (2.67)$$

$$u = \alpha v \qquad (2.68)$$

in which the velocity of unperturbed water usually is considered as zero.

The Boussinesq and KdV equations both describe solitary wave phenomena in shallow water. Essentially, they are the same. The main difference is that the Boussinesq equation can describe the waves propagating in two directions while the KdV equation only allows one. The following relation will lead the two sets of equations to transform from each other:

$$v + \frac{1}{6}\beta\frac{\partial^2 v}{\partial x^2} = \eta - \frac{1}{4}\alpha\eta^2 + \frac{1}{3}\beta\frac{\partial^2 \eta}{\partial x^2} \qquad (2.69)$$

$$\frac{\partial \eta}{\partial t} = -\frac{\partial \eta}{\partial x} \qquad (2.70)$$

In Boussinesq equations, if we restrict waves to propagate in one direction, the condition (2.70) should be satisfied: that is not surprising because the lowest order equations (α, β both $\rightarrow 0$ in (2.66)) actually is a set of ordinary wave equations.

In terms of the fluctuation quantity η, the KdV equation can be represented as:

$$\frac{\partial \eta}{\partial t} + \frac{\partial \eta}{\partial x} + \frac{3}{2}\alpha\eta\frac{\partial \eta}{\partial x} + \frac{1}{6}\beta\frac{\partial^3 \eta}{\partial x^3} = 0 \qquad \text{---------- (2.71)}$$

This form also is connected with the more common form of the KdV equation which usually is written as:

$$\frac{\partial \zeta}{\partial t} + \zeta\frac{\partial \zeta}{\partial x} + \varepsilon^2\frac{\partial^3 \zeta}{\partial x^3} = 0 \qquad \text{---------- (1. 4)}$$

through the transformation shown below:

$$\zeta = 1 + 1.5\,\alpha\eta \qquad (2.72)$$

$$\varepsilon^2 = \frac{1}{6}\beta \qquad (2.73)$$

Combining (2.67) and (2.72), the relation between ζ and h is built up as

$$\zeta = 1.5\ h - 0.5$$

---------- (2.74)

The similarities between the Boussinesq and KdV equations under various conditions have been shown numerically in Sec. 4.3).

4. Computational results

We mainly treat KdV equation (1.4) and Boussinesq equations (2.14)- (2.15) which are expressed in terms of the total water depth h . For comparison reasons, we will discuss the results of KdV and Boussinesq equations of the fluctuation depth (2.71) and (2.66).

The grid points are set up with $\Delta x = 1/40$ or $1/50$, $\Delta t = 1/600$ or $1/800$ to satisfy the CFL instability criterion: $\gamma[\Delta t/(\Delta x)^3] < 1$ where $\gamma = \varepsilon^2$ in KdV equation and $\gamma = (1/3)\beta$ in Boussinesq equation. The small parameter β in Boussinesq equation varies from 0 to 0.0007 , then ε in KdV equation is determined correspondingly from (2.73). Throughout section II, the numerical scheme designed is denoted as the fourth order scheme, and the scheme adopted from [23] will be called the second order scheme. Generally, two types of initial conditions have been used: a half sine function spreading over

20 grid points whose width is much wider than the width of a soliton, and a single hump whose width is comparable with that of a soliton, the amplitudes of them are changed for different cases and both of them are placed over the unperturbed water level.

This section is explained from 3 aspects: in the first part, the influence of different time-dependent boundary conditions and different initial conditions in KdV equation is discussed; in 4.2), we will present the results from the Boussinesq equations: 4.2.1) results from initial excitations; 4.2.2) soliton collisions; 4.2.3) reflection of solitons at boundary; 4.2.4) boundary induced solitons; in the last section 4.3), we will compare the results from Boussinesq and KdV equations.

4.1). Some important results from KdV equation.

In Chu et al[23], they restricted themselves to the case of $\zeta_0 = 0$ and carefully observed the solitons induced only by the fixed boundary conditions. We concentrate on analyzing the influence of different time-varying boundaries to the soliton induced under both cases of $\zeta_0 = 0$ and $\zeta_0 \neq 0$. We shall see that the different unperturbed water levels will lead to totally different pictures of the solitons induced by the

boundary.

For the initial excitation, if an arbitrary initial hump is given, the soliton will be formed afterwards: if the width of the initial hump is much wider than that of soliton, several solitons will be formed afterwards; if the width of the initial hump is comparable with the width of soliton, a single soliton will be formed. Although these results were well known long ago, we have still done some work in this area. This is not only for checking our numerical scheme, but also for comparing with the results obtaining from Boussinesq equation.

We have worked on two initial conditions: a half sine function and a narrow single hump, both are placed over $\zeta_0 = 1.0$. The fourth order scheme is used.

For the first case (wider single hump of amplitude 0.75), 4 solitons are formed as shown in Figs. 1.1.1 - 1.1.2 for time t = 1.0 and t = 3.0. Through the transformation (2.72) and (2.73), the solitons in terms of fluctuation η are shown in Figs 1.1.3 (for t = 1) and Fig. 1.1.4 (for t = 3). Figs 1.2.1 and 1.2.2 show the results for the fluctuation amplitude calculated directly from (2.71) under the equivalent initial hump whose amplitude is 1.0 while $\alpha = 0.5$. The unperturbed fluctuation level η_0 should be taken as zero that is obvious. These figures are identical with Figs. 1.1.3 and 1.1.4, which proves the correctness of the transformation of (2.72) and

(2.73) and the reliability of our scheme.

Giving an initial hump whose width is comparable with the soliton's, a single soliton is formed. Calculated from (1.4) numerically, we can see that the amplitude of the soliton gets bigger and the width gets smaller if ε decreases. The results are shown in 4.3) in order to compare with Boussinesq case.

For the boundary induced soliton problem, the work is done generally according to two categories. First, we expand Chu's results. We simply adopt their scheme and parameters: $\varepsilon = 0.022$, $\zeta_0 = 0$, but work out solitons under different boundary excitations; or we keep a fixed boundary condition, but let ζ_0 be finite instead. The results from latter will be compared with that from Boussinesq equation, so we use the corresponding fourth order scheme and parameters as for Boussinesq, such as $\varepsilon = 0.00898$, $\zeta_0 = 1.0$.

For the first case, we had tried several different time dependent functions as our boundary conditions, such as cosine, sine, periodic square function and random function with a fixed expectation, etc.. The typical cases are the cosine and random functions, these results deserve special attention in this section.

For the cosine function induction, $\zeta_b = 0.5\{1 + \cos(t)\}$ and $\zeta_0 = 0.5$, the results are as predicted: the solitons are induced one by one with different amplitudes whose envelope is strongly influenced by the boundary cosine function. The

speeds of solitons with bigger amplitudes are higher. After few time intervals, the solitons with higher speeds would pass over the ones with lower speeds, the solitons are "lined up" according to their amplitudes. These effects are shown in Figs. 1.3.1 - 1.3.4. They are very similar with Zabusky and Kruskal [5].

The results from the random boundary with a fixed expected value surprised us the most. When we put in this random condition, we were expecting some chaotic behavior to come out, such as solitons with random amplitudes, and perhaps soliton turbulence. In contrast, we got a very regular behavior --- solitons (Figs. 1.4.1 - 1.4.2) which are formed as if we were using a fixed value boundary (that is equal the expectation value of the random function which is 0.5 in this case) shown in Figs. 1.4.7 - 1.4.8. We then tried to hold every random value for few time steps, such as 5 or 10 time steps, and we got similar regular results displayed in Figs. 1.4.3 to 1.4.6. These astonishing results lead to the conclusion that the solitary wave phenomena are integrated effects, and are extremely regular and very stable objects. Baransky also made similar calculations which agree with our results (private communication).

In these two examples, both boundary conditions used to induce solitons change, but they change at different time scales. The period for the cosine function is 2π, that for

the random function is a few time steps (1 ~ 10) 1/600 . This suggests a conclusion: when the period of boundary variation is much bigger than soliton maturing time, the amplitudes of solitons (envelope) are strongly influenced by the shape of the boundary function; if the time scale of the boundary is much smaller than the soliton maturing time, these perturbations almost have no effects on forming solitons, only the expectation of these perturbations plays the dominant role.

We also work on the steady boundary case, but ζ_0 is not zero any more. In fact, after we got the Boussinesq solitons induced by fixed boundary and realized that the results are correct although they look totally different from Fig. 1.5.1 taken from [23], we came back to this case. Let $\varepsilon = 0.022$, the grids are set up as $\Delta x = 1/40$, $\Delta t = 1/600$ and second order scheme is used. Fig. 1.5.1 from [23] describes the solitons induced by taking boundary $\zeta_b = 1.0$ and the initial condition $\zeta_0 = 0.0$. Figs. 1.6.1 - 1.6.5 display the results of $\zeta_b = 1.75$ and $\zeta_0 = 1.0$, while Figs. 1.7.1 - 1.7.4 display $\zeta_b = 1.75$ and $\zeta_0 = 0.5$. These examples clearly show that Fig. 1.5.1 is the extreme limit as ζ_0 approaches zero. As long as ζ_0 increases, the solitons born do not immediately have equal amplitudes any more because it takes a longer time to make solitons mature.

In order to compare boundary induced KdV solitons with

Boussinesq's, we work on the situation in which $\zeta_0 = 1.0$, $\varepsilon = 0.00898$ and choose the fourth order numerical scheme. The results are shown in Figs. 1.8.1 - 1.8.2 where boundary condition is preset as $\zeta_b = 1.15$ and $t = 1.0$ and $t = 3.0$ respectively. The situation is similar to the case shown in Figs. 1.6.1 - 1.6.5.

4.2). Results from Boussinessq equation

Since Boussinesq equation can handle the solitons traveling in two directions, more advanced topics such as soliton collision and reflection etc. can be studied besides the problems of initial and boundary excitations.

The typical parameters are chosen as: $\beta = 0.000484$, $h_0 = 1.0$, $u_0 = 0.0$. The grids are set up as $\Delta x = 1/40$, $\Delta t = 1/600$. Fourth order scheme is used. A half sine function and a single narrow hump are the two types of initial functions used in this section. No matter how big the amplitudes a_{ih} they have, the former covers 20 grid points, so its width is in general much bigger than the width of a soliton; the width of the latter is chosen to be closer to that of soliton. The figures, describing the numerical results, typically show the distributions of the total water depth or the fluctuation water level.

Any conditions different from above will be indicated specifically.

4.2.1). Results of initial excitation

Since any initial perturbation will excite solitons which will symmetrically propagate into two opposite directions. If a half sine function is chosen as our initial hump, the main characters can be summarized in the table 1 below, where w is the width of the soliton, No. is the number of solitons formed, and τ is the time needed for forming a soliton.

The parameter β controls the width of the soliton. If β is larger, the soliton is wider. The amplitude of the initial hump a_{ih} basically determines the amplitudes of the solitons.

Table 1.

a_{ih}	0.25	to	1.25	(β is fixed)
β	0.0008	to	0.0001	(a_{ih} is fixed)
w	big		small	
No.	2		5	
τ	long		short	

The result of the balance of the dispersive and nonlinear effects will form a soliton. If a_{ih} is fixed , the bigger β will make a little stronger dispersive effect than the nonlinear effect, then the width of soliton will be larger and the time needed to form it will be longer and from the mass conservation, the number of solitons could be formed is smaller. If β is fixed, bigger amplitude a_{ih} will make a stronger nonlinear effect than the dispersive effect, the soliton width will be smaller, more solitons will be formed and the time needed to form them is shorter.

Giving a half sine function as an initial excitation, we

Table 2.

a_{ih}	No.	a	w	Figs.
0.25	2	~ 0.184	~ 0.071	2.1.1 - 2.1.2
0.50	3	~ 0.384	~ 0.067	2.1.3 - 2.1.4
0.75	3 ~ 4	~ 0.584	~ 0.062	2.1.5 - 2.1.6
1.00	4	~ 0.750	~ 0.059	2.1.7 - 2.1.8
1.25	4 ~ 5	~ 0.890	~ 0.053	2.1.9 - 2.1.11

fix β to 0.000484 and change the amplitudes of initial humps from 0.25 to 1.25, the results are displayed in the the table 2, where a and w are the approximate amplitude and width of the leading soliton. As an example, only one velocity profile is shown in Fig. 2.1.11 : when the solitons propagate toward opposite directions, two sets of velocities having different signs also propagate toward opposite directions.

If the half sine function with fixed amplitude 0.5 is used to excite the solitons, we change β, the results are

Table 3.

β	No.	a	w	Figs.
0.000000	5			2.2.1 - 2.2.2
0.000100	4	~ 0.329	~ 0.059	2.2.3 - 2.2.4
0.000300	3 ~ 4	~ 0.372	~ 0.062	2.2.5 - 2.2.6
0.000484	3	~ 0.384	~ 0.067	2.1.3 - 2.1.4
0.000700	2 ~ 3	~ 0.383	~ 0.080	2.2.7 - 2.2.8

shown in the table 3 above, where a and w are defined as

before.

If a single hump of amplitude 0.82 is given as an initial function, two solitons are formed and propagate away in opposite directions. As long as β increases, the soliton width gets wider and its amplitude gets smaller. The numbers are shown in the table 4 below where a and w are the amplitude and width of the single soliton, and the figures are displayed in Figs. 2.3.1 - 2.3.8.

Berezin and Karpman [27] analyzed numerically the relation between the widths of initial hump and solitons for KdV equation. subsequently the inverse-scattering method gives the theoretical results. Our Boussinesq results are very close to theirs.

Table 4.

β	a	w	Figs.
0.000100	0.4341	~ 0.083	2.3.1 - 2.3.2
0.000300	0.4172	~ 0.092	2.3.3 - 2.3.4
0.000400	0.4056	~ 0.097	2.3.5 - 2.3.6
0.000484	0.3925	~ 0.104	2.3.7 - 2.3.8

4.2.2). Soliton collision.

We have worked on the soliton collision problems where solitons either propagate in the same direction or in the opposite directions. The former is familiar from KdV equation, while the latter is new. For both cases, we start with Boussinesq equations (2.14) and (2.15), but the results come out quite differently.

For the head-on collision, we first consider the collision between two single solitons which are formed by letting the widths of initial humps be close enough to that of solitons. We have worked on collisions of pairs of solitons with different amplitudes, the results are summarized as follows.

If the two initial humps of amplitudes 0.58 and 0.82 are given at t = 0.0, the solitons of amplitudes 0.61 and 0.91 are formed soon and they propagate toward each other. As they get closer, their amplitudes get bigger. At t = 0.898 , they started to overlap and the common peak a of 0.983 locates at x = 5.125 . This peak a gradually increases until it reaches its maximum a = 1.609 at x = 5.075 and t = 0.933 , then it starts to decrease, at t = 0.968, this single peak gets to as low as a = 0.838 at x = 5.025. At t = 0.970, the two solitons split and their amplitudes at that moment are 0.87 and 0.52 located at x = 5.025 and x = 5.15

respectively. So the soliton overlap time equals 0.070 . As time goes on, they finally will reach their original amplitudes. This general process is shown in Figs. 3.1.1 - 3.1.3: at t = 0.5 , the two solitons propagate toward each other but have not collided yet; at t = 1.0 , these solitons just collided and passed each other but have not totally split; at t = 1.5 , they split totally and propagate away from each other.

If the two initial humps are identical and their peaks are 0.82, the two solitons formed are identical and their amplitudes are 0.91 at the beginning. As they propagate toward each other, their amplitudes get bigger and bigger. At t = 0.858 , the two peaks reach 1.025 and are just one grid apart. At t = 0.860 , they started to overlap and the common peak a of 1.081 locates at x = 5.15 , this peak increases until t = 0.885 , it reaches the maximum a = 2.142 at the same grid, then it starts to decrease, and at t = 0.918 , the single peak gets to as low as a = 0.858 , then the two solitons split. As time goes on, they reach their original amplitudes. The soliton overlap time in this case is 0.058 . If the peaks of two initial humps are chosen to be 0.58 , the situation is similar with that of 0.82 . We exhibit these results in Fig. 3.2.1 - 3.2.3. At the time t = 0.5, 1.0, 1.5, the solitons are in the stages of before collision, overlap and after collision respectively.

If the two peaks of initial humps are 0.27 and 0.82 , the amplitudes of solitons formed are 0.26 and 0.91 at the beginning. The solitons start to propagate toward each other until t = 0.942 , they locate at x = 4.95 and x = 5.05 with amplitudes of 0.260 and 0.961 . At t = 0.943, they started to overlap and the common peak a = 0.971, this peak increases until it reaches the maximum a = 1.299 at t = 0.983 and x = 5.0 , then starts to decrease, at t = 1.025, the single peak gets to as low as a = 0.929, then at t = 1.023, the two solitons split and their amplitudes are 0.91 and 0.23 , as time goes, they reach their original amplitudes. The soliton overlap time in this case is 0.082.

From the above analysis, we find out some very important results which are that no matter what amplitudes the original two solitons have, when they collide, they simply overlap and the "joint" amplitude gradually reaches its maximum which is much bigger than the sum of the two original solitons' amplitudes, such as $1.61 > 0.91 + 0.61 = 1.58$; $2.14 > 0.91 + 0.91 = 1.82$ and $1.30 > 0.91 + 0.26 = 1.17$; since the soliton with bigger amplitude has a larger velocity, the collision time for a pair of solitons with larger amplitudes is shorter.

We also observe the head-on collision of series of solitons produced by two half sine functions as the initial conditions. The parameters and the grid are set up as before.

In the first case, we let these two half sine functions be identical, that is they have the same amplitudes 0.5 and their peaks are 300 grid points apart. The results are shown in Figs. 3.3.1 - 3.3.10. Figs. 3.3.1 and 3.3.2 exhibit the solitons formed and propagated toward the center just before collision during the time period t = 0.5 to t = 2.5 ; Fig. 3.3.3 shows the corresponding solitons in velocity space at t = 2.5. Figs. 3.3.4 - 3.3.8 show the process of collision of this series of solitons, both in total water depth and velocity, during the time period t = 3.0 - 4.0 . After collisions, the two sets of solitons leave each other totally and propagate in opposite directions, shown in Figs. 3.3.9 and 3.3.10 , while t = 4.5 and 7.0 respectively.

In the second case, we let these two initial half sine functions placing over $h_0 = 0.5$ have amplitudes differing by a factor of 10 : 0.05 and 0.5 , shown in Fig. 3.4.1, they are 220 grid points apart. Figs. 3.4.2 and 3.4.3 show the solitons in h and u at t = 2.0 , before collision; Figs 3.4.4 - 3.4.7 give the pictures of series collisions in h and u between the two sets of solitons at time t = 3.0 and t = 4.0 ; at t = 5.0 , the two sets of solitons (in h and u) totally split and propagate to the opposite directions, shown in Figs. 3.4.8 and 3.4.9.

When the two single solitons propagate in the same

direction, then collide, the situation is even more interesting. We have worked on two cases: in the first one, amplitudes of initial humps are 0.27 and 0.82 and in the second, they are 0.58 and 0.82 . The initial humps are 20 grid points apart.

The two initial humps of amplitudes 0.27 and 0.82 were given at t = 0 . The amplitudes of solitons formed afterwards are 0.26 and 0.94 . So the ratio between amplitudes of two initial humps is 3.03 and the ratio between amplitudes of two solitons is 3.6 . Since the soliton with bigger amplitude has a higher speed, it soon catches up the soliton with smaller amplitude (lower speed). At t = 1.32 , they start to overlap and the "joint" peak a = 0.835 is at x = 6.275 . As time goes on, this joint amplitude a soon decays to its minimum value 0.720 at x = 6.05 and t = 1.458 , after passing this point, this peak increases to 0.851 at x = 5.825 and t = 1.600 , then splits into two single solitons of amplitudes 0.854 (at x = 5.825) and 0.279 (at x = 5.925) at time t = 1.602 . The minimum of "joint" amplitude is smaller than the sum of two original soliton amplitudes: 0.720 < 0.94 + 0.26 = 1.20 . The whole overlap time period is 0.28 . After collision, the solitons will soon restore to their original shapes. This collision process is exhibited in Figs. 3.5.1 - 3.5.5: the first two figures show the solitons at t = 0.5 and t = 1.0, these two solitons are getting in touch that is shown

in the latter; the overlap of solitons at t = 1.5 is shown in Fig. 3.5.3; Figs. 3.5.4 and 3.5.5 show that the solitons leave each other at t = 2.0 and t = 2.5 .

When the two initial humps with amplitudes of 0.58 and 0.82 are given at t = 0, the solitons will be formed with amplitudes 0.61 and 0.91 later. The ratio of amplitudes for a pair of initial humps is 1.52 and the ratio of a pair of soliton amplitudes is 1.51 . The fast moving soliton gradually gets closer to the slow moving one, and their amplitudes gradually get closer too. Until t = 3.633 , the two solitons of amplitudes 0.682 and 0.686 are located at x = 2.975 and x = 3.075 , they are 3 grid points apart. From time t = 3.635 to t = 3.642, these two solitons of very close amplitudes are trying to exchange their positions instead of overlapping, till t = 2.362 , this exchange process finishes and the peak of 0.690 locates at x = 2.975 and the peak of 0.677 locates at x = 3.075 . So the switching time for these two solitons is 0.0167 . Then these two solitons keep propagate in the same direction and restore to their original shapes gradually.

The results of collision of solitons traveling in the same direction are similar to the results from KdV equation [20].

Now we can clearly see the difference between two different types of collisions. When the solitons travel in the same direction and collide, if the amplitude ratio of the

solitons (just steadily formed, that is way before collision) is ~ 3.6 , the two solitons overlap and the "joint" amplitude gradually decreases to its minimum which is much smaller than the sum of the two original soliton amplitudes, after passing through this minimum value, it increases and then the two solitons split and leave each other totally; if the soliton amplitude ratio is ~ 1.51 , these two solitons although catch up with each other, but they will never overlap, instead, they try very hard to switch their peaks, after a moment (~0.0167), two solitons indeed exchange their positions, the soliton of bigger amplitude becomes the leading soliton. Around the switching period, the soliton amplitudes are very close to each other. For the head-on collision, no matter what soliton amplitude ratio is, when a pair of solitons collide, they overlap and the "joint" amplitude increases till its maximum which is much bigger than the sum of two original amplitudes, then it decreases and finally split.

In [7], for the KdV equation, Lax gave a theoretical criterion for the collision of solitons traveling in the same direction: if the ratio of two solitons is less than 2.62 , these two solitons will exchange their positions instead of overlapping while they collide; if the ratio of this pair of solitons is bigger than 2.62 , then they will overlap while they collide. Our numerical results for the Boussinesq equation fit that criterion very well. Hirota et al [13] had

similar results for a different type of Boussinesq equation (1.11).

4.2.3). Soliton reflection at left boundary

Soliton reflection essentially should be the same as the head-on collision of two identical solitons. We work on two cases: (1) a single left going soliton reflecting at the left boundary; (2) two solitons in sequence reflect at the left boundary. In the latter case, after the first one reflects, it will collide with the second one which is still traveling to the left but not hits the wall yet.

Figs. 4.1.1 - 4.1.4 show the whole reflection process of a single soliton. A soliton of amplitude 0.94 starts to hit the left boundary at t = 3.59. The amplitude at left boundary at this moment is 1.12 , then it gradually reaches it maximum 1.68 at t = 3.61. Soon after this moment, this soliton starts to move to the right and leaves boundary slowly. Its amplitude at the boundary decays to 0.99 while t = 3.64 . When t = 3.67, the reflected soliton first time appears at the third grid. The time period for the soliton negotiating with the boundary is 0.053 . The amplitude of the reflected soliton finally reaches 0.67 which is much lower than its original amplitude.

We also let two solitons travel to the left, one follows the other. Their amplitudes are $a_1 = 0.14$ and $a_2 = 0.056$. From the Figs.4.2.1 - 4.2.4, we can see: the first soliton hits the left boundary at $t = 4.81$ with amplitude 0.1961, then it grows until that its amplitude gets to $a = 0.2765$ at $t = 4.85$; when the second soliton hits $x = 0$ at $t = 5.20$, its maximum amplitude is $a_2 = 0.1095$. After the first soliton reflects at boundary, it meets the second soliton at $x = 0.175$ while $t = 5.02$, their joint amplitude is 0.1900 which is little smaller than the sum of the two individual amplitudes. After both solitons reflect from the left boundary, their amplitudes are little lower than before: $a_1 = 0.13$ and $a_2 = 0.049$.

From the results of head-on collision, we know that the joint amplitude should be much bigger than the sum of two original amplitudes, and after collision, the solitons should restore to their original stages without losing their identities. In our cases, some how the situations are little different. While a single soliton hits the boundary, its maximum amplitude 1.68 is lower than the double of its amplitude ~ 1.88. For the case (2), the solitons collide after one reflected, their maximum joint amplitude is lower than the sum of the two individual amplitudes. Finally, after

reflection, soliton cannot restore to its original amplitude. It looks to us that there is some energy lose during the reflection.

A possible explanations we can give is that our numerical scheme closed to the boundary area is not too perfect. The characteristics method being used in this thesis already is a very approximate method, especially the local characteristics method used for the reflection problem. After reflection, a lot of noise has been brought in, and they take some energy away, so the solitons cannot get back to the amplitudes they have before the collisions. This phenomenon can be clearly observed from Figs. 4.1.4 and 4.2.4.

4.2.4). Boundary induced soliton in Boussinesq equation

As the same as the KdV equation, we also got solitons induced by suitable boundary conditions.

For the problem of soliton induced by a fixed boundary value, at the beginning, we thought we would get similar pictures as Fig. 1.5.1; in fact, what we got is quite similar to the collisionless shocks shown in Fig. 1.5.2. That puzzled us for a very long time. We first thought that was due to unexpected strong viscosity effects which might be brought in by the numerical scheme, because certain viscosity is

necessary in order to form a collisionless shock. But eventually we found out that idea was wrong. What we have now are normal solitons although their amplitudes have "exponential like" envelopes. For the collisionless shock, the length and the amplitude of the shock are fixed, they do not change as the shock propagates. In our case, the length of the wave train gets longer and longer and the amplitude gets bigger as the soliton goes. This is one key distinguishable border between the soliton and collisionless shock. As time evolves, the amplitudes of solitons grow until the first born solitons get mature, then these mature solitons propagate stably and more and more solitons born later get mature in following. This is the other key difference from the collisionless shock.

If we let the preset boundary be $h_b = 1.1$, the process of forming solitons is shown in Figs. 5.1.1 - 5.1.5 which cover the time period from $t = 1.0$ to $t = 18.0$. Among these pictures, Figs. 5.1.1 and 5.1.2 give the detail processes at $t = 1.0$ and $t = 2.0$ in the smaller domain $x = 0.0$ to $x = 4.0$. The Figs. 5.2.1 and 5.2.2 display the soliton forming at $t = 4.0$ and $t = 14.0$ while the boundary of the total water depth is preset at $h_b = 1.5$.

Figs. 5.1 and 5.2, especially Figs. 5.1.5 and 5.2.2, make us clearly see that since the ratios between the disturbance

amplitude and the unperturbed water level for these two sets of figures are different, the shapes of soliton envelopes are totally different, so as the solitons mature degrees: for a case of bigger ratio 0.5/1.0, at t = 14.0, a few solitons induced already reach their mature stages, but for the situation of smaller ratio 0.1/1.0, even at t = 18.0 , there is still no mature soliton being formed. This proves that: the ratio of perturbed amplitude and unperturbed water level is dominating the process of soliton maturing in the problem of boundary inducing solitons. Combining the results from KdV and Boussinesq equations, we can conclude that if this ratio is different, the shape of the soliton envelope is different; if this ratio is smaller, the soliton maturing time needed is very long; if it is bigger, the soliton maturing time is shorter; if this ratio approaches infinity, as the case exhibited in Fig 1.5.1, solitons will mature practically as soon as they are born.

The result of $h_0 = 0$ can not be obtained from the Boussinesq equation, because the unperturbed water level approaching zero cannot be handled by the Boussinesq model.

We then let the boundary $h_b(t)$ change periodically, such as a series of half sine function of period 0.5 and amplitude 0.05, placed over $h_0 = 0.5$. How solitons form and mature can be clearly observed that is very interesting, and

the results are displayed in Figs. 5.3.1 - 5.3.4. In Fig. 5.3.1, three solitons of first set start to form during the first time unit; at $t = 3.0$, the first set of solitons are getting close to the mature stage while the third set of solitons just start to appear; when $t = 5.0$, the first set of solitons are fully mature so as the leading soliton in the second set, and the leading soliton in the second set is slowly catching up the shortest soliton in the first set; in Fig. 5.3.4, the solitons born first are mature and start to line up according to their amplitudes.

We also let $h_b(t)$ change as one complete sine function first, then followed the fixed boundary value. The boundary sine function of amplitude 0.05 and period 0.5 is placed over $h_b = 0.55$ which is also the fixed boundary value followed. The unperturbed water level is $h_0 = 0.5$. In this case, generally speaking, solitons are come in as two groups: from the sine function and from the fixed boundary value. In Fig. 5.4.1 of $t = 1.0$, the solitons are just formed; in Figs. 5.4.2 - 5.4.6 which cover the period of $t = 2.0$ to $t = 16.0$, the solitons from the fixed boundary are gradually catch up and pass the solitons formed from the oscillation boundary and gradually mature.

4.3). Comparison between the results of Boussinesq and kdV equations

In section II. 3., we already explained the relationship between Boussinesq and KdV equations theoretically. When we numerically control solitons to propagate in one direction in Boussinesq equation, the results are almost identical with KdV solitons if same working conditions and numerical schemes are offered for both situations.

Here we explain these conditions again: fourth order schemes are used both for Boussinesq and KdV equations; $\beta = 0.000484$, $h_0 = 1.0$, $u_0 = 0.0$, so $\varepsilon = 0.00898$ (from (2.73)) and $\zeta_0 = 1.0$ correspondingly. The grids for both sets of equations are set up as: $\Delta x = 1/40$, $\Delta t = 1/600$.

Let us discuss the boundary excitation first. Through the transformation (2.74), if preset boundary $h_b = 1.1$ for Boussinesq equation, the preset boundary for KdV equation should be $\zeta_b = 1.15$. The numerical results for KdV equation shown in Figs. 1.8.1 and 1.8.2 almost are exactly the same as the results for Boussinesq equation shown in Figs. 5.1.1 and 5.1.2.

For the initial excitation situations, if the half sine

functions spreading over 20 grid points are offered to Boussinesq and KdV equations, the numerical results are displayed in Figs. 6.1.1. - 6.1.2 for Boussinesq equation while the amplitude of initial hump is taken as 0.1 and in Figs. 6.2.1. to 6.2.2 for KdV equation while the amplitude of initial hump is taken as 0.15 correspondingly. These two sets of solitons are almost identical, respectively.

Table 5 shows the comparison between single solitons obtained from KdV and Boussinesq equations. For both cases, the single soliton traveling to the right is induced by a narrow single hump whose amplitude for KdV case is 1.23

Table 5.

KdV case			Boussinesq case		
β	~ a	~ w	β	~ a	~ w
0.00000	1.3781	0.0529			
0.00408	1.3704	0.0767	0.000100	0.9549	0.0746
0.00707	1.3552	0.0820	0.000300	0.9457	0.0817
0.00818	1.3408	0.0850	0.000400	0.9237	0.0866
0.00898	1.3236	0.0879	0.000484	0.9149	0.0906

and that for Boussinesq case is 0.82 . Δx and Δt are chosen as 1/50 and 1/800 . Fourth order schemes are used. The relation between the amplitudes of solitons from KdV and Boussinesq equations are very close to the theoretical prediction (2.74), the difference is around 2%.

5. Few comments on the numerical schemes

The numerical results are very sensitive to the numerical scheme chosen. If the scheme is not suitable, we can not either avoid the numerical instability or get the correct results. When Chu's paper was worked out, nine months had been spent on the boundary numerical scheme. For the boundary induced soliton and soliton reflection problems of Boussinesq equation, we had spent five months on the boundary difference approximation. The schemes we used now are stable (within certain range of parameters), although they have not been proved to be so.

The numerical scheme is the difference approximation to the exact differential equation. When we use this scheme to do our calculation, a lot of numerical dispersive and dissipative terms actually have been brought into our calculation. These unexpected terms may greatly influence our final results if we

did not choose the scheme carefully. The typical examples are the situations of $\beta = \varepsilon = 0$ in the Boussinesq and KdV equations. The theoretical explanations of $\varepsilon=0$ for KdV equation was given by Lax in [17].

In the case of soliton stimulated by the pure initial conditions, if ε is taken to be zero, the key dispersive term disappears from the KdV equation. Thereby the soliton is not supposed to be formed. The only results we could get are weak solutions or shocks. A similar situation should occur in the Boussinesq equations when β is taken to be zero. But when we really did so, we actually got solitons no matter from KdV or from Boussinesq equations numerically. At the beginning, that surprised us very much. But when we looked into the difference schemes with great care, it is not strange any more.

We use the second order leap-frog approximation for the KdV equation as an example to describe this phenomenon. The numerical scheme for KdV equation is like:

$$\frac{\zeta_j^{n+1} - \zeta_j^{n-1}}{2\,\Delta t} + \frac{\zeta_{j-1}^n + \zeta_j^n + \zeta_{j+1}^n}{3}\left(\frac{\zeta_{j+1}^n - \zeta_{j-1}^n}{2\,\Delta x}\right)$$

$$+ \varepsilon^2 \frac{\zeta^n_{j+2} - 2\,\zeta^n_{j+1} + 2\,\zeta^n_{j-1} - 2\,\zeta^n_{j-2}}{2\,\Delta x^3} = 0$$

---------- (2.75)

After expansion in Taylor series, this difference equation approximates the differential equation

$$\zeta_t + \frac{1}{3!}\zeta_{3t}\,\Delta t^2 + \frac{1}{5!}\zeta_{5t}\,\Delta t^4 + \ldots$$

$$+ \zeta\zeta_x + \left(\frac{1}{6}\zeta\zeta_{3x} + \frac{1}{3}\zeta_x\,\zeta_{2x}\right)\Delta x^2 + \left(\frac{1}{18}\zeta_{2x}\,\zeta_{3x} + \ldots\right)\Delta x^4$$

$$+ \varepsilon^2\,\zeta_{3x} + \varepsilon^2\,\zeta_{5x}\,\Delta x^4 + \ldots = 0$$

---------- (2.76)

From this, we clearly can see that all the following terms

$$\zeta_{3x}\left\{\varepsilon^2 + \frac{1}{6}\zeta\,\Delta x^2 + \frac{1}{18}\zeta_{2x}\,\Delta x^4 + \ldots\right\}$$

---------- (2.77)

will contribute to the dispersive effect and all the terms as

$$\zeta_{2x}\left\{\frac{1}{3}\zeta_x\,\Delta x^2 + \frac{1}{18}\zeta_{3x}\,\Delta x^4 + \ldots\right\}$$

---------- (2.78)

will contribute to the dissipative effect. In other word, except the original form of the KdV equation, all terms of the rest part of (2.76) are brought in due to the difference approximation.

Let us compare two dispersive terms: the original term $\varepsilon^2 \zeta_{3x}$ and the additional term $\{(1/6)\ \zeta\ \Delta x^2\ \zeta_{3x}\}$. Since ε usually is taken as 0.022, the order of magnitude of ε^2 is about 5×10^{-4}. If Δx is chosen as $1/40$ and we assume the order of magnitude of ζ to be 1.0, $\Delta x^2/6$ is approximated to 1.04×10^{-4}. These two terms have the same order of magnitude. That is why even if we let ε to be zero in the KdV equation, there are still enough dispersive effects left, so we still can get solitons numerically. This result is shown in Figs. 7.1.1 - 7.1.2 for initial stimulation where besides $\varepsilon = 0.0$, $\Delta x = 1/40$, $\Delta t = 1/600$, $\zeta_0 = 0.0$, the initial condition is a half sine function of amplitude 1.0 , second order leap-frog scheme is used. The similar result for boundary stimulation is displayed in Figs. 7.2.1. - 7.2.2 where the boundary is preset to $\zeta_0 = 1.0$ and the rest are the same as for the initial stimulation.

If we change the numerical scheme for the term $\zeta\zeta_x$ to

$$\zeta_j^n \left(\frac{\zeta_{j+1}^n - \zeta_{j-1}^n}{2\,\Delta x} \right) \qquad \text{---------- (2.79)}$$

then the main dissipative term disappears from (2.78). The solitons will be formed but not too stable. Soon after t = 2.0, the calculation blows up. This result is displayed in Figs. 7.3.1 - 7.3.2. This missing dissipative term is impossible to compensate artificially.

When we deal with the second order numerical scheme of Boussinesq equation, as the same reason, the unexpected dispersive and viscosity terms are brought in. Besides the original dispersive term: $1/3\ \beta\ h_{3x}$, the other most important dispersive terms contributed by the scheme are $1/6\ \Delta x^2\ h_{3x}$ and $1/6\ \Delta x^2\ u\,u_{3x}$. If β is chosen as 0.022^2 , $\beta/3 \sim 1.6*10^{-4}$. If $\Delta x = 1/40$ and $u \sim 1.$, $\Delta x^2/6$ is approximated to $1.04*10^{-4}$. The orders of magnitudes of the coefficients in front of h_{3x} and u_{3x} are the same: 10^{-4} . So, it is quite clear that the solitons can be formed numerically even when β

is equal zero.

For the same physical problem, due to the reason explained, the results from numerical schemes of second order and fourth order accurate are different. We use KdV equation as our example. The result from second order accurate scheme is displayed in Figs. 7.4.1 - 7.4.2 and the result from fourth order accurate is exhibited in Figs. 7.5.1. - 7.5.2. The initial hump is a half sine function with amplitude 0.75 .

Analyzed the fourth order numerical scheme where $\zeta\zeta_x$ is written as

$$\frac{4}{3}\,\frac{\zeta^n_{j+1}+\zeta^n_j+\zeta^n_{j-1}}{3}\,\frac{\zeta^n_{j+1}-\zeta^n_{j-1}}{2\,\Delta x}-\frac{1}{3}\,\frac{\zeta^n_{j+2}-\zeta^n_{j-2}}{2\,(2\Delta x)}\,, \qquad (2.80)$$

the terms contributed to the dispersion are

$$\zeta_{3x}\,\{\,\varepsilon^2-\frac{2}{27}\,\zeta_{2x}\,\Delta x^4+\ldots\ldots\,\} \qquad (2.81)$$

The number of solitons formed from the second order scheme is 3 and from the fourth order scheme is 4. This is due to that the dispersive effect is much weaker in the fourth order scheme.

If we carefully select our numerical methods, both these

unexpected effects can be suppressed to certain extent to meet the needs of the problems.

III. Ion acoustic soliton

1. Physical model and derivation of Boussinesq-type equation

Various people have worked on ion acoustic solitary waves induced by initial excitation theoretically and experimentally. For theoretical simplicity, they neglected boundary conditions which actually might be very important. Many physical cases indeed lead to this type of problem. But no one had studied the ion acoustic solitary waves from the point of view of the boundary - initial excitation. That is why it is also our main concern in this part of the thesis.

First, we like to exhibit the basic two fluid equations for plasma and their working conditions; we explain how the ion acoustic wave is derived from them and show their solitary wave nature by deriving the Boussinesq-type equations from them. Then we will set up the dimensionless equations and suitable boundary - initial conditions for our boundary induced ion acoustic soliton problem.

1.1). Two fluid equations and ion acoustic waves

We will deal with the two component plasma without external magnetic field. The necessary condition of existence

for the ion acoustic wave: $T_e >> T_i$ still holds for the ion acoustic soliton, otherwise, Landau damping will prevent the formation of the ion acoustic wave. Since we choose the cold ion plasma approximation, T_i is taken as zero. Long wave approximation, $k\lambda_{De} << 1$, is considered, where λ_{De} is the electron Debye shielding length. We shall be only interested in one dimensional case.

The standard two fluid equations are our starting point. The equations of continuity and momentum and the equations of states for both ion and electron are as follows:

for ion:

$$\frac{\partial n_i}{\partial t} + \frac{\partial n_i u_i}{\partial x} = 0 \qquad \text{---------- (3. 1)}$$

$$\frac{\partial u_i}{\partial t} + u_i \frac{\partial u_i}{\partial x} = - \frac{e n_i}{m_i n_i} \frac{\partial \phi}{\partial x} - \frac{1}{m_i n_i} \frac{\partial P_i}{\partial x} \qquad \text{---------- (3. 2)}$$

$$P_i = n_i K T_i = 0 \qquad (T_i = 0) \qquad \text{---------- (3. 3)}$$

for electron:

$$\frac{\partial n_e}{\partial t} + \frac{\partial n_e u_e}{\partial x} = 0$$

---------- (3. 4)

$$\frac{\partial u_e}{\partial t} + u_e \frac{\partial u_e}{\partial x} = \frac{e n_e}{m_e n_e} \frac{\partial \phi}{\partial x} - \frac{1}{m_e n_e} \frac{\partial P_e}{\partial x}$$

---------- (3. 5)

$$P_e = n_e \kappa T_e$$

---------- (3. 6)

Poisson equation

$$\frac{\partial^2 \phi}{\partial x^2} = - 4 \pi e \ (n_i - n_e)$$

---------- (3. 7)

where the notations are conventional: n, m, u, P and T stand for density, mass, velocity, pressure and temperature; ϕ for electric potential, e for electron charge; subscripts e and i stand for the spices of electron and ion; κ stands for Boltzmann constant.

Neglecting the inertia of electrons , (3. 5) and (3. 6) are combined as

$$\frac{e}{m_e} \frac{\partial \phi}{\partial x} - \frac{\kappa T_e}{m_e n_e} \frac{\partial n_e}{\partial x} = 0$$

---------- (3. 8)

from which we see that the electrons follow the Boltzmann distribution

$$n_e = n_0 \exp\left(\frac{e\phi}{\kappa T_e}\right) \qquad \text{---------- (3. 9)}$$

where n_0 is defined as the unperturbed density of plasma (same for ions and electrons) throughout this section.

The equations (3.1) - (3.3), (3.7), (3.8) govern the ion acoustic waves and ion acoustic solitons.

Through the following two aspects: to derive the wave equations and to get the dispersion relation, it is very easy to see that these equations govern the ion acoustic waves.

If we let $n_e = n_i = n$, then linearize the equations as

$$n = n_0 + n_1 + n_2 + \cdots\cdots \qquad (3.10)$$

$$u = u_0 + u_1 + u_2 + \cdots\cdots$$

$$= u_1 + u_2 + \cdots\cdots \qquad (u_0 = 0) \qquad (3.11)$$

where u_0 is unperturbed velocity of plasma assumed at rest, the equations become

$$\frac{\partial n_1}{\partial t} + n_0 \frac{\partial n_1}{\partial x} = 0$$

$$\frac{\partial u_1}{\partial t} = - \frac{e}{m_i} \frac{\partial \phi}{\partial x}$$

$$e\, n \frac{\partial \phi}{\partial x} - \kappa\, T_e \frac{\partial n_1}{\partial x} = 0$$

---------- (3.12)

Eliminating u_1 and ϕ from above equations, we can get the ion acoustic wave equation

$$\frac{\partial^2 n_1}{\partial t^2} - \frac{n_0}{n} c_s^2 \frac{\partial^2 n_1}{dx^2} = 0$$

If the equation is kept up to first order approximation, then

$$\frac{\partial^2 n_1}{\partial t^2} - c_s^2 \frac{\partial^2 n_1}{\partial x^2} = 0$$

---------- (3.13)

which is the wave equation with wave speed (the ion-acoustic speed)

$$c_s^2 = \frac{\kappa T_e}{m_i}$$

---------- (3.14)

If we linearize, then Fourier transform the whole equations (3. 1) - (3. 7) without letting $n_e = n_i = n$, but using the electron Boltzmann distribution and the condition $e\phi << \kappa T_e$, we get a set of equations for ions:

$$
\begin{aligned}
&- i\omega u_i = - \frac{e}{m_i} ik\phi \\
&- i\omega n_i + n_0 ik u_i = 0 \\
&- k^2\phi = - 4\pi e n_i + \frac{1}{\lambda_{De}^2}\phi
\end{aligned}
\qquad \text{----------} \quad (3.15)
$$

where

$$
\lambda_{De} = \sqrt{\frac{\kappa T_e}{4\pi n_0 e^2}}
$$

is the electron Debye length.

The dispersion relation for ion acoustic wave is as

$$
\omega^2 = \frac{k^2 c_s^2}{1 + k^2 \lambda_{De}^2}
\qquad \text{----------} \quad (3.16)
$$

For $k\lambda_{De} << 1$, we have again $\omega^2/k^2 = c_s^2$ for dispersionless waves.

substituting (3. 3) into (3. 2) and (3. 9) into (3. 7), we simplify the set of equations for ion further:

$$\frac{\partial n}{\partial t} + \frac{\partial (n u)}{\partial x} = 0 \qquad \text{---------- (3.17)}$$

$$\frac{\partial u}{\partial t} + u \frac{\partial u}{\partial x} = - \frac{e}{m} \frac{\partial \phi}{\partial x} \qquad \text{---------- (3.18)}$$

$$\frac{\partial^2 \phi}{\partial x^2} = 4\pi e \{ n_0 \exp(\frac{e\phi}{\kappa T_e}) - n \} \qquad \text{---------- (3.19)}$$

Henceforth, the subscript i is omitted, but all quantities used without subscript are understood to be the quantities for ion unless indicated specifically.

1.2). Ion acoustic solitons and Boussinesq equation

Many papers about solitary waves induced by the initial excitation were based upon this set of equations (3.17) -

(3.19). To study the solitary waves of this set of equations, Washimi and Taniuti [19] derived a KdV equation from them under the small parameter approximation and single direction propagation. Since the ion acoustic waves obtained from (3.13) are allowed to travel in two directions and the solitary waves traveling in two directions are essentially governed by the Boussinesq-type equations, we believe that the plasma two fluid equations should essentially relate to the Boussinesq-type equations. Under the first order approximation, indeed, we have derived such a set of equations.

The main principle to derive this Boussinesq equation is to try to eliminate the terms involved potential ϕ.

Since there is a small difference between the densities of electron and ion, we let:

$$n_e = n_0 \exp\left(\frac{e\phi}{\kappa T_e}\right)$$

$$= n_i + n'$$

$$= n + n' \qquad \text{----------} \quad (3.20)$$

where n' is a small deviation of n_e from n_i and we emphasize again that all the subscript for ion will be suppressed for simplicity.

substituting (3.20) into Poisson equation, (3. 7) becomes

$$\frac{\partial^2 \phi}{\partial x^2} = - 4\pi e n' \qquad (3.21)$$

From (3. 8), we can get

$$- \frac{e}{m} \frac{\partial \phi}{\partial x} = - \frac{c_s^2}{n_e} \frac{\partial n_e}{\partial x}$$

---------- (3.22)

Substitute (3.20) and (3.21) into the ion momentum equation (3. 2), then

$$\frac{\partial u}{\partial t} + u \frac{\partial u}{\partial x} = - \frac{e}{m} \frac{\partial \phi}{\partial x}$$

$$= - \frac{c_s^2}{n} \left[\frac{\partial n}{\partial x} - \frac{n'}{n} \frac{\partial n}{\partial x} + \frac{\partial n'}{\partial x} + \cdots\cdots \right]$$

---------- (3.23)

In order to find the derivative of n', we go through the Poisson equation (3.21) and get

$$\frac{\partial n'}{\partial x} = \frac{1}{4\pi e} \frac{\partial^3 \phi}{\partial x^3}$$

$$= \frac{\kappa T_e}{4\pi e^2} \frac{\partial^2}{\partial x^2} \left\{ \frac{1}{n} \left[\frac{\partial n}{\partial x} - \frac{n'}{n} \frac{\partial n}{\partial x} + \frac{\partial n'}{\partial x} + \cdots\cdots \right] \right\}$$

---------- (3.24)

substituting (3.24) into (3.23), we get

$$\frac{\partial u}{\partial t} + u \frac{\partial u}{\partial x} = - \frac{c_s^2}{n} \{1 - \frac{n'}{n}\} \frac{\partial n}{\partial x}$$

$$- \frac{c_s^2}{n} \frac{\kappa T_e}{4\pi e^2} \frac{\partial^2}{\partial x^2} \{ \frac{1}{n} [\frac{\partial n}{\partial x} - \frac{n'}{n} \frac{\partial n}{\partial x}] + \ldots\ldots \}$$

---------- (3.25)

If only zero order terms are kept, the equations for ions become:

$$\frac{\partial n}{\partial t} + \frac{\partial nu}{\partial x} = 0$$

---------- (3.26)

$$\frac{\partial u}{\partial t} + u \frac{\partial u}{\partial x} + \frac{c_s^2}{n} \frac{\partial n}{\partial x} + \frac{c_s^2}{n} \frac{\kappa T_e}{4\pi e^2} \frac{\partial^2}{\partial x^2} \{ \frac{1}{n} \frac{\partial n}{\partial x} \} = 0$$

---------- (3.27)

These are the Boussinesq-type equations for ion acoustic waves, from which solitons can be found.

If we linearize equations (3.26) and (3.27) by letting

$$n = n_0 + n" \qquad (3.28)$$

$$u = 0 + u" \qquad (3.29)$$

where n_0 is defined as before and there was no plasma flow. The superscript " means the first order approximation.

Linearizing this set of equations and Fourier transforming them, we again get the dispersion relation (3.16).

1.3). Physical model for boundary induced soliton

We now start to discuss our boundary induced ion acoustic soliton problem. We will build the dimensionless equations and set up the suitable boundary and initial conditions.

The plasma was prepared in the following way: it is in an infinite one-dimensional domain; the unperturbed density n_0 is a constant (same for ion and electron); u_0 is the average speed of plasma, if there was no plasma flow, u_0 is taken as zero; only one grid in the domain carries a small fixed potential ϕ_0 ; obviously, when $x \to \pm\infty$, $\phi(x,t) \to 0$.

For simplicity, we will start with equations (3.17) - (3.19) instead of the Boussinesq equations (3.26) and (3.27).

We choose λ_{De} , t_0 and c_s as our normalization standards, t_0 are defined as

$$t_0 = \frac{1}{\omega_{pi}} = \sqrt{\frac{m}{4\pi n_0 e^2}}$$

λ_{De} is the electron Debye shielding and c_s is the ion acoustic wave speed, as defined before, t_0 is the length of time during which ion travels an electron Debye length λ_{De} at c_s . c_s falls between the thermal velocities of ion and electron. For the electric potential ϕ , we normalize it according to the quantity Φ

$$\Phi = \frac{\kappa T_e}{e}$$

The density is normalized to n_0 .

Our dimensionless equations then look like

$$\frac{\partial n^*}{\partial t^*} + \frac{\partial n^* u^*}{\partial x^*} = 0 \qquad \text{---------- (3.30)}$$

$$\frac{\partial u^*}{\partial t^*} + u^* \frac{\partial u^*}{\partial x^*} = - \frac{\partial \phi^*}{\partial x^*} \qquad \text{---------- (3.31)}$$

$$\frac{\partial^2 \phi^*}{\partial x^{*2}} = \exp(\phi^*) - n^* \qquad \text{---------- (3.32)}$$

The boundary conditions are set up as:

for potential:

$$\phi \rightarrow 0, \qquad \text{as } x \rightarrow \pm \infty$$

$$\phi = \phi_0 \qquad \text{at } x = x_0$$

for density and velocity:

The boundary conditions are set up as:

$$n(x,t) = n_0 \qquad \text{as } x \rightarrow \pm \infty$$

$$u(x,t) = u_0 \qquad \text{as } x \rightarrow \pm \infty$$

The initial conditions are set up as:

$$n(x,0) = n_0$$

$$u(x,0) = u_0$$

The relation between u_0 and ϕ_0 should satisfy:

$$\frac{1}{2} m u_0^2 > e\phi_0$$

After normalization, these conditions become:

for boundary conditions:

$$\text{as } x \to \pm\infty \qquad \phi^* \to 0 \tag{3.33}$$

$$n^*(x,t) = 1.0 \tag{3.34}$$

$$u^*(x,t) = u^*_0 \tag{3.35}$$

$$\text{at } x = x_0 \qquad \phi^*(0,t) = \phi^*_0 \tag{3.36}$$

for initial conditions

$$n^*(x,0) = 1.0 \tag{3.37}$$

$$u^*(x,0) = u^*_0 \tag{3.38}$$

The relation between u_0 and ϕ_0 becomes:

$$\frac{1}{2} u_0^{*2} > \phi_0^* \tag{3.39}$$

In the following, the superscript * is omitted, all the quantities are understood to be dimensionless.

2. Numerical methods and results

For solving the first two equations (3.30) and (3.31), the

ordinary second order leap-frog numerical schemes are used.

Among these three equations, the Poisson equation (3.32) for potential should be calculated first. In the real physical situation, as mentioned before, the two boundaries are set up like: at $x = 0$, $\phi(0,t) = \phi_0$, (i. e. (3.36)); as x approaches infinity, ϕ approaches zero, (i. e. (3.33)). For the situation of the two fixed boundaries given, the shooting method is very usable. The essence of the shooting method is to change the two boundary condition problem into two initial condition problem. But when we tried this method in our case, we met great difficulties.

In numerical calculations, we have to use the finite domain instead of infinite one, so how to choose the condition artificially at outer finite boundary becomes crucial, in other words, the outer boundary is not exactly defined any more. By shooting method, we should pick up a trial function $\phi(x,0)$ for this finite domain to start with, in principle, after several shooting, we would get the numerical solution for the equation. We have used the exponential function as a trial function. The shooting method works well in the smaller domain, such as $5 \sim 6$ Debye lengths, but this small domain is not big enough for the ion acoustic soliton to be formed and to propagate. When we tried to work on a bigger domain,

the numerical instability was very hard to avoid. The reason is very clear: if we choose the outer boundary at around ten Debye lengths away, our trial function ϕ at that point is approximated to 10^{-8}; ϕ_0 at $x = 0$ is chosen to be less than 1.0 ; so in the shooting method, the amplification should be as high as $10^{7 \sim 8}$ which is very difficult to achieve in numerical calculation even if we use the quadruple precision computer.

To avoid this difficulty, we restrict ourself only in the situation of $\phi_0 << 1.0$. Under this small ϕ_0 approximation, we find out an integration solution of the Poisson equation,

$$\phi(x,t) = \phi(x_0,t)\ \exp(x_0 - x) - \int_x^\infty \frac{1 - n(\xi,t)}{2} \exp(x - \xi)\ d\xi$$

$$+ \int_{x_0}^\infty \frac{1 - n(\xi,t)}{2} \exp(2\,x_0 - \xi - x)\ d\xi$$

$$+ \int_{x_0}^x \frac{n(\xi,t) - 1}{2} \exp(- x + \xi)\ d\xi$$

---------- (3.40)

and use this solution in the rest of the calculation instead of solving the exact Poisson potential equation. In (3.37), x_0 is the position of the grid point where the potential barrier

is prescribed, in our case x_0 is taken at $x = 0$.

When the ion flow with certain kinetic energy passes over the potential grid, the ions will be expelled by the positive potential at this grid and run away very fast. Then very deep dips in potential and density are formed right after the grid and gradually get deeper and deeper until the calculation blows. This is another difficulty met in this problem. The main cause of this phenomenon is that we have not considered the dynamic behavior of the electrons (we assume that the electrons obey the Boltzmann distribution). In order of smoothing out this dip, we have added some artificial viscosity around the grid in the numerical scheme. That basically solved the problem and the typical numerical results are shown in Figs. 8.1.1 and 8.1.2.

Fig. 8.1.1 shows a typical solution $\phi(x)$ at some 600 time steps. Indeed, soliton like waves propagate both upstream and downstream of the grid. Unfortunately, due to adding the small amount of dissipation ($\upsilon = 0.4$) around the grid (four points on each side), soliton amplitudes are not the same any more. The density has the similar profile. The 'unavoided' dip behind the grid is clearly shown in the figure. Fig. 8.1.2 shows the ion velocity $u(x)$ at the same time. The spike in velocity behind the grid is the corresponding behavior to the

density cavity, already explained above. In this calculation, $\phi_0 = 0.05$, $u_0 = 0.4$. The numerical grids are set up as $\Delta x = 0.6$ and $\Delta t = 0.1$.

IV. Conclusion

In this conclusion, We emphasize again the major original contributions made in this thesis.

1. About the KDV equation: For the constant boundary condition, we extend the work into the finite (nonzero) unperturbed water level cases and point out that the ratio between the disturbance amplitude and the unperturbed water level determines the soliton maturing time.

When we deal with the unperturbed water level approaching zero and the time-dependent boundary conditions, the ratio between the time-scale of the boundary conditions and the soliton maturing period plays the key role in determining the envelop of solitons induced. The random boundary condition can also produce a series of 'constant amplitude' solitons as the constant boundary condition does.

2. About the Boussinesq equation: All the results of

solitons induced from the mixed boundary-initial conditions are the new developments in this area. Due to the advantage of Boussinesq equation over the KdV equation, the soliton reflection at boundary and solitons head-on collision are discussed for the first time. Because of the difficulty of treating the boundary conditions at a wall for the Boussinesq equation, the reflection results are less accurate but the collision results are very precise.

The results from two fully non-linear KdV and Boussinesq equations are compared for the first time, and agree extremely well.

3. About the ion acoustic solitons: For th efirst time,We derived a set of Boussinesq equations from the standard two fluid equations of the cold ion plasma. It theoretically proves the essential nature of solitary wave solutions of the cold ion plasma. The ion acoustic solitons induced by boundary condition are also obtained.

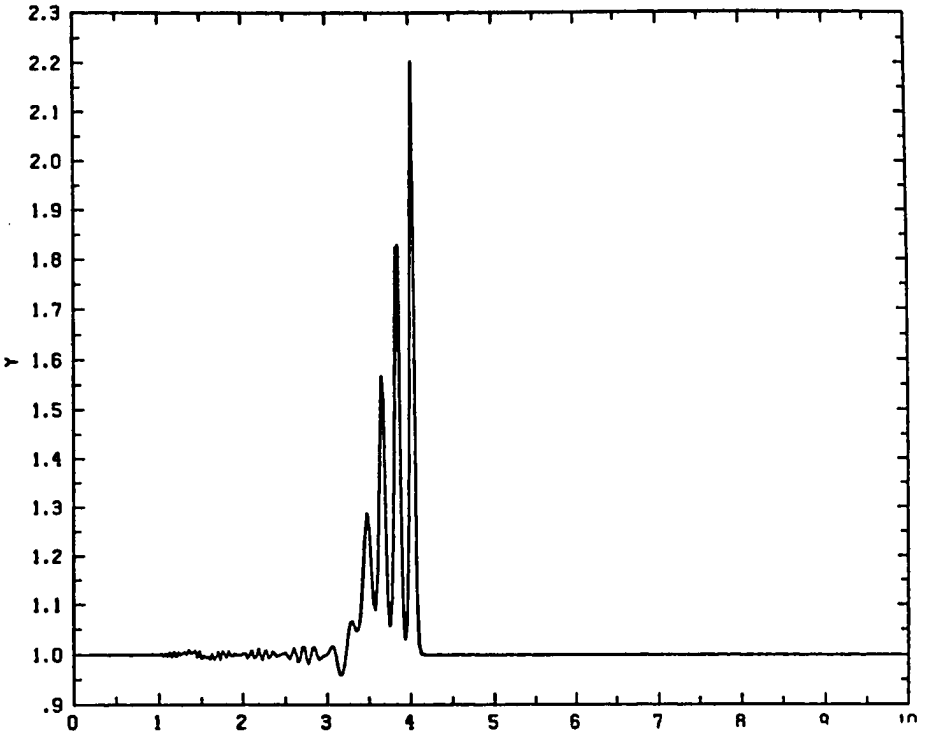

Fig. 1.1.1

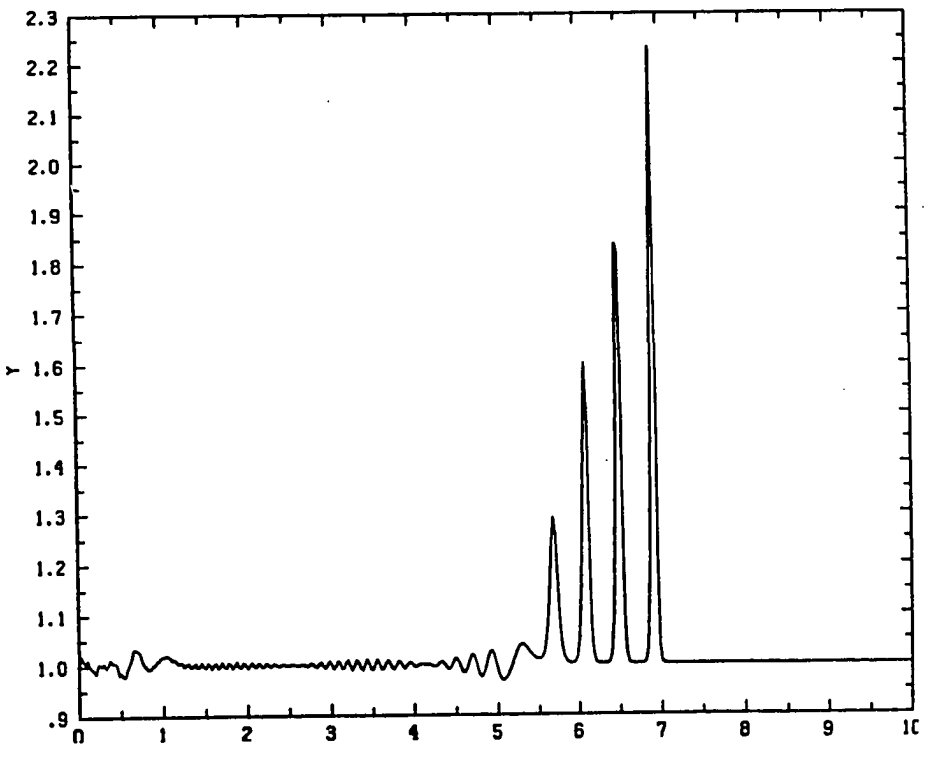

Fig. 1.1.2

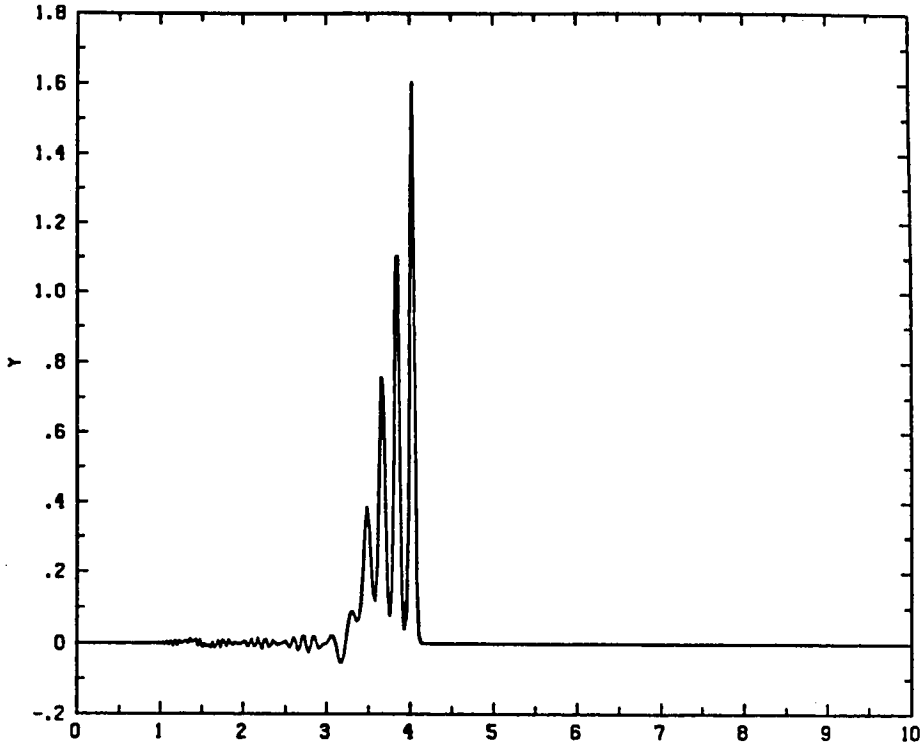

Fig. 1.1.3

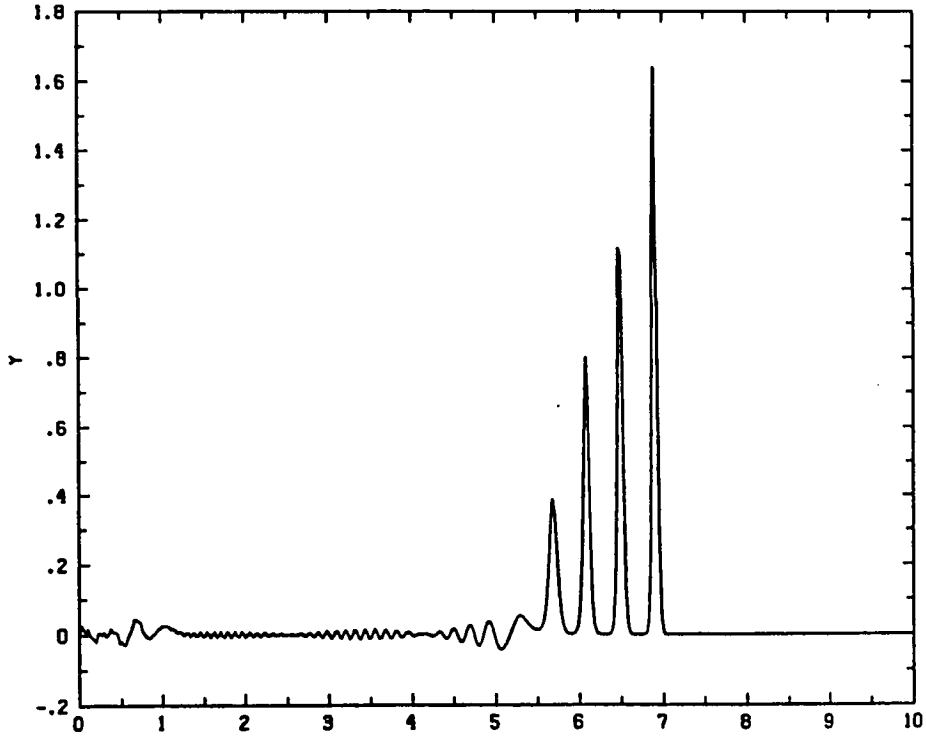

Fig. 1.1.4

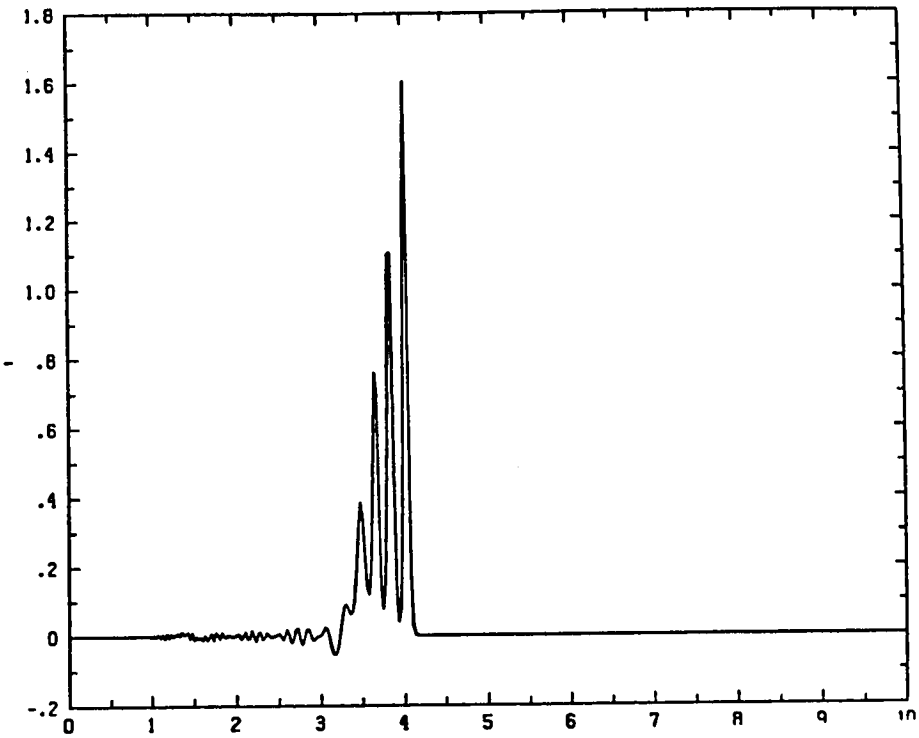

Fig. 1.2.1

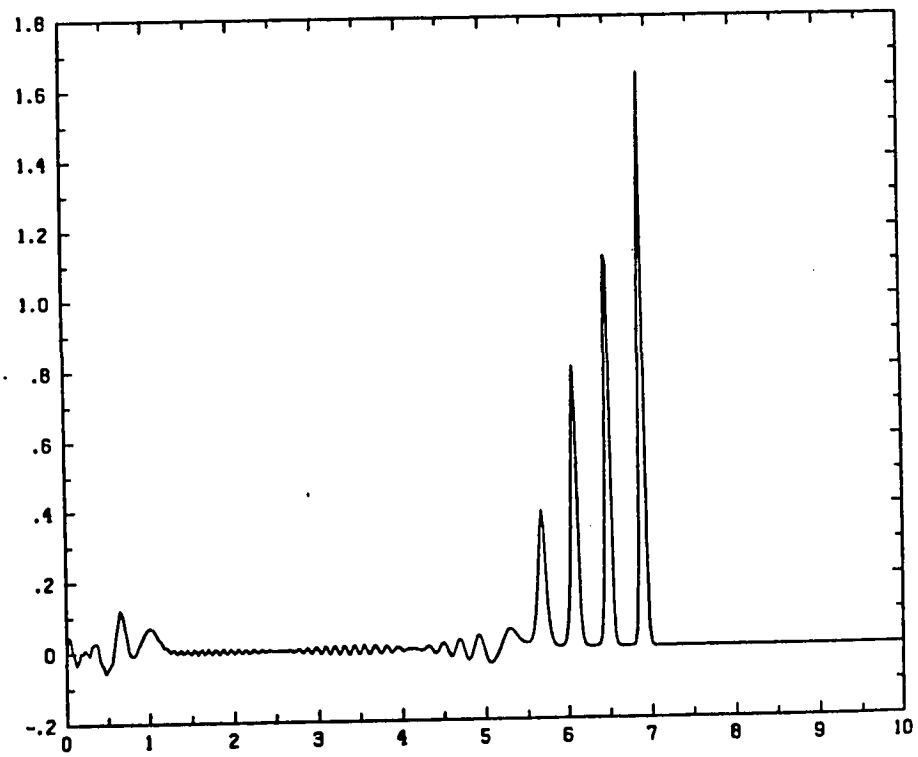

Fig. 1.2.2

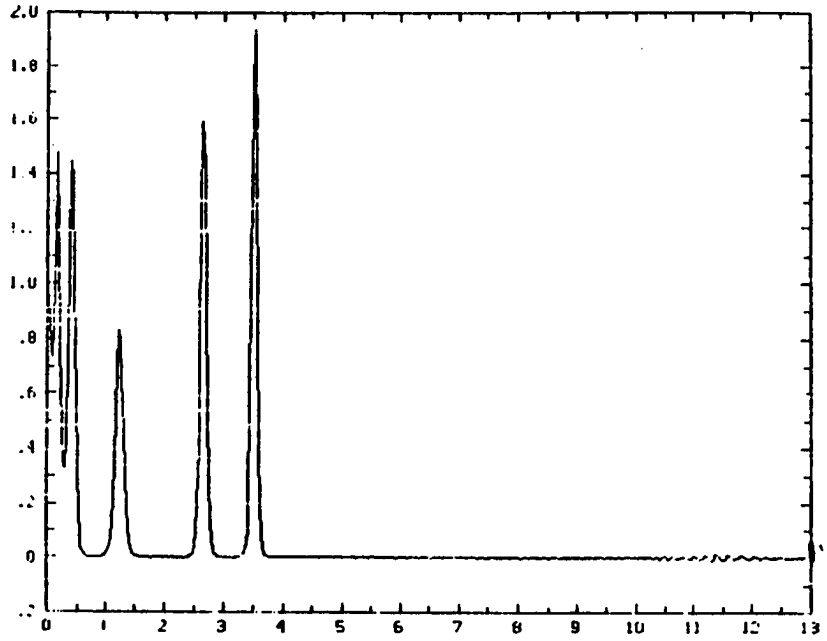

Fig. 1.3.1

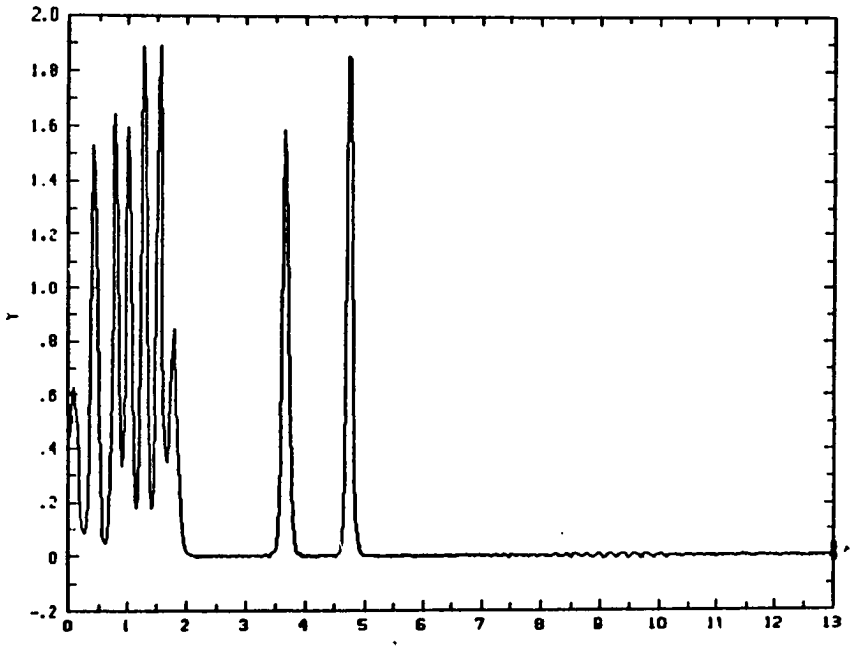

Fig. 1.3.2

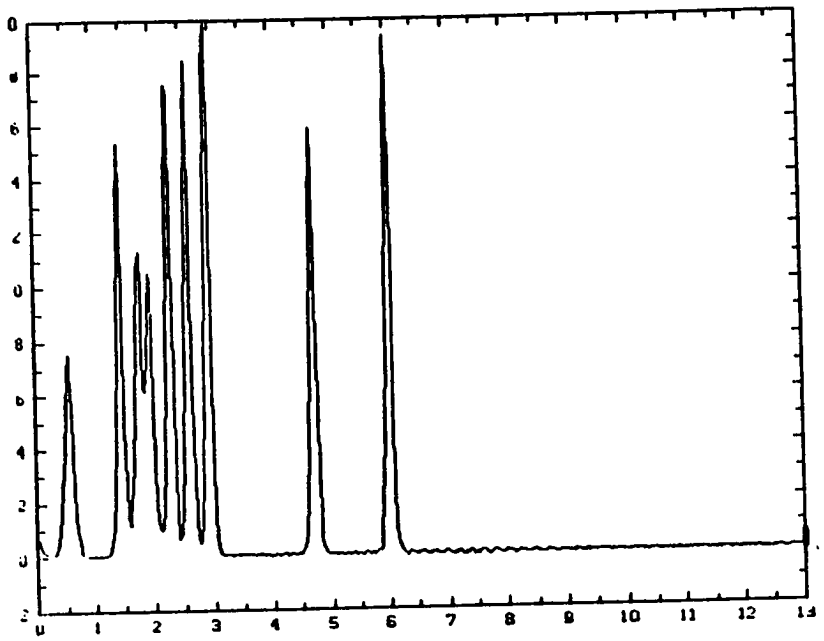

Fig. 1.3.3

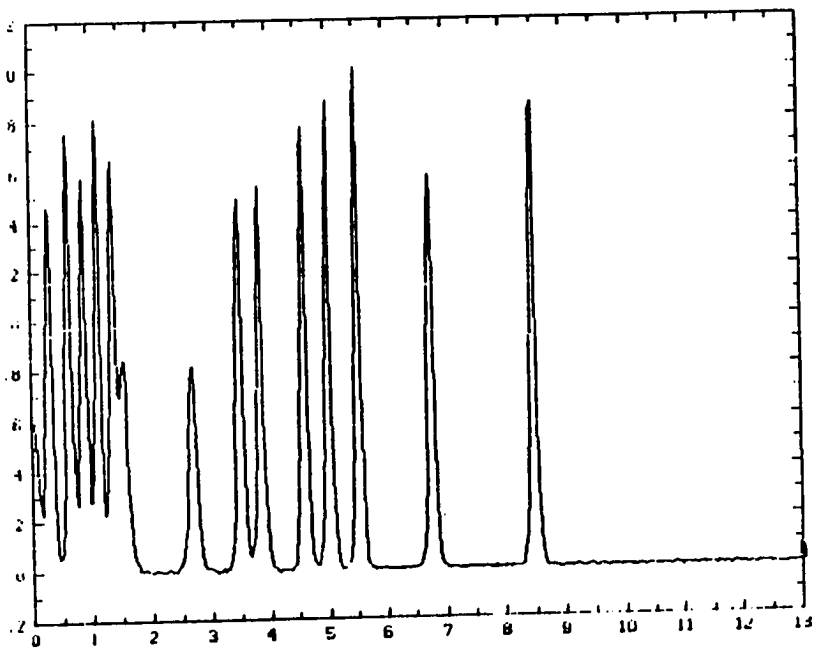

Fig. 1.3.4

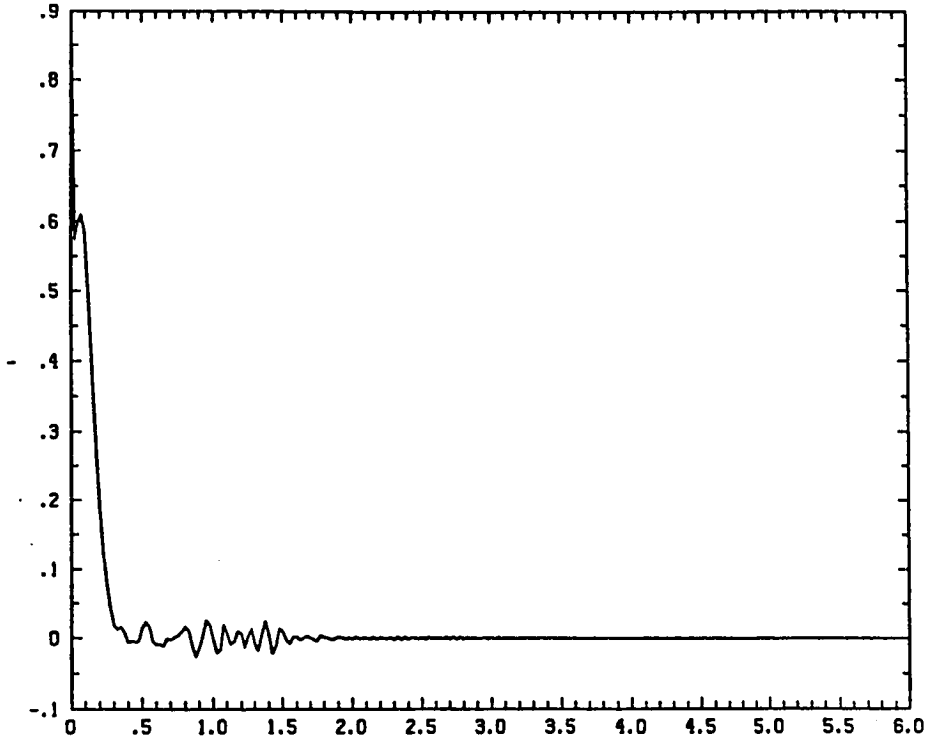

Fig. 1.4.1

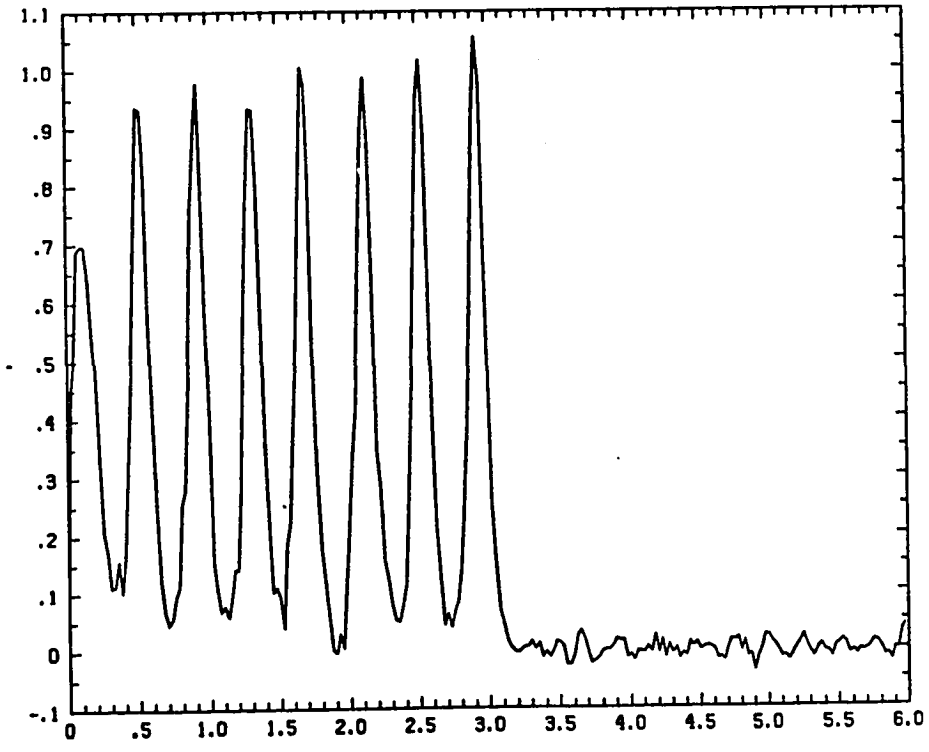

Fig. 1.4.2

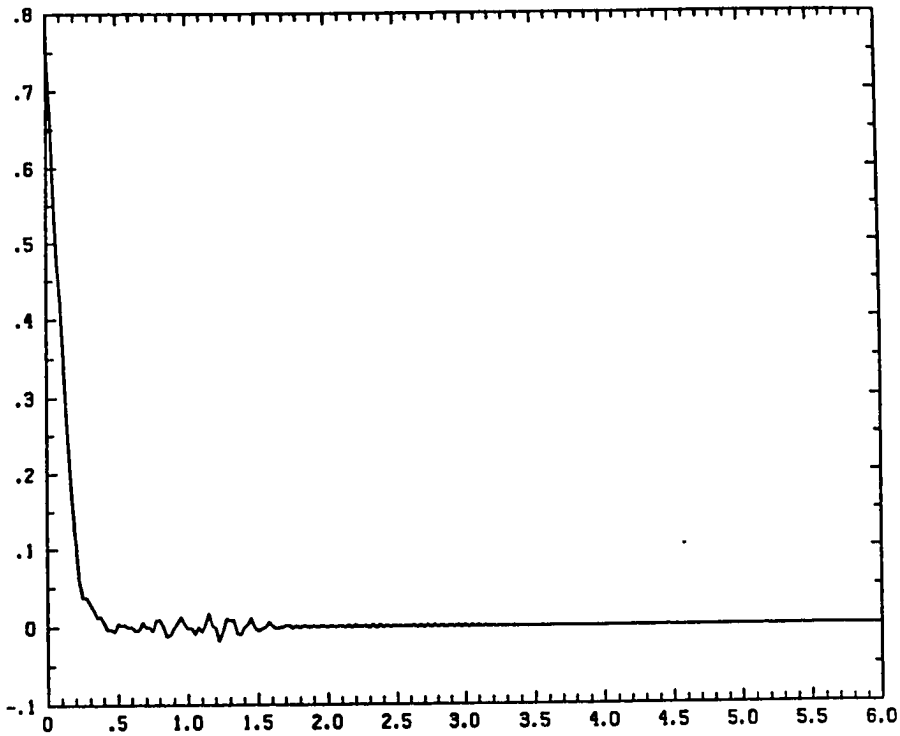

Fig. 1.4.3

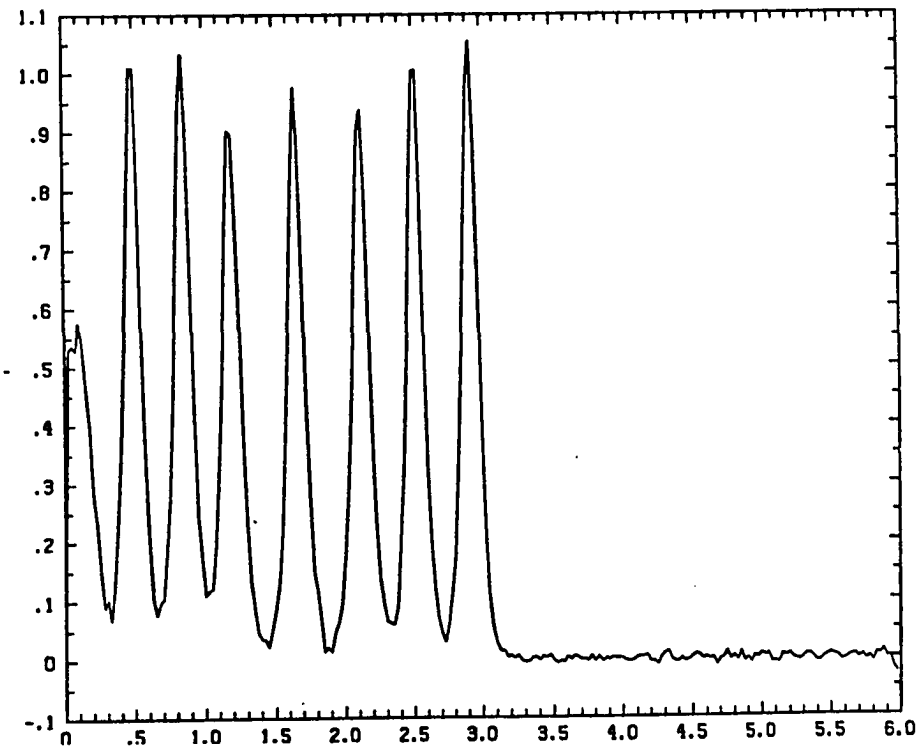

Fig. 1.4.4

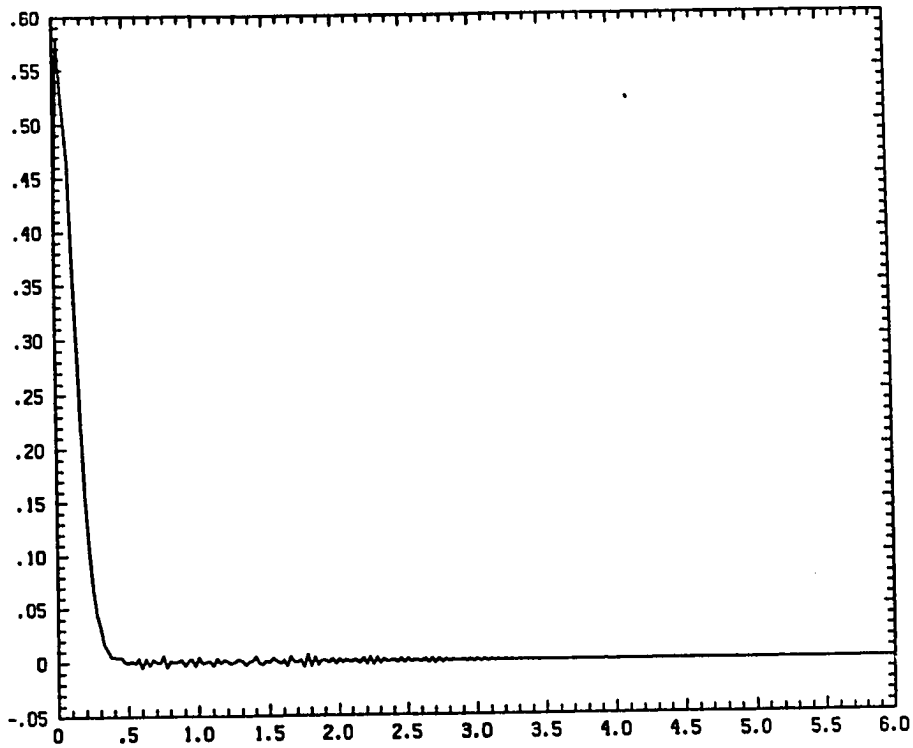

Fig. 1.4.5

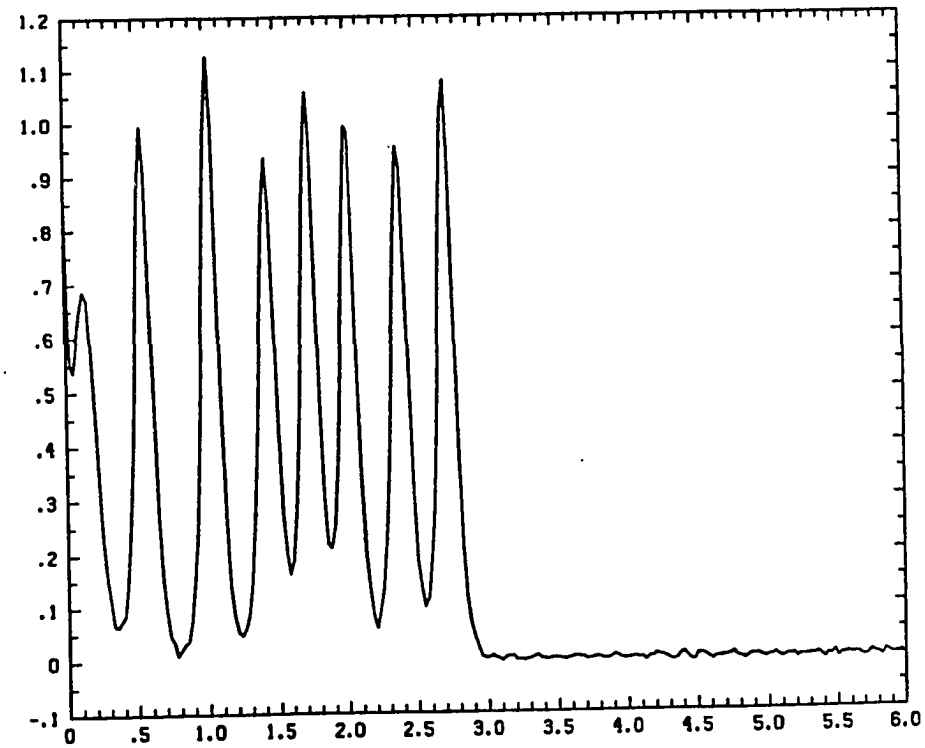

Fig. 1.4.6

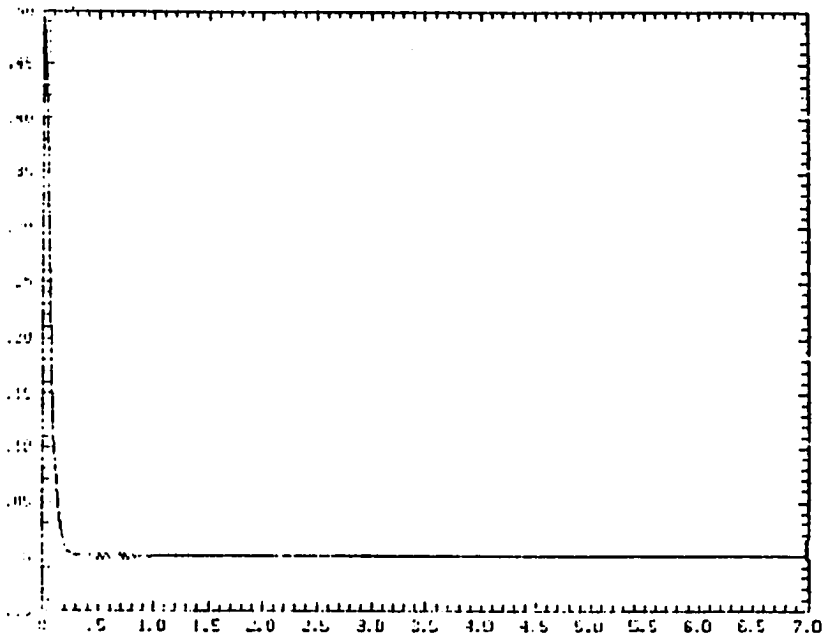

Fig. 1.4.7

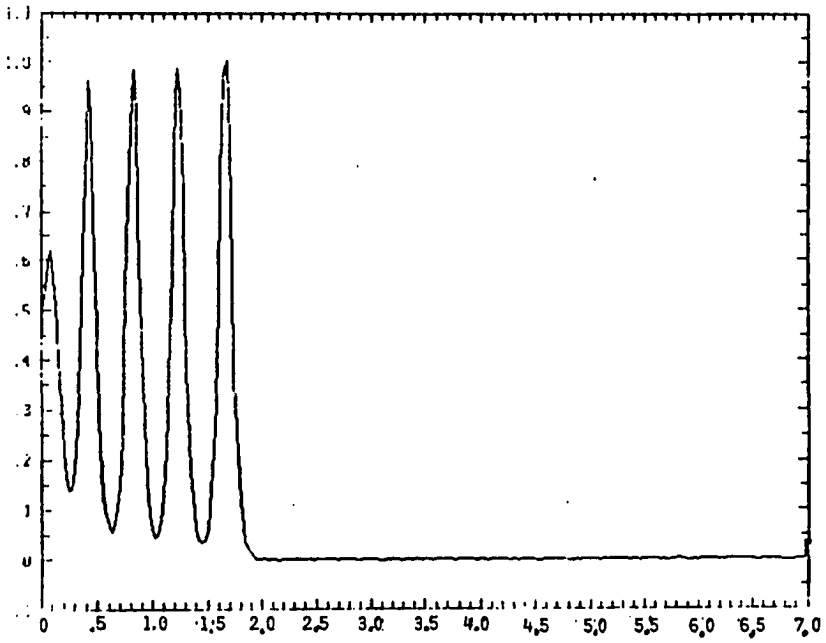

Fig. 1.4.8

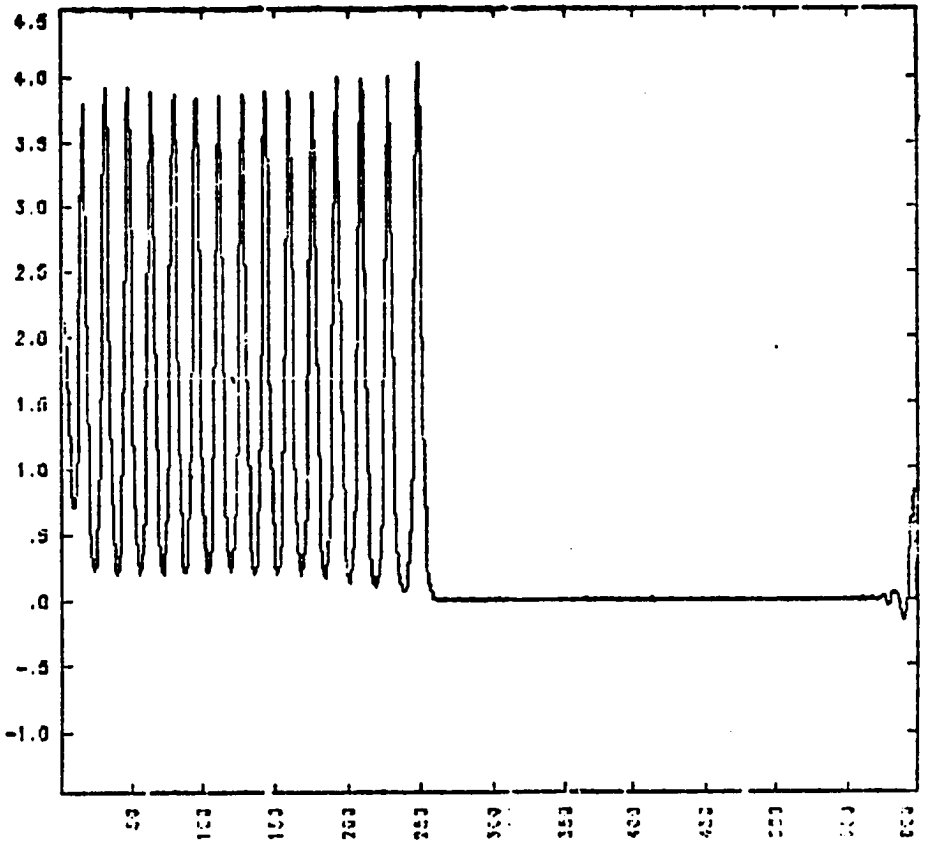

Fig. 1.5.1

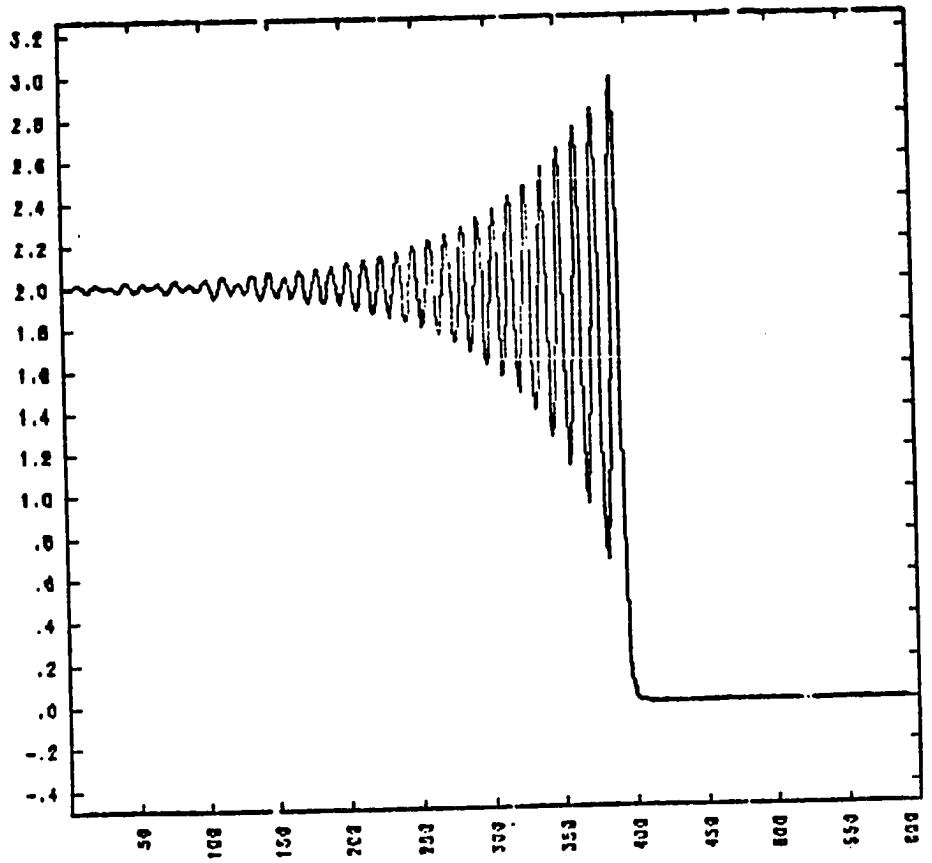

Fig. 1.5.2

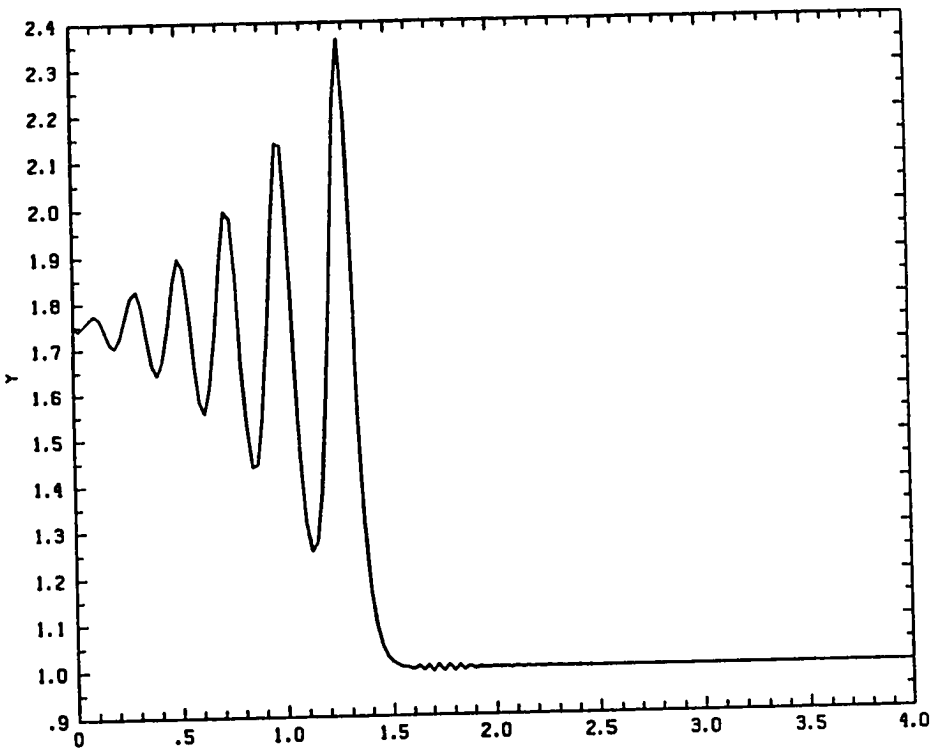

Fig. 1.6.1

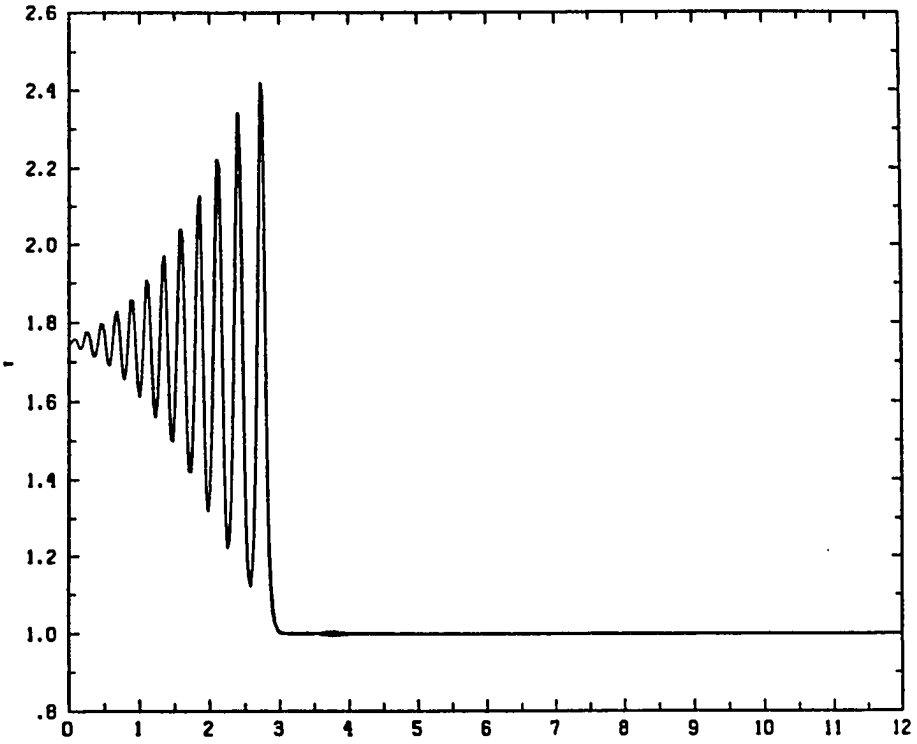

Fig. 1.6.2

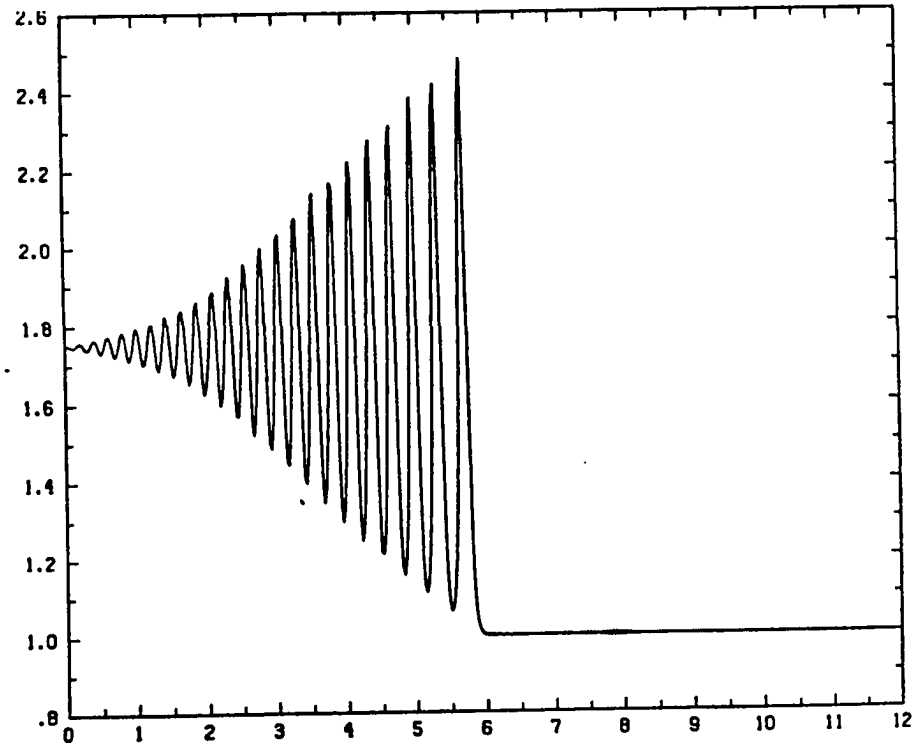

Fig. 1.6.3

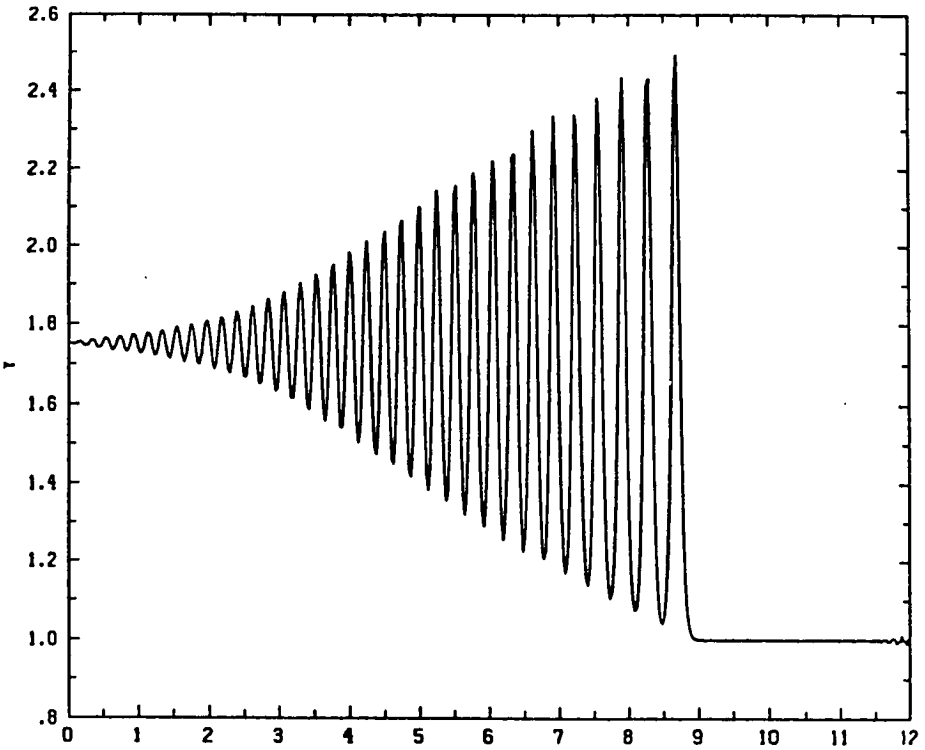

Fig. 1.6.4

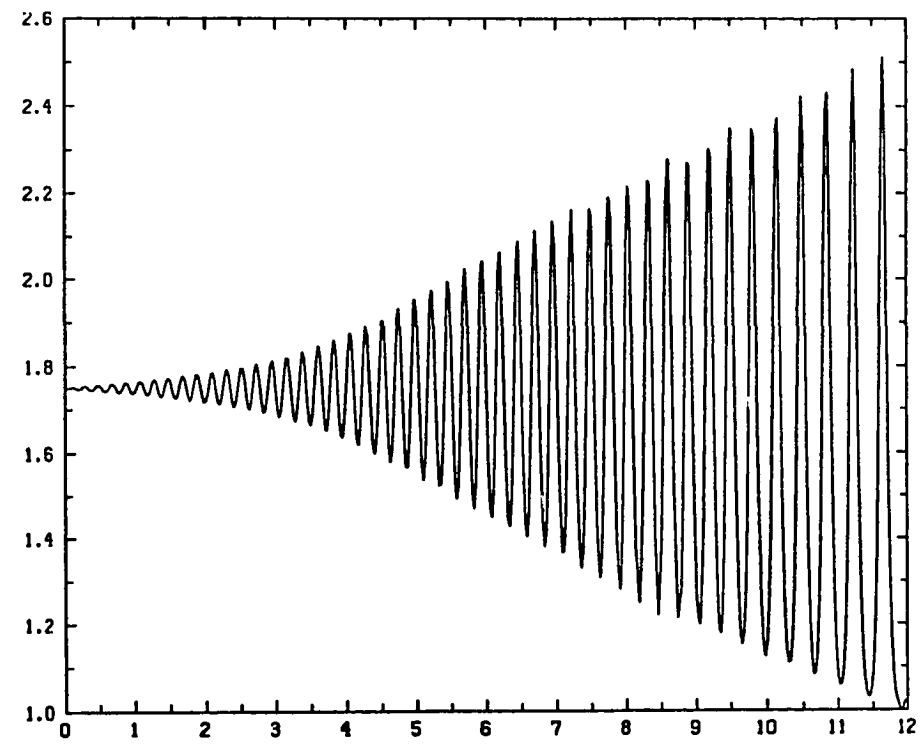

Fig. 1.6.5

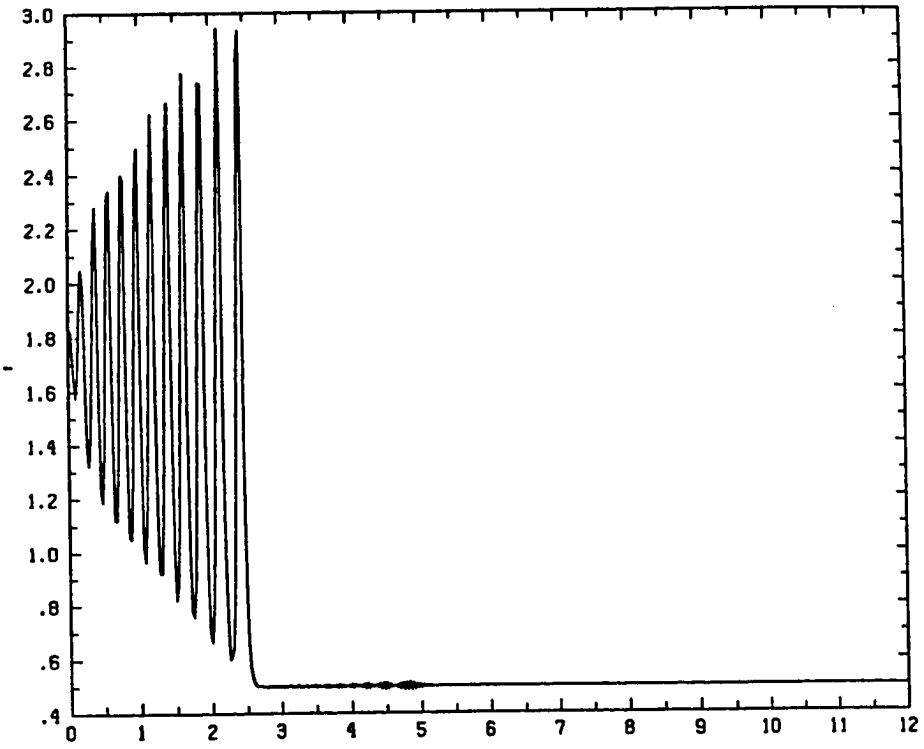

Fig. 1.7.1

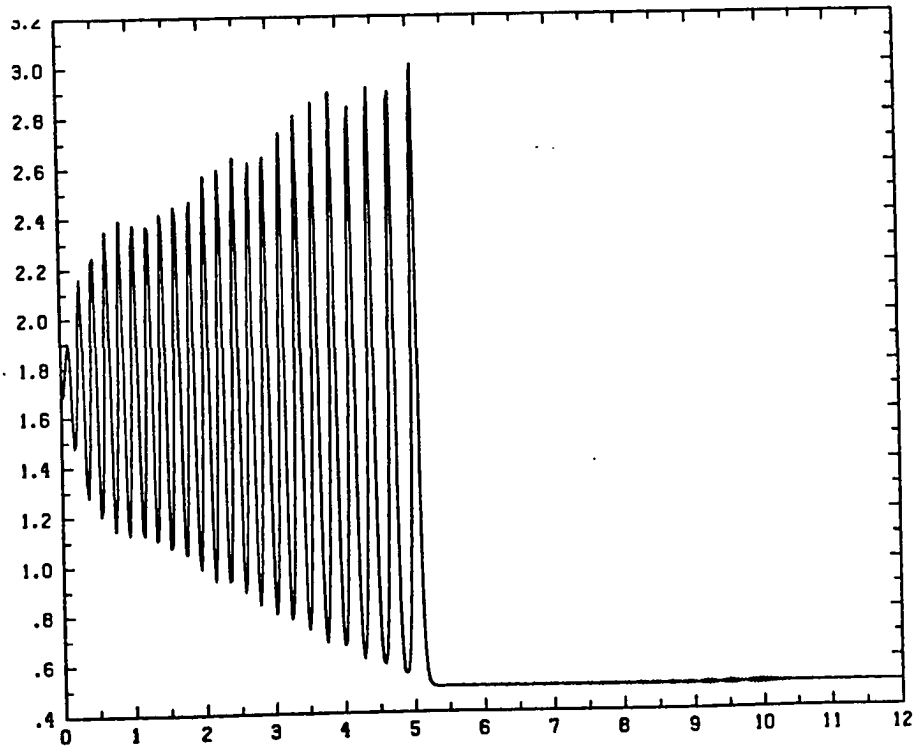

Fig. 1.7.2

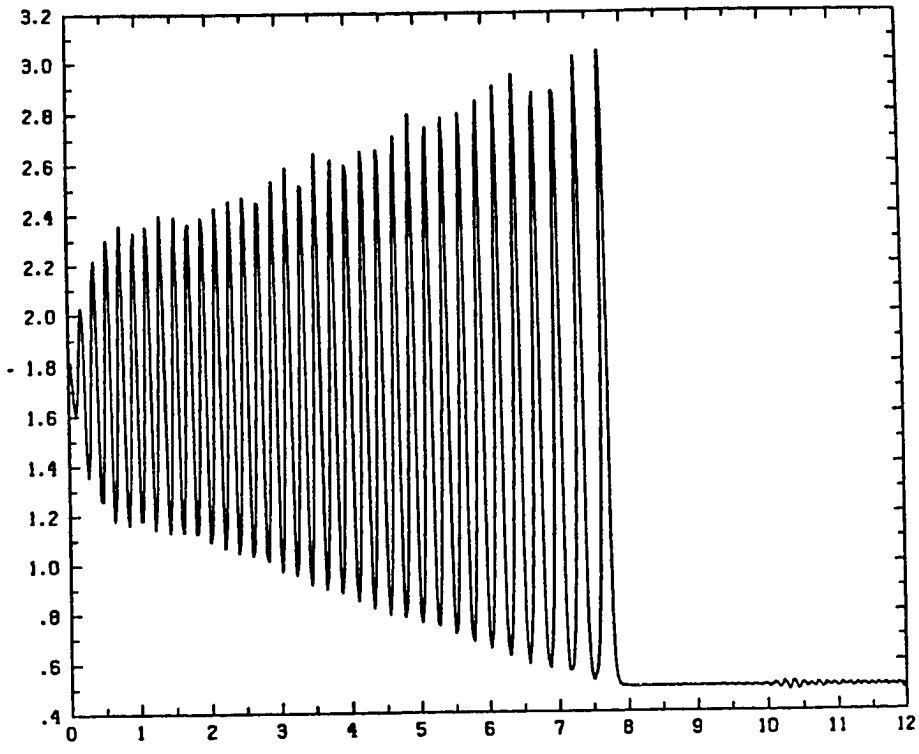

Fig. 1.7.3

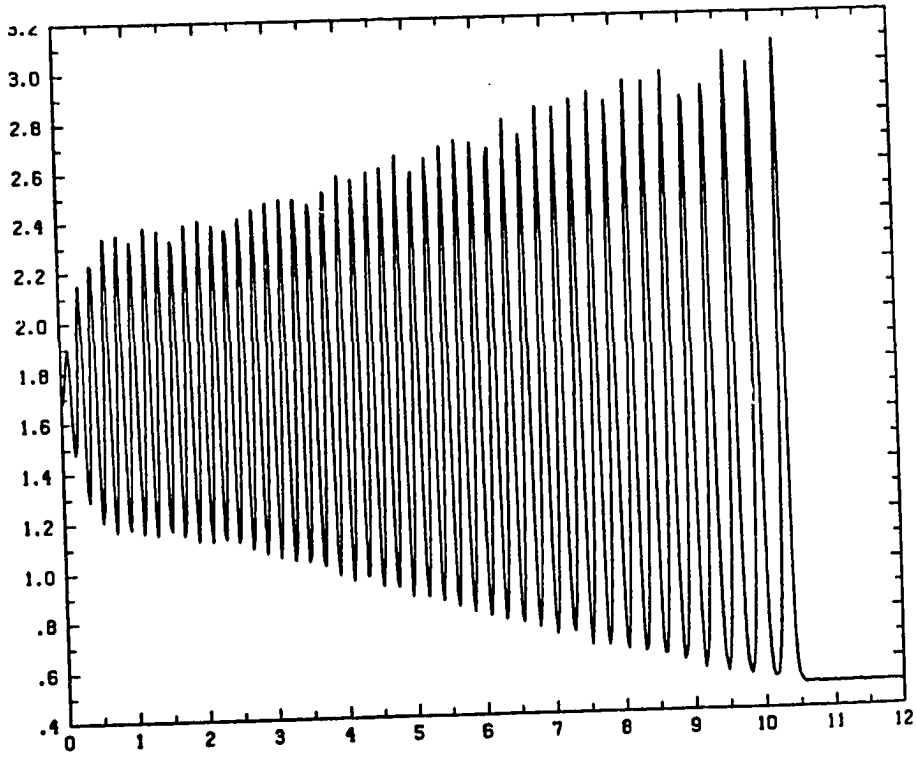

Fig. 1.7.4

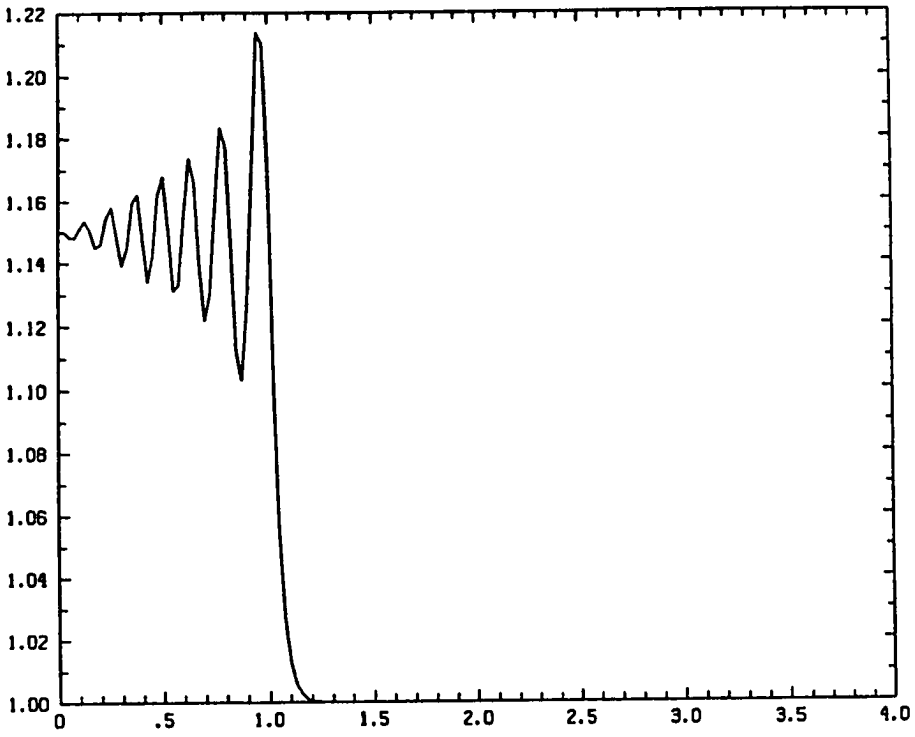

Fig. 1.8.1

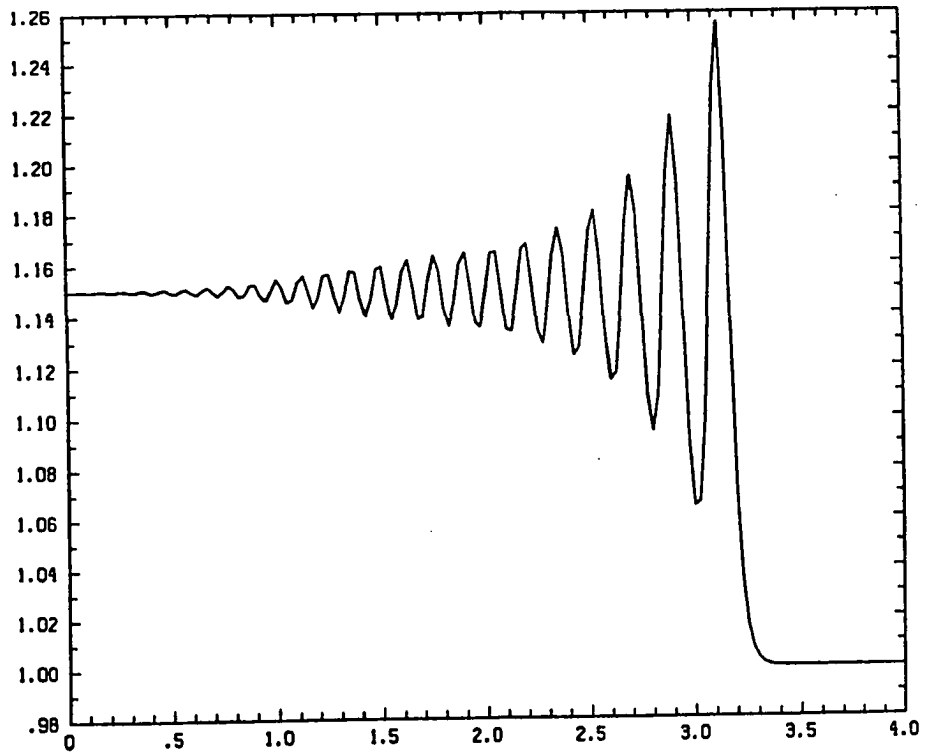

Fig. 1.8.2

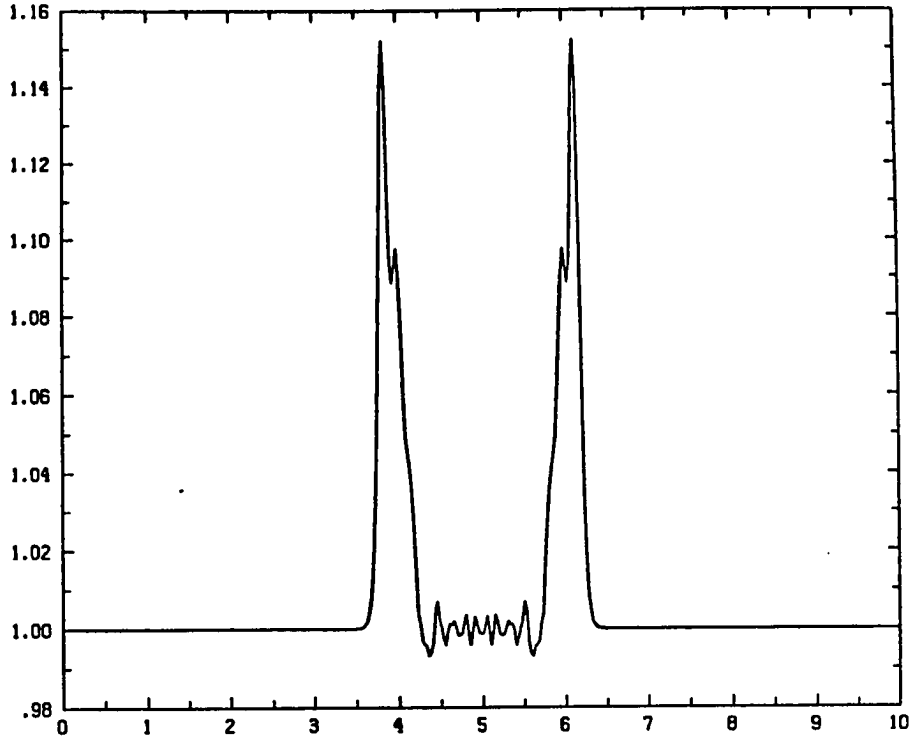

Fig. 2.1.1

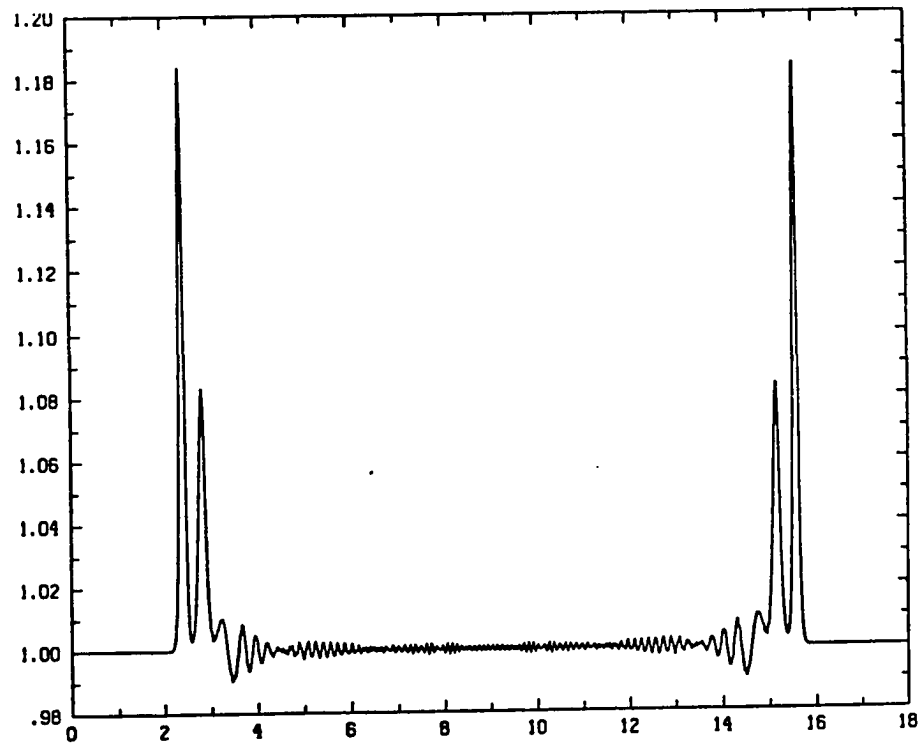

Fig. 2.1.2

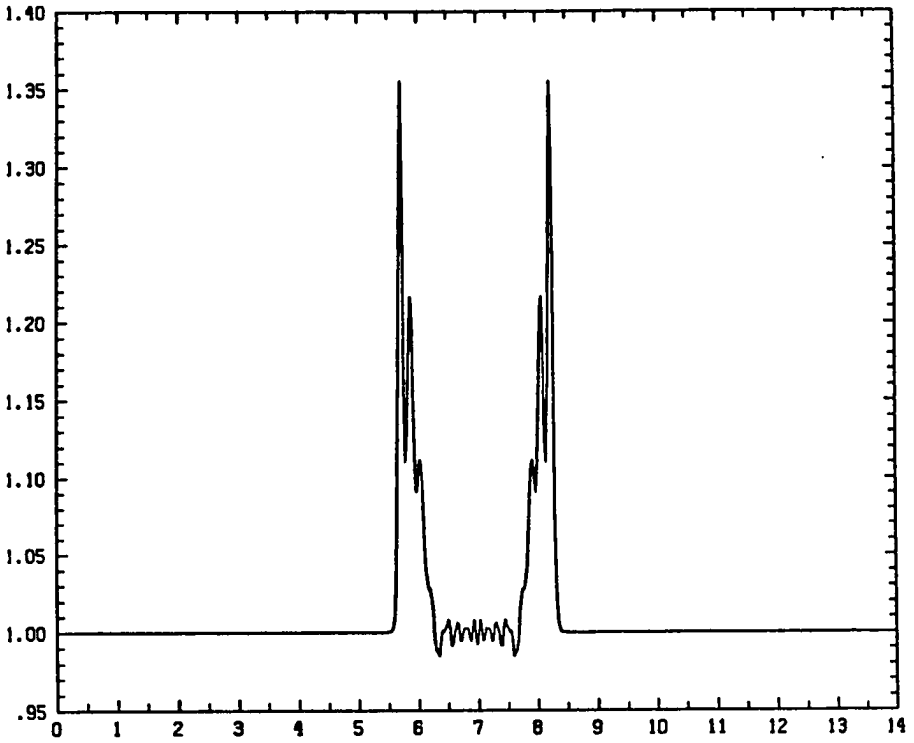

Fig. 2.1.3

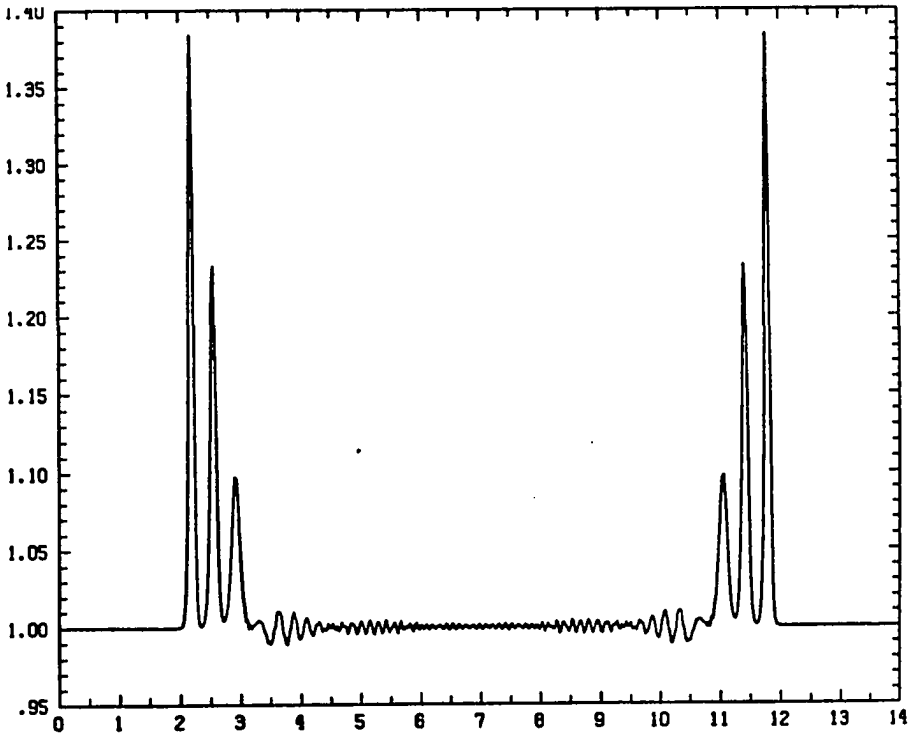

Fig. 2.1.4

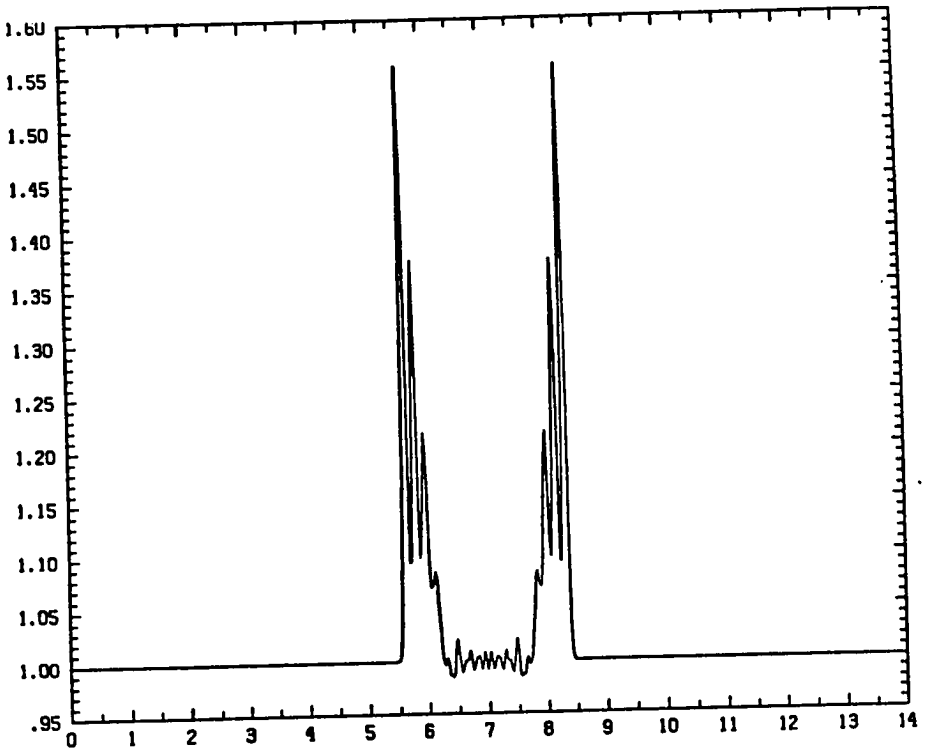

Fig. 2.1.5

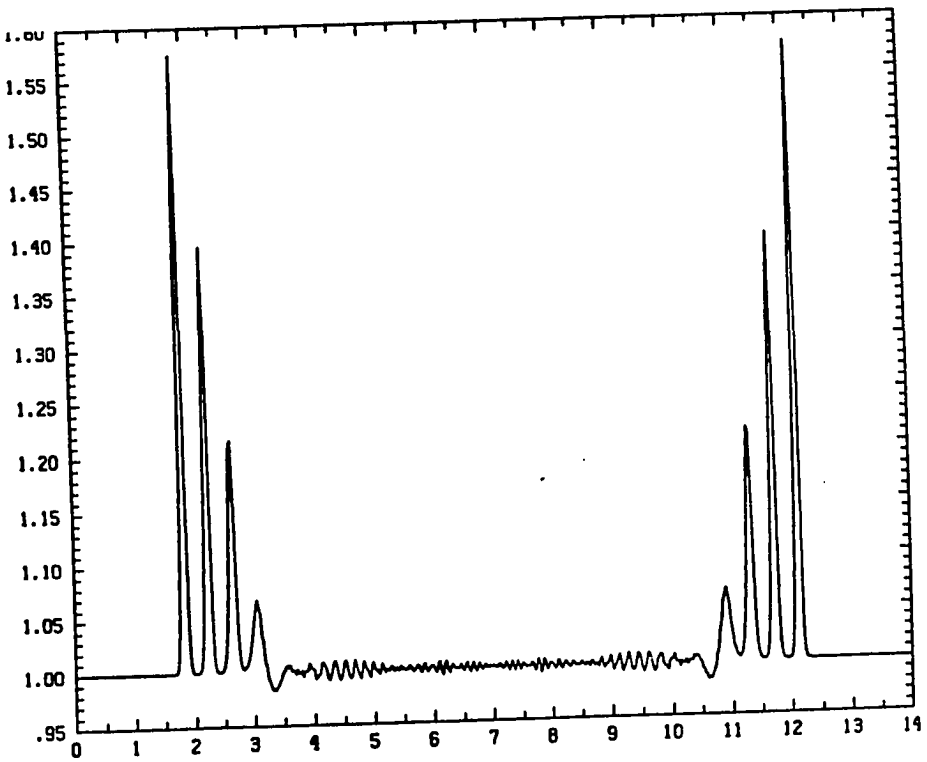

Fig. 2.1.6

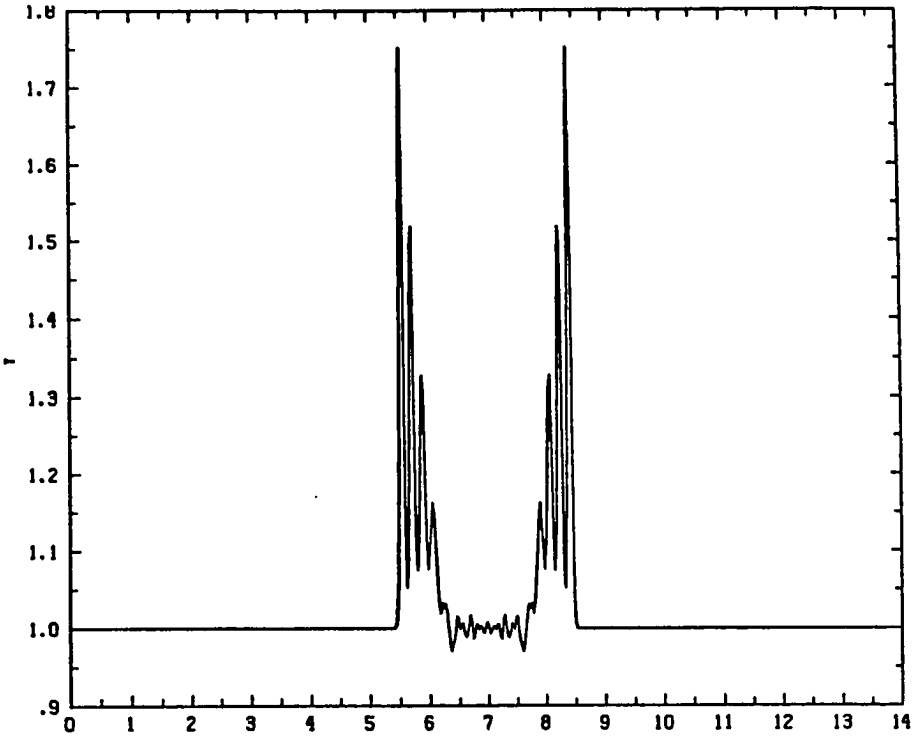

Fig. 2.1.7

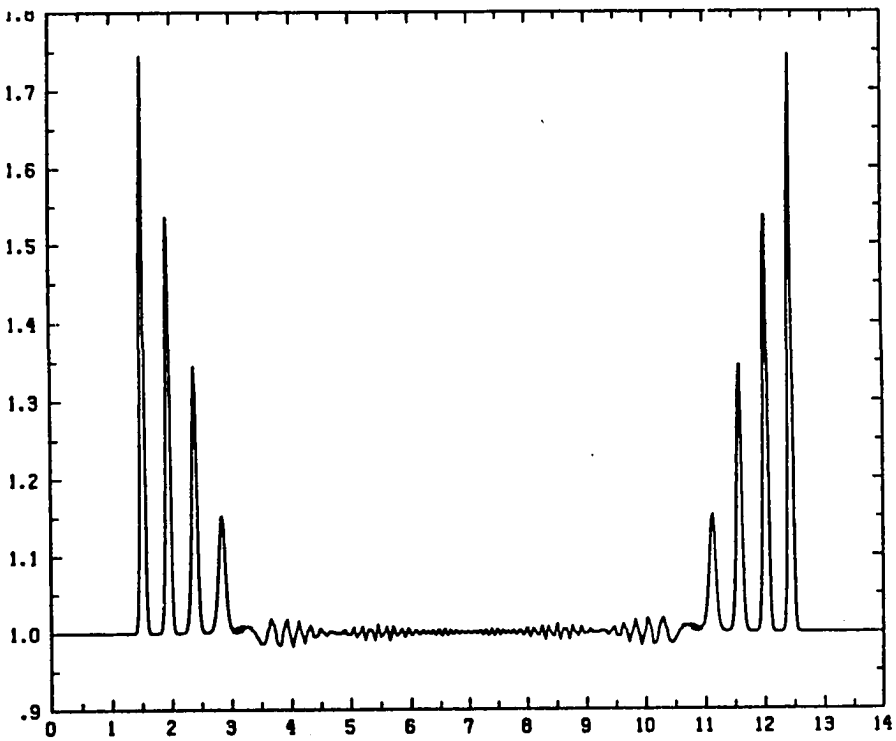

Fig. 2.1.8

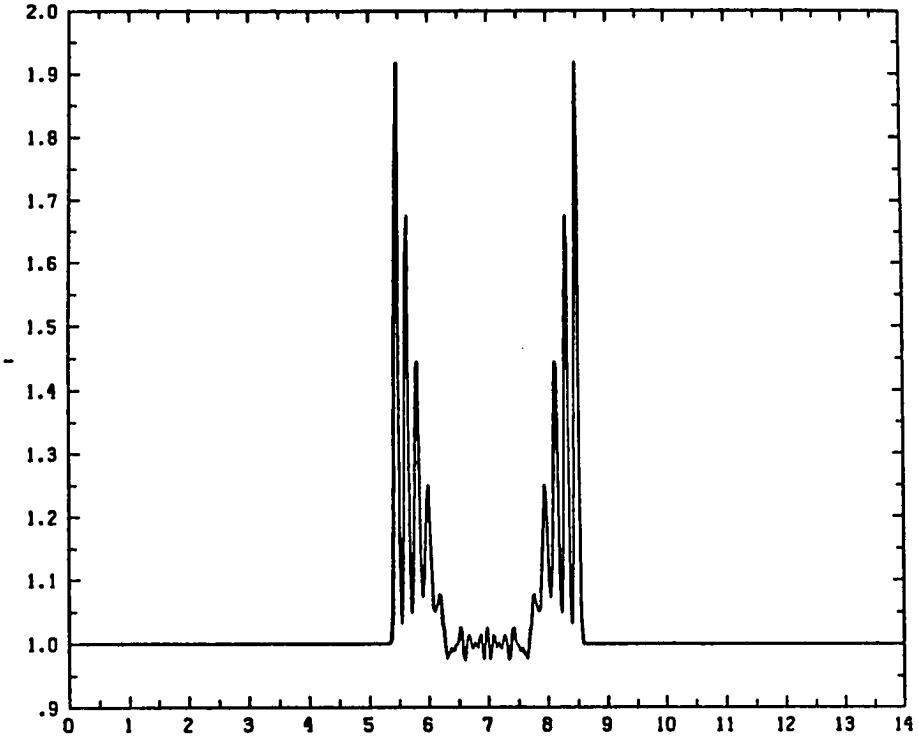

Fig. 2.1.9

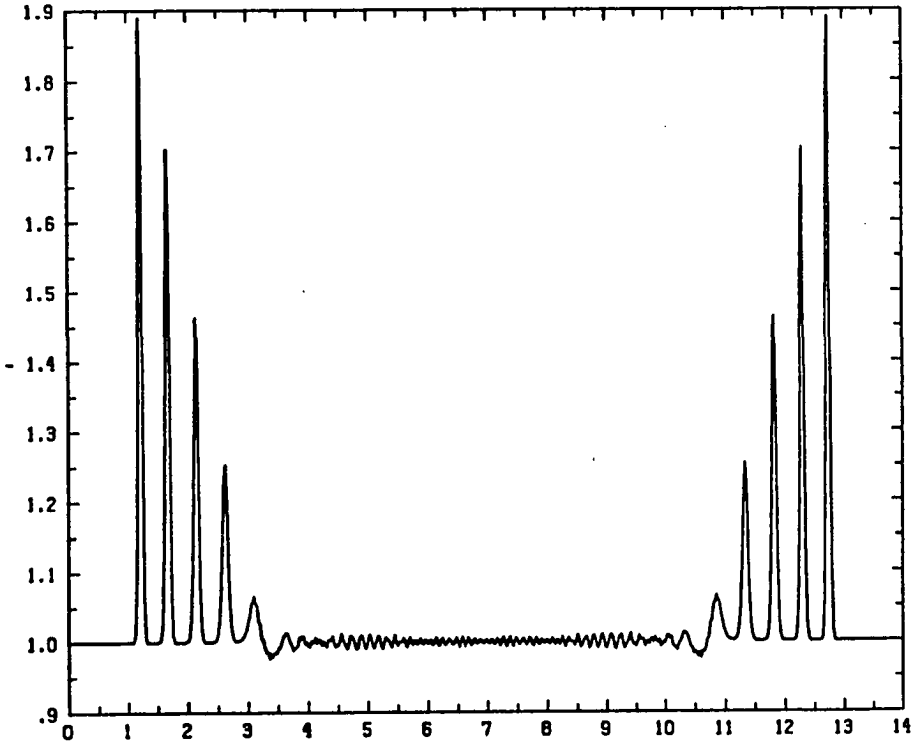

Fig. 2.1.10

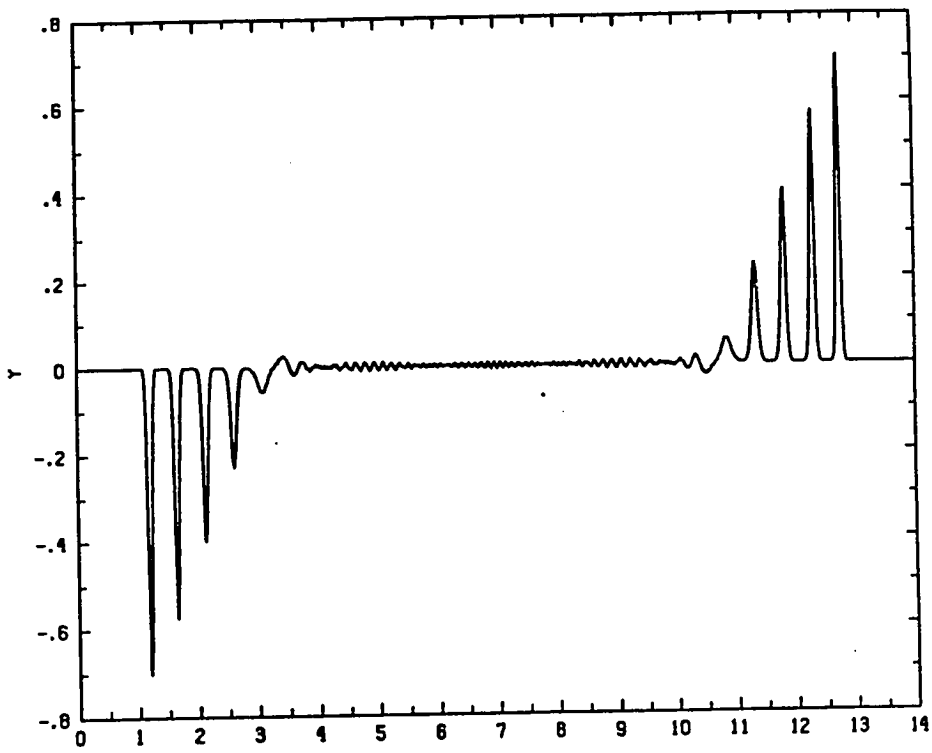

Fig. 2.1.11

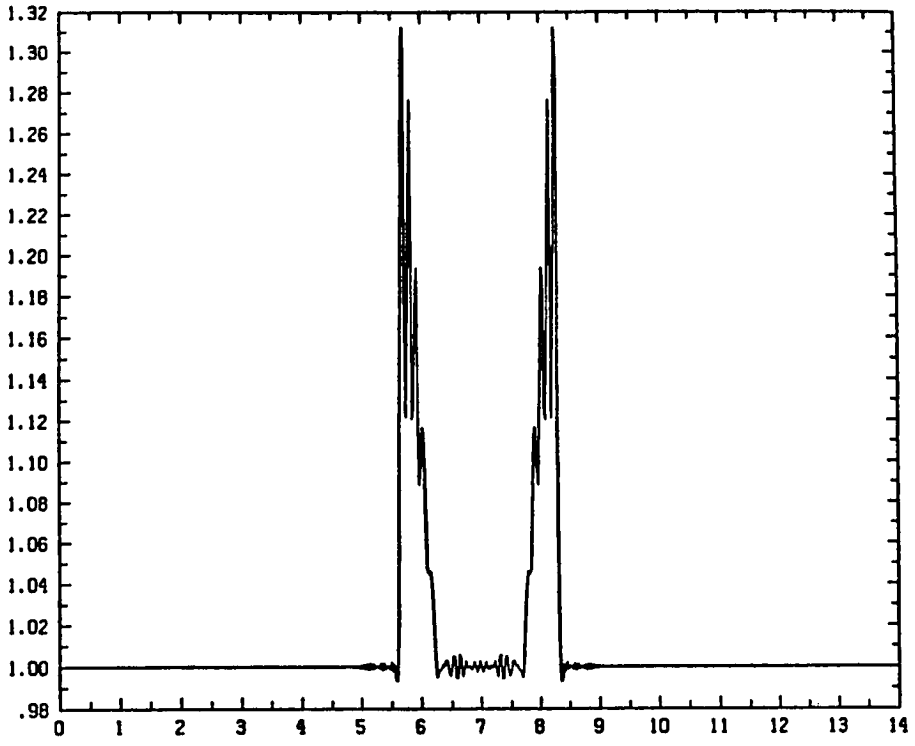

Fig. 2.2.1

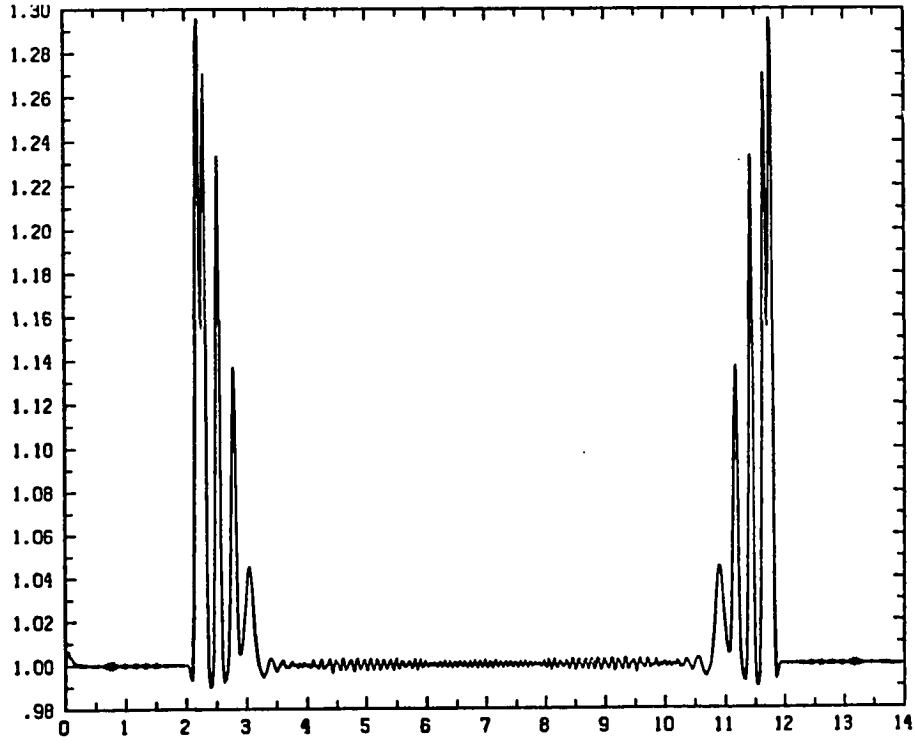

Fig. 2.2.2

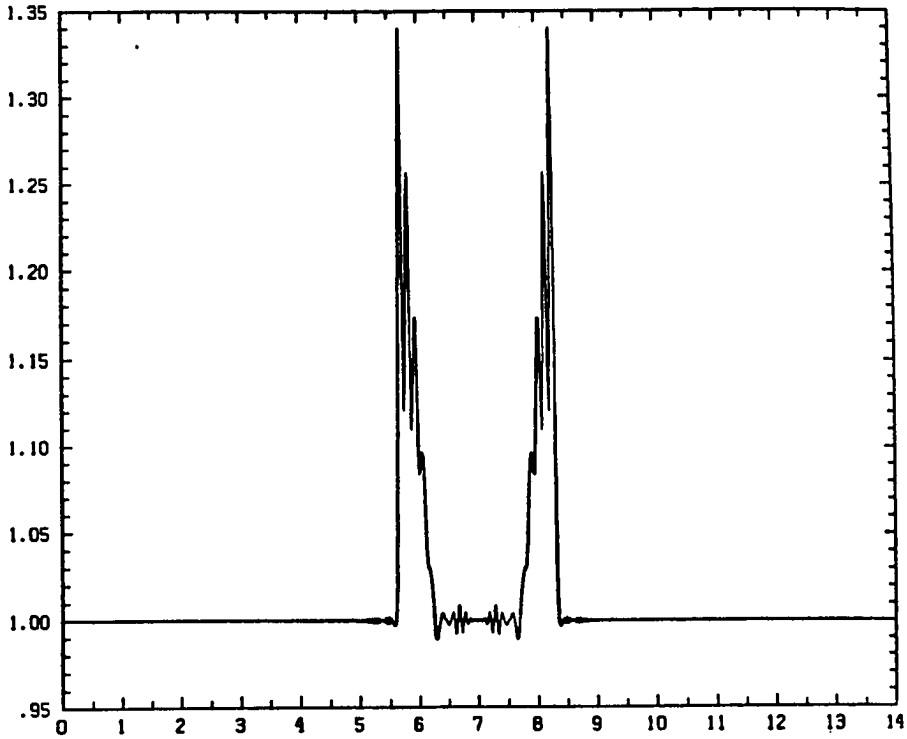

Fig. 2.2.3

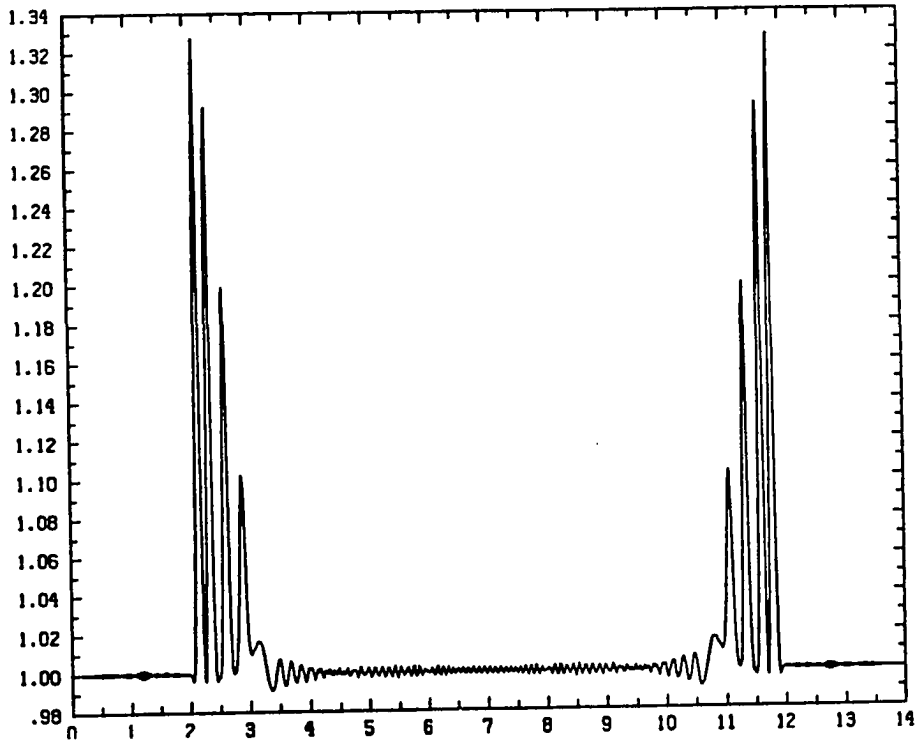

Fig. 2.2.4

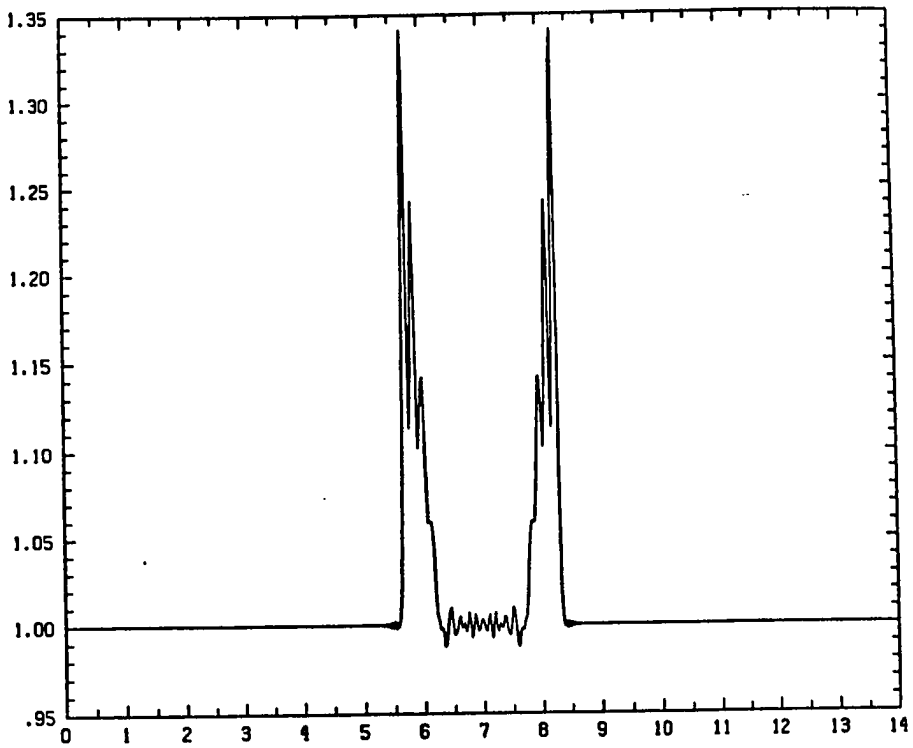

Fig. 2.2.5

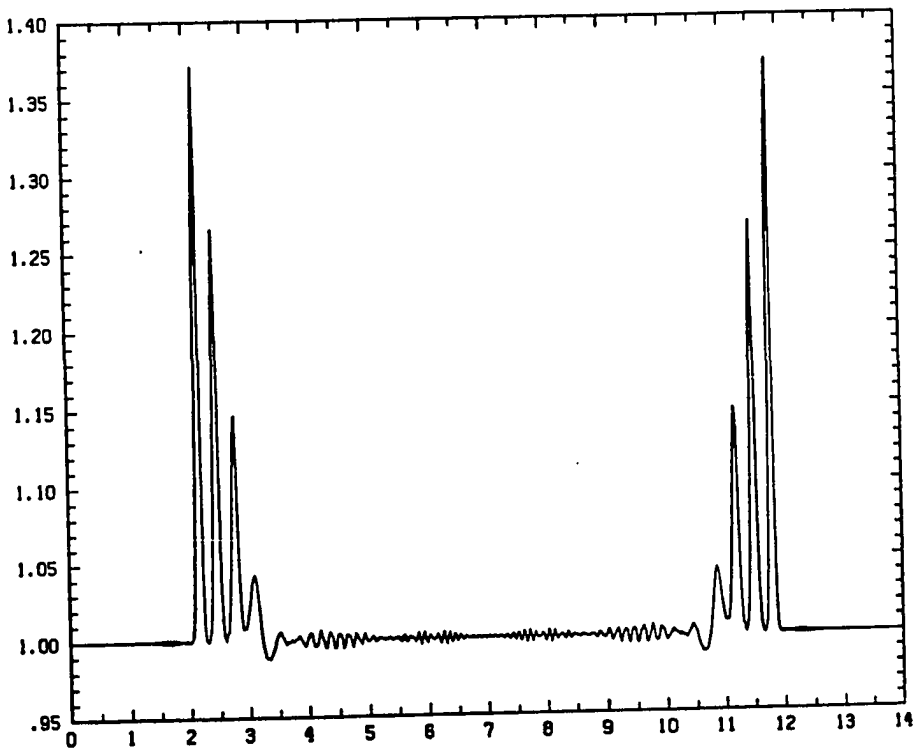

Fig. 2.2.6

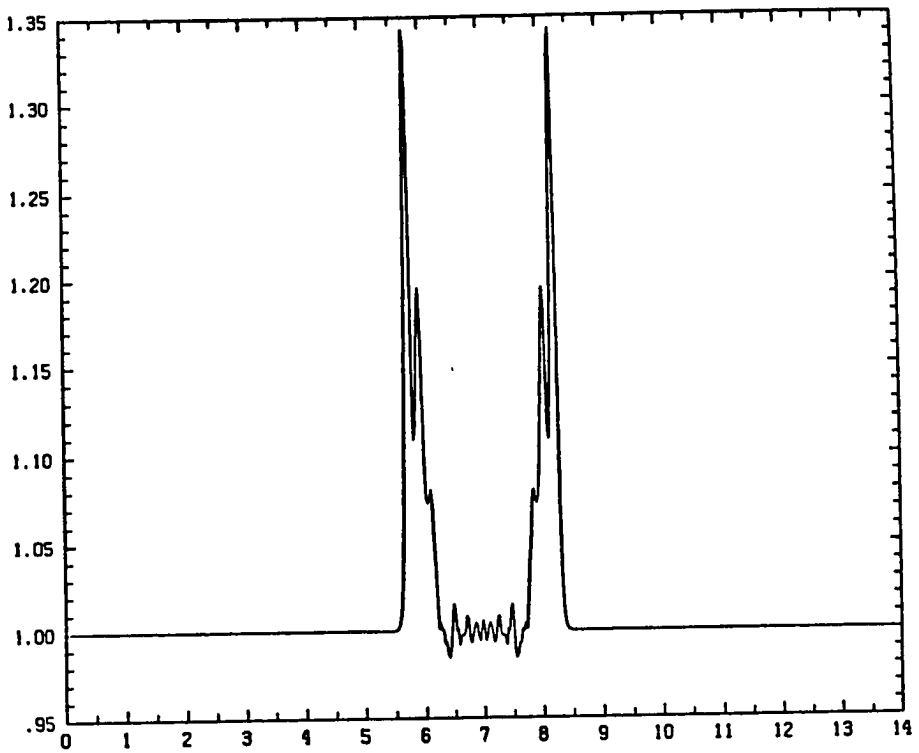

Fig. 2.2.7

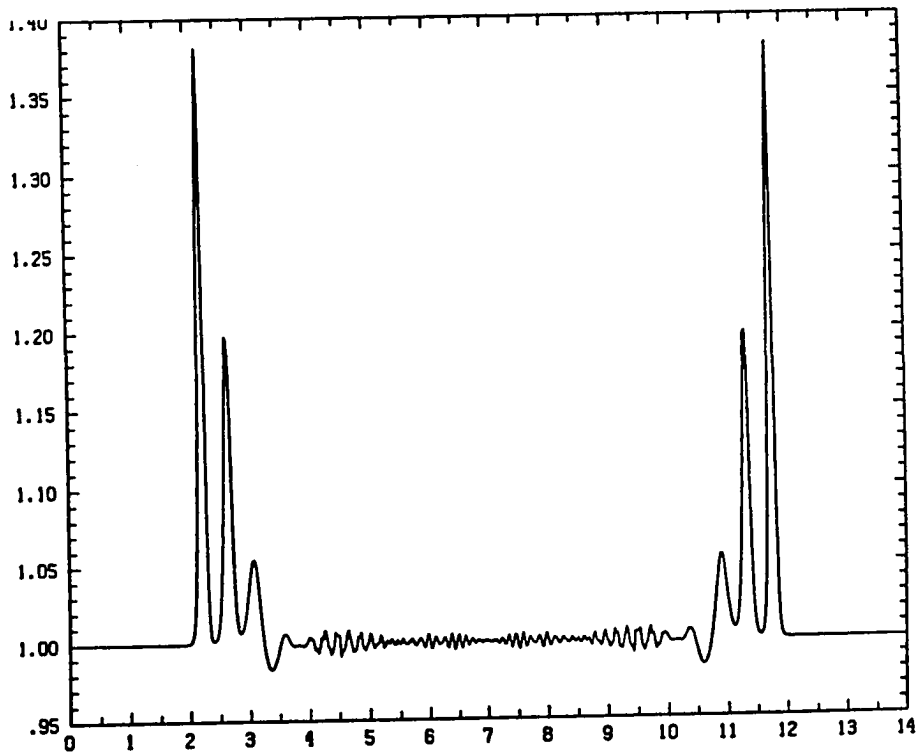

Fig. 2.2.8

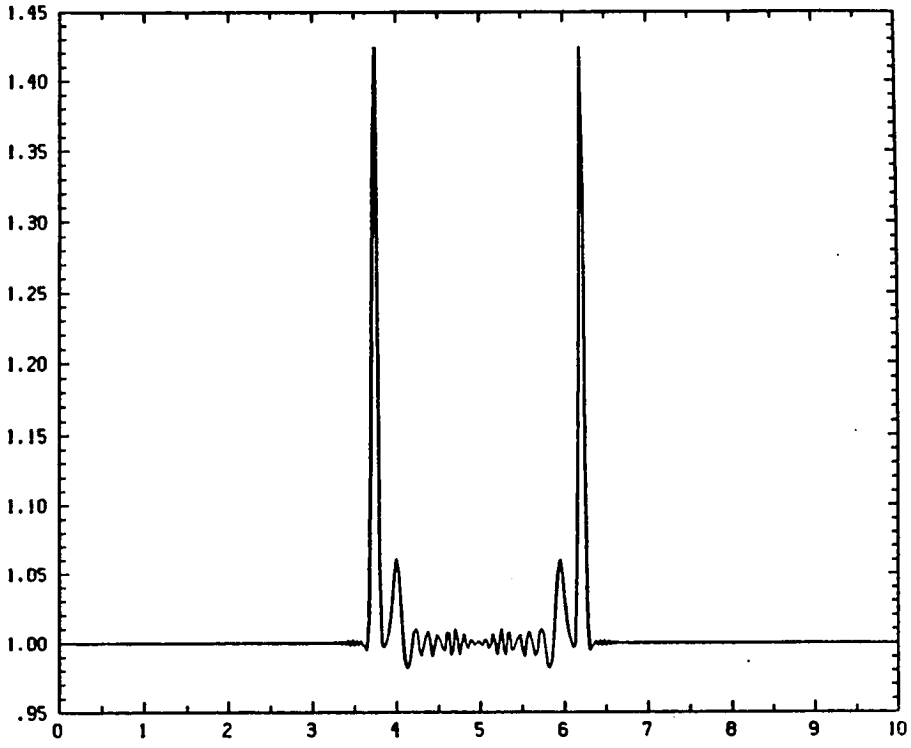

Fig. 2.3.1

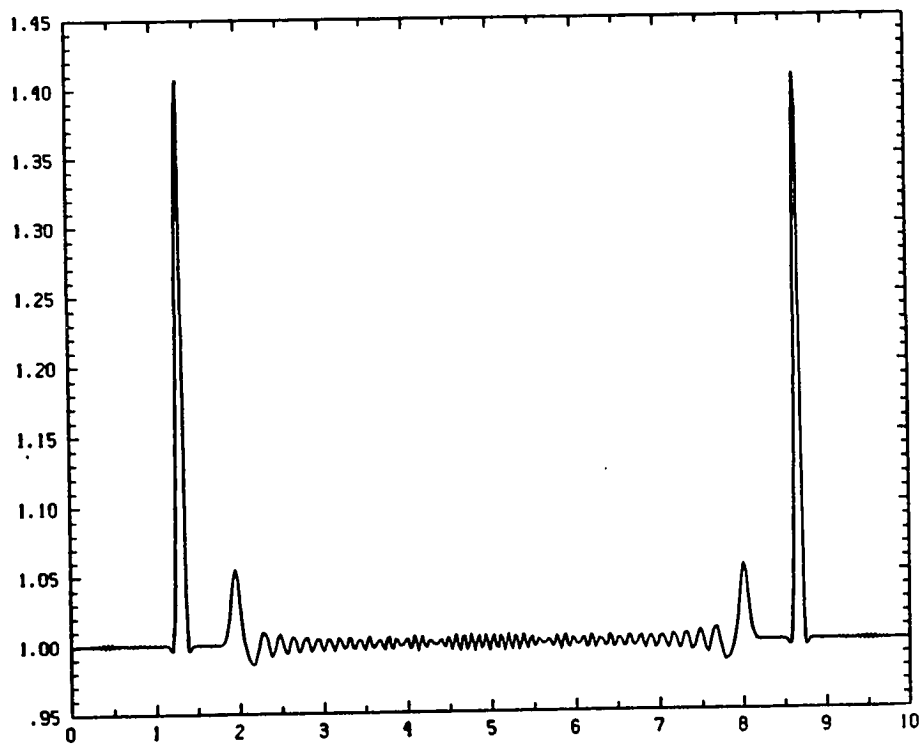

Fig. 2.3.2

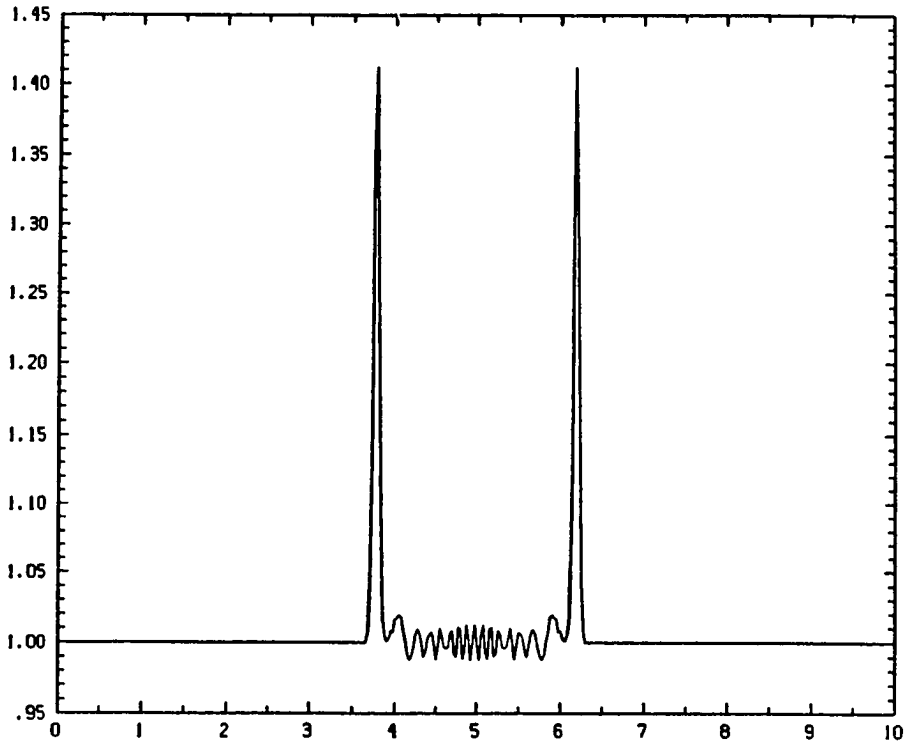

Fig. 2.3.3

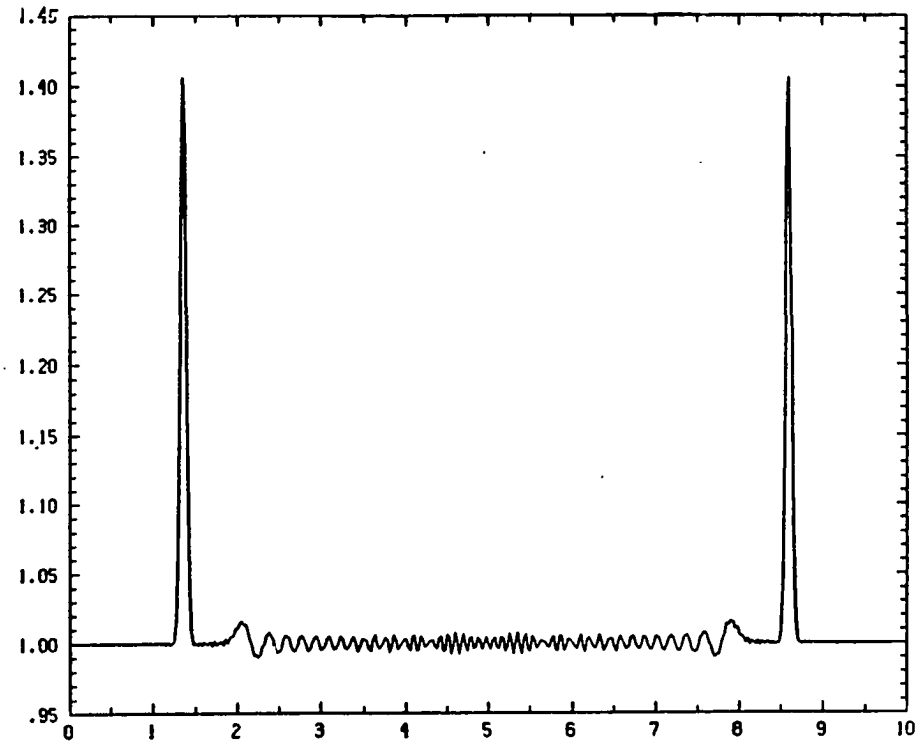

Fig. 2.3.4

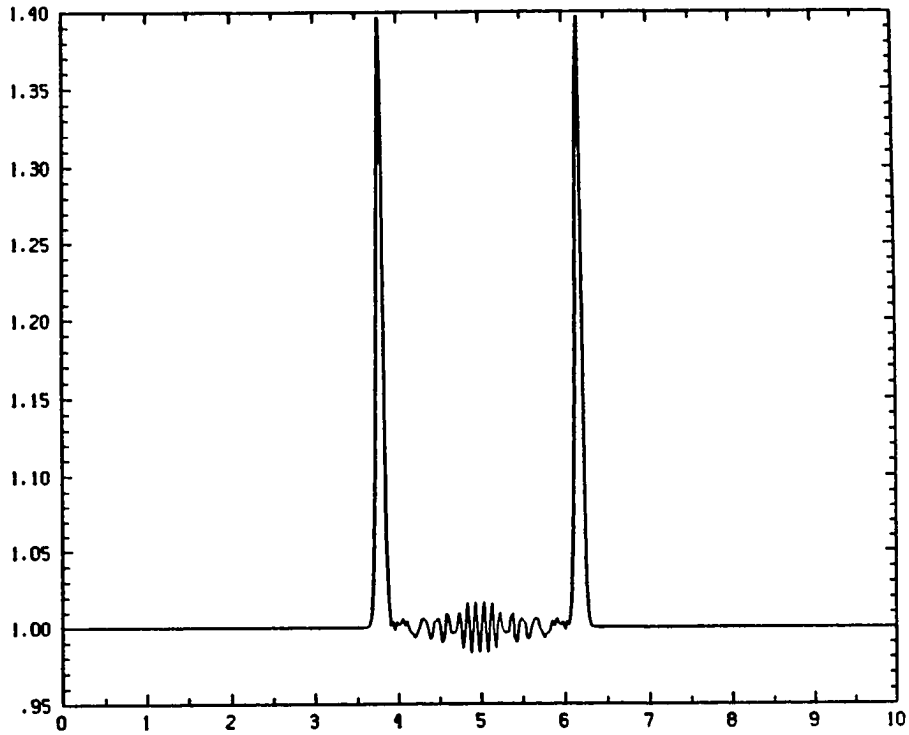

Fig. 2.3.5

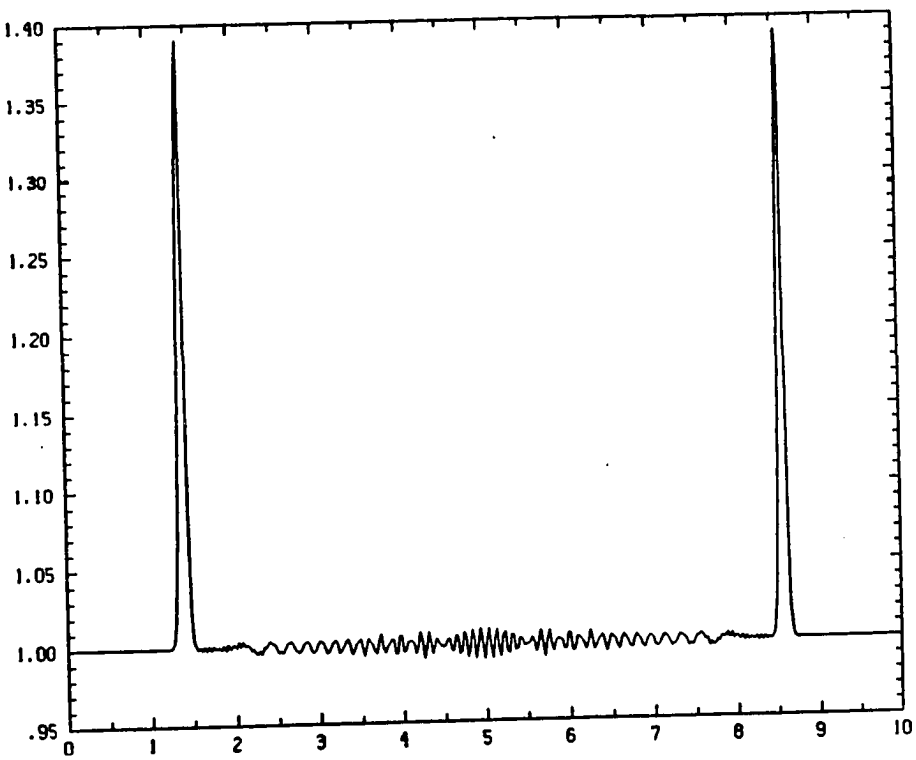

Fig. 2.3.6

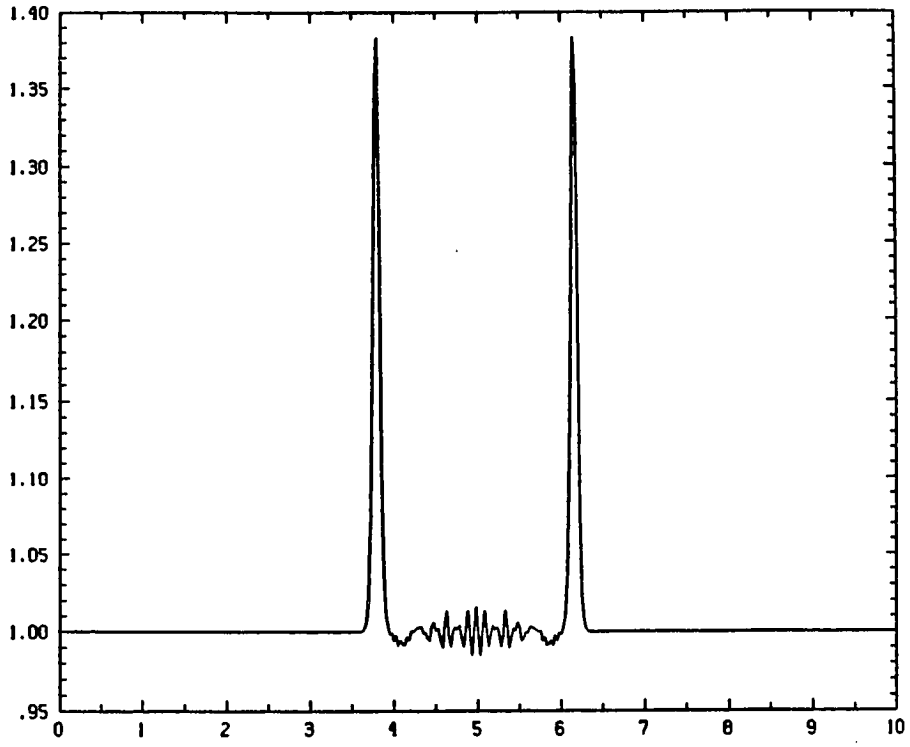

Fig. 2.3.7

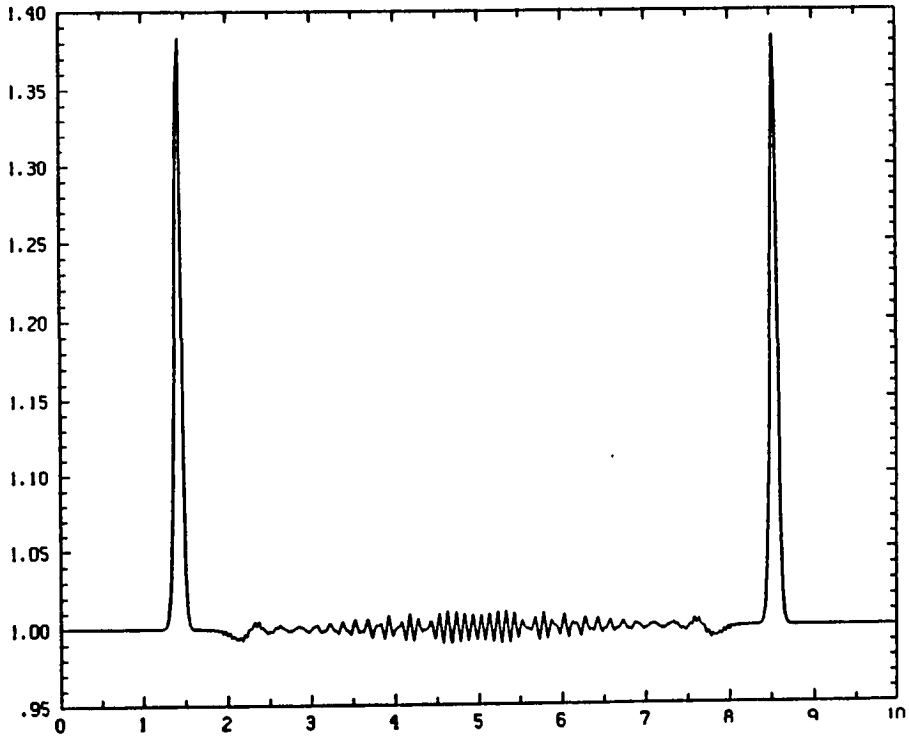

Fig. 2.3.8

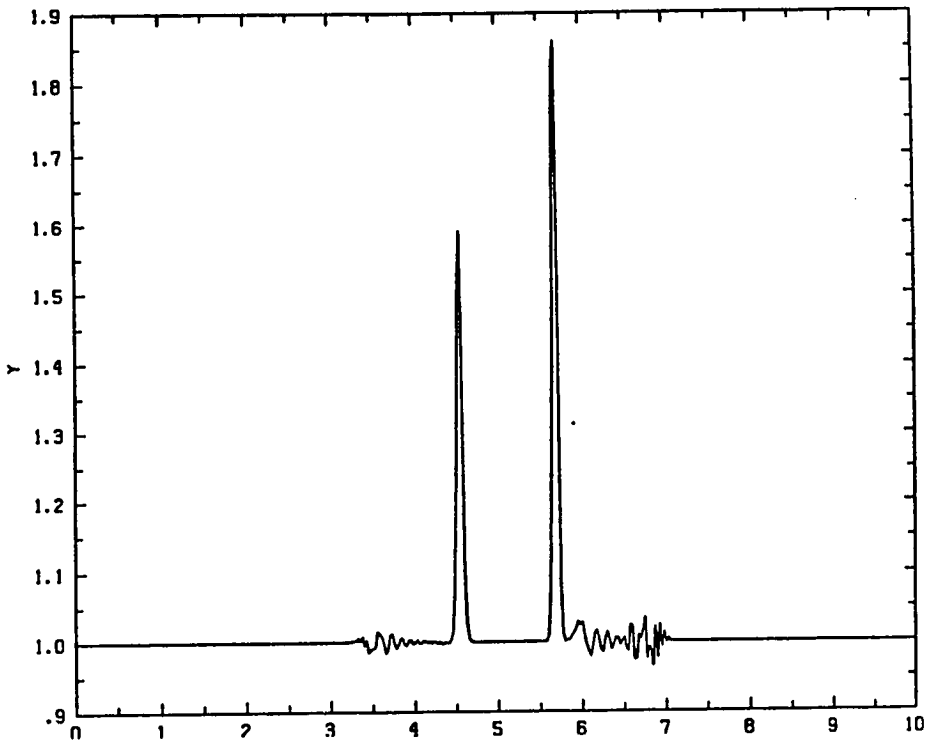

Fig. 3.1.1

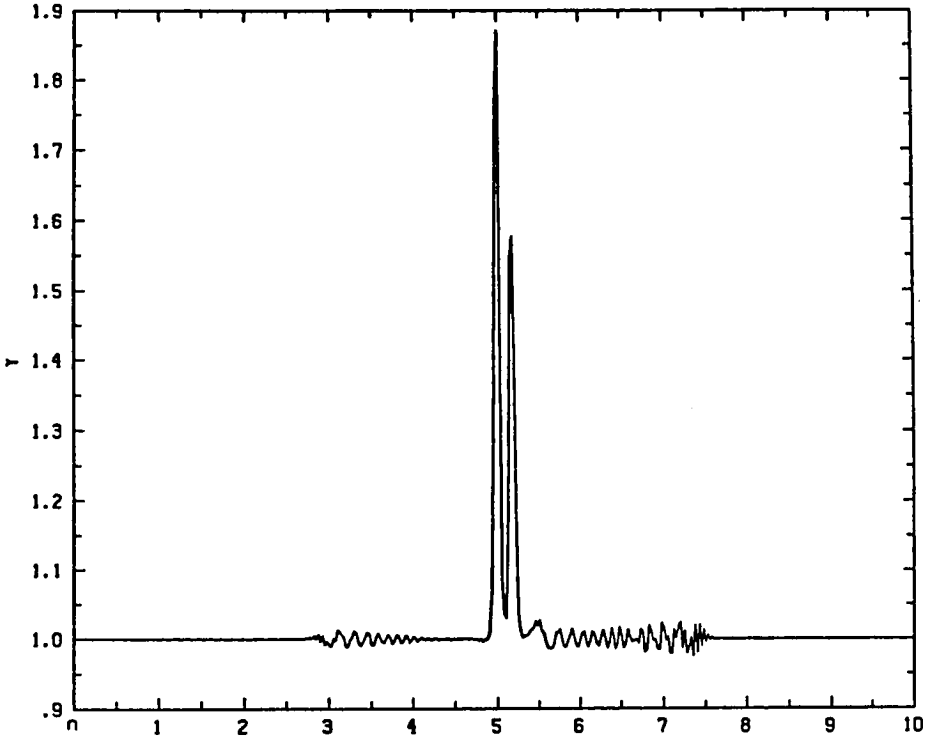

Fig. 3.1.2

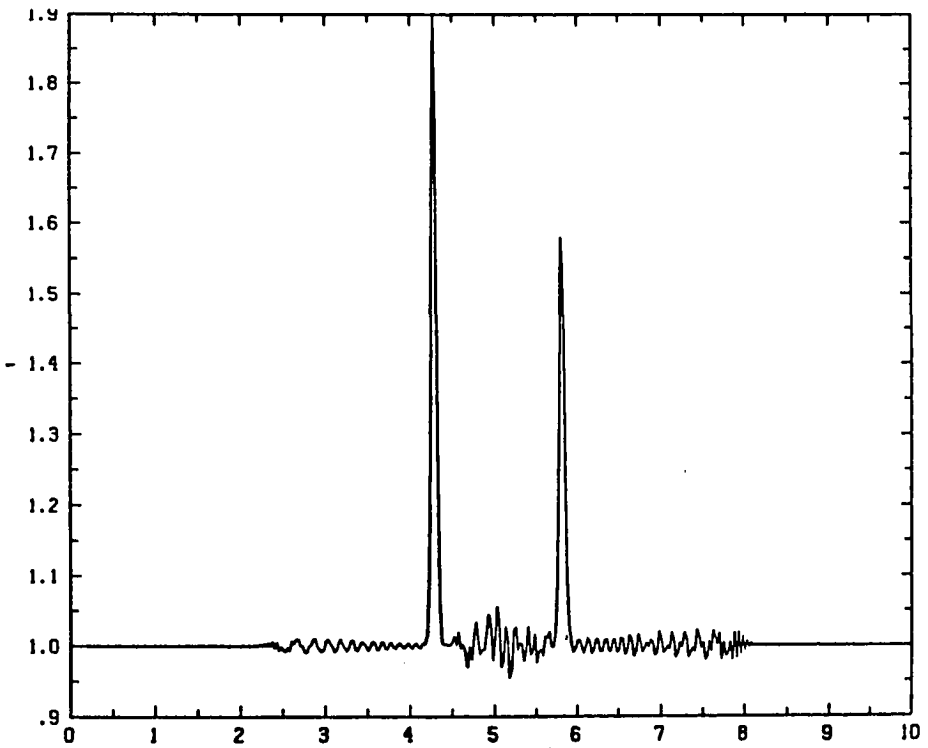

Fig. 3.1.3

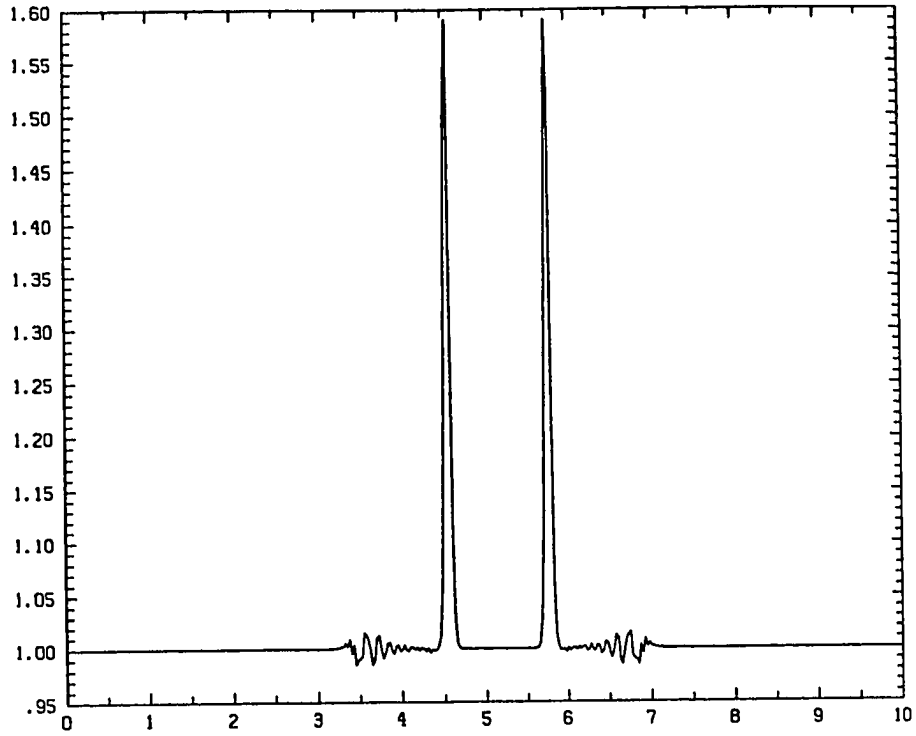

Fig. 3.2.1

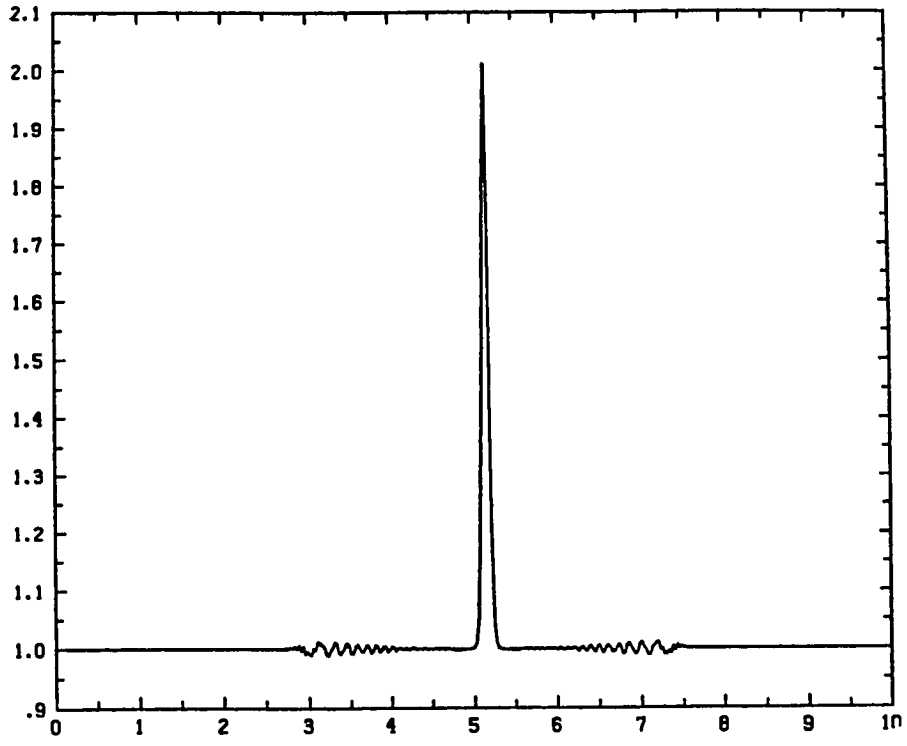

Fig. 3.2.2

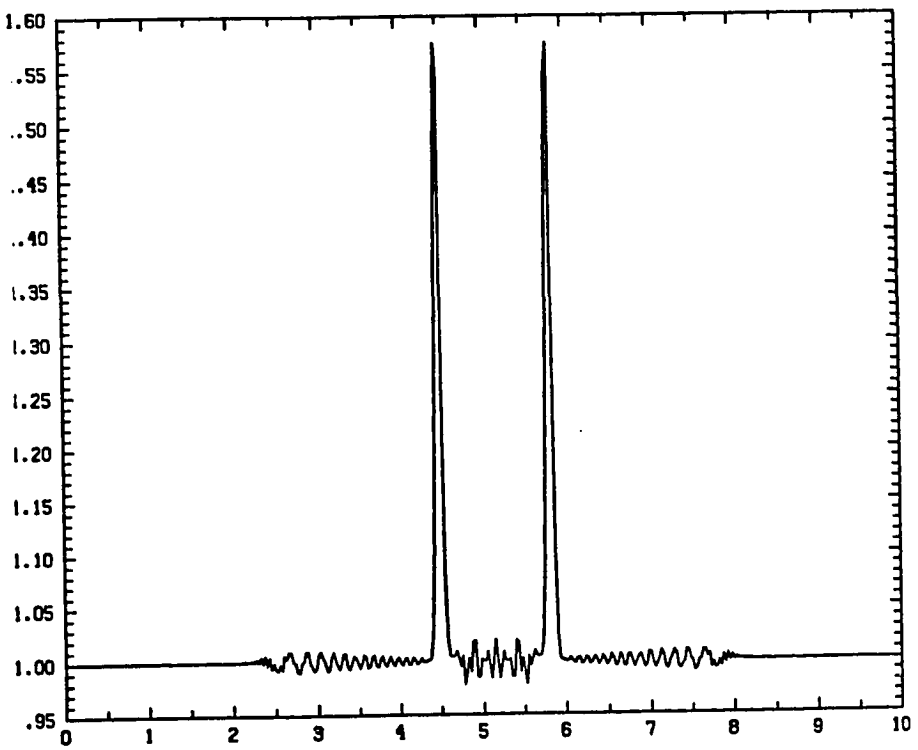

Fig. 3.2.3

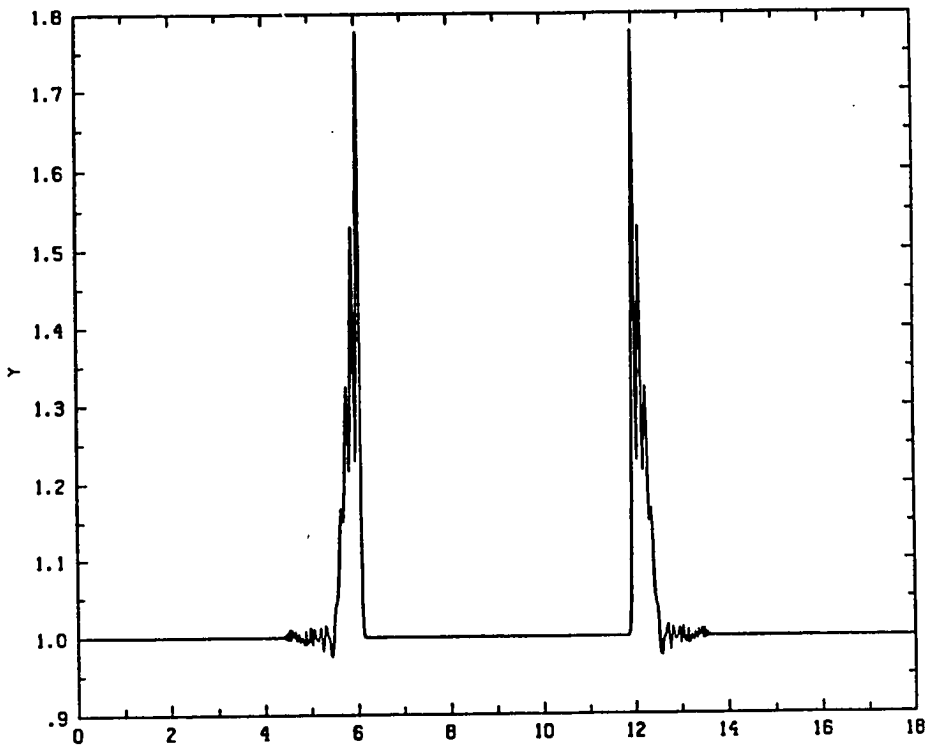

Fig. 3.3.1

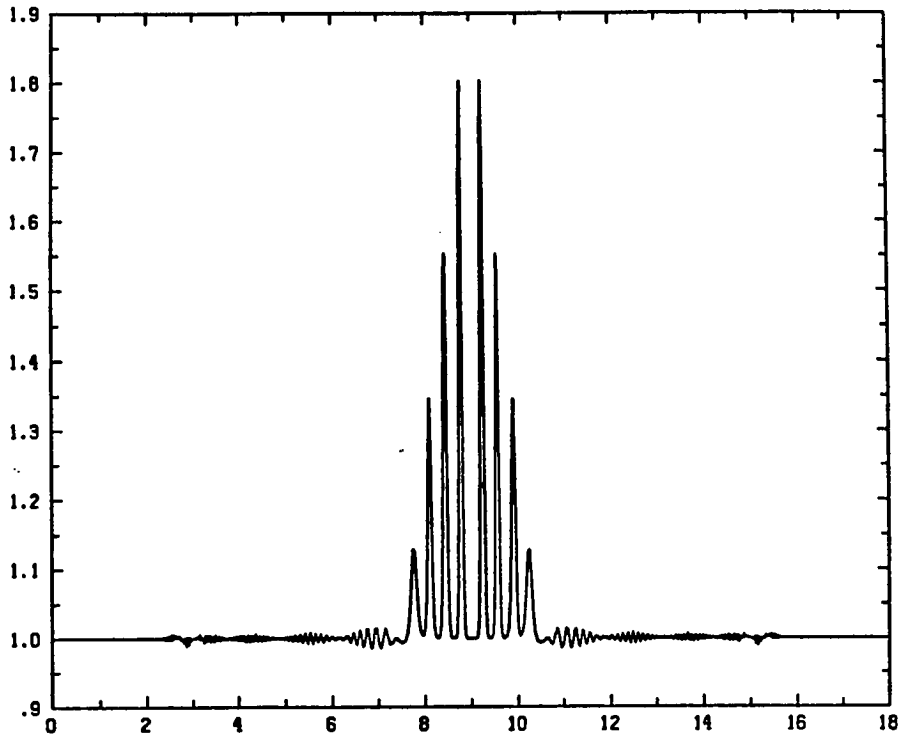

Fig. 3.3.2

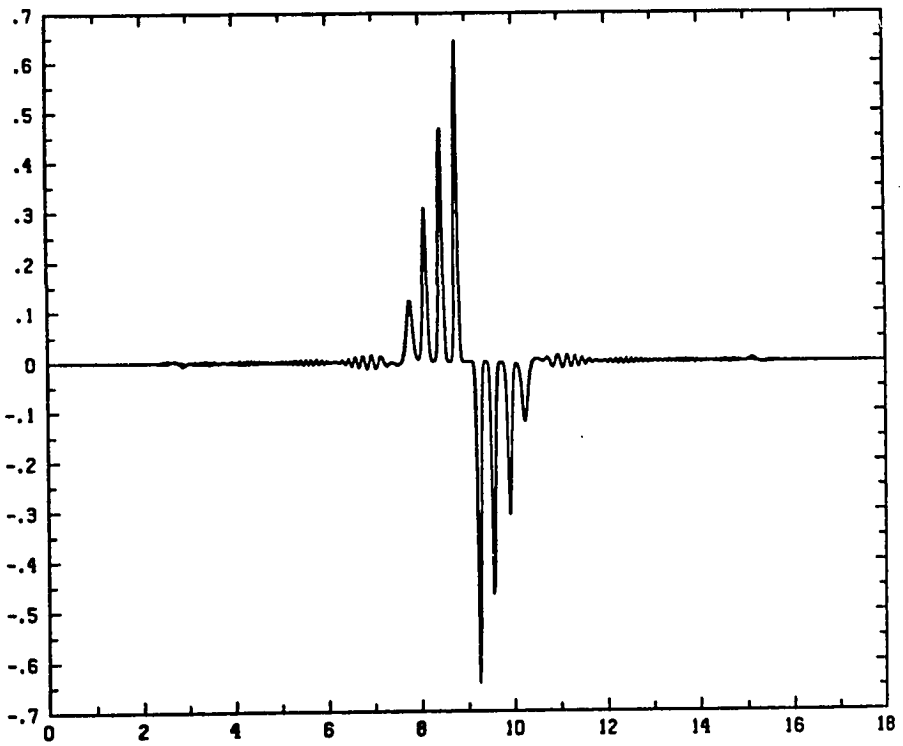

Fig. 3.3.3

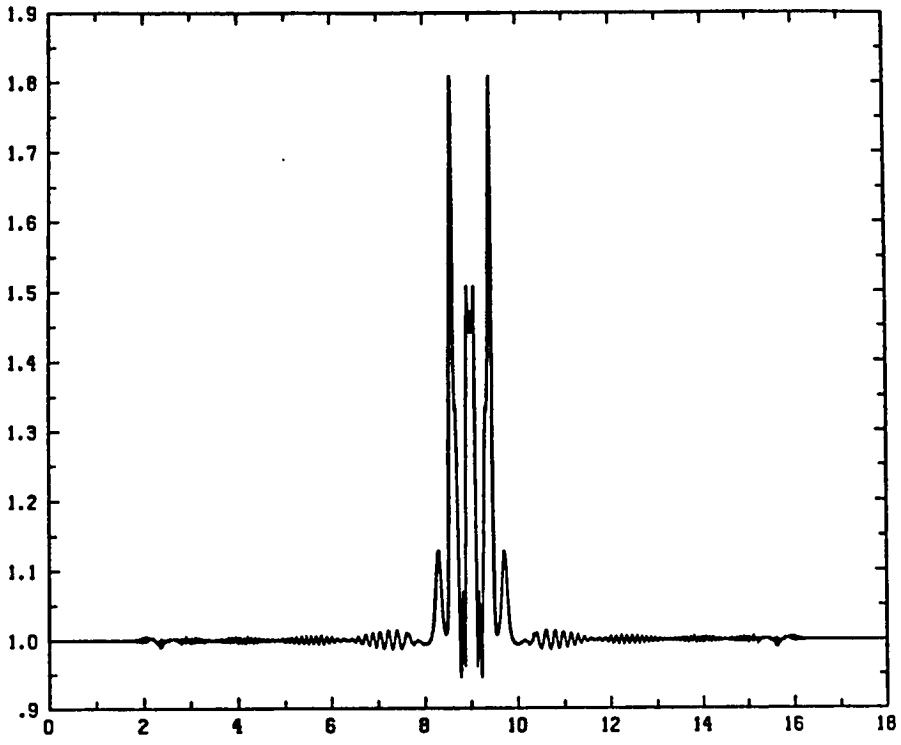

Fig. 3.3.4

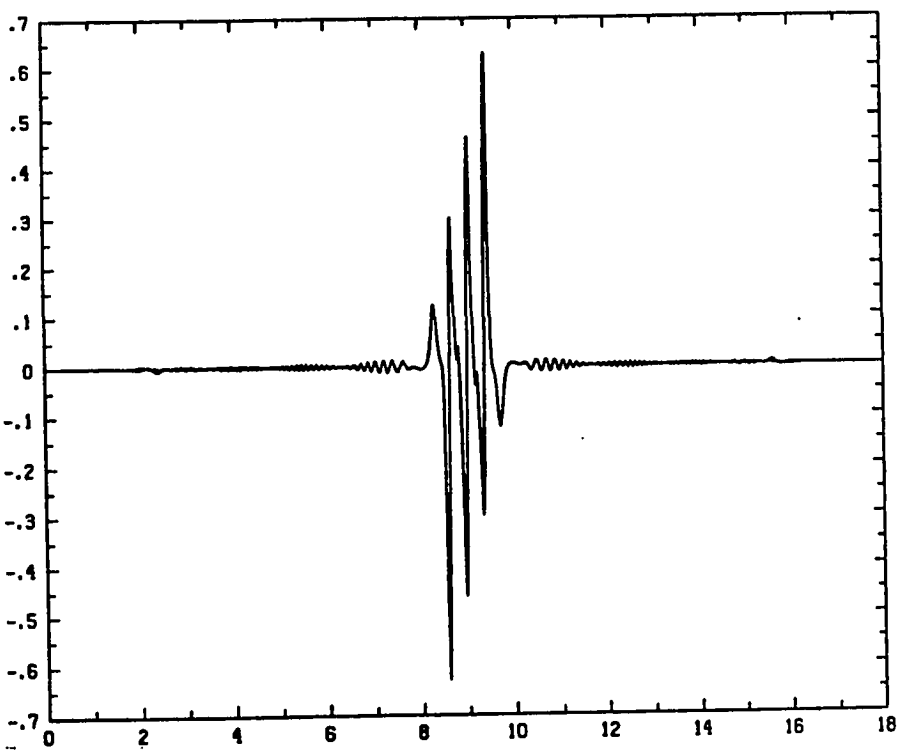

Fig. 3.3.5

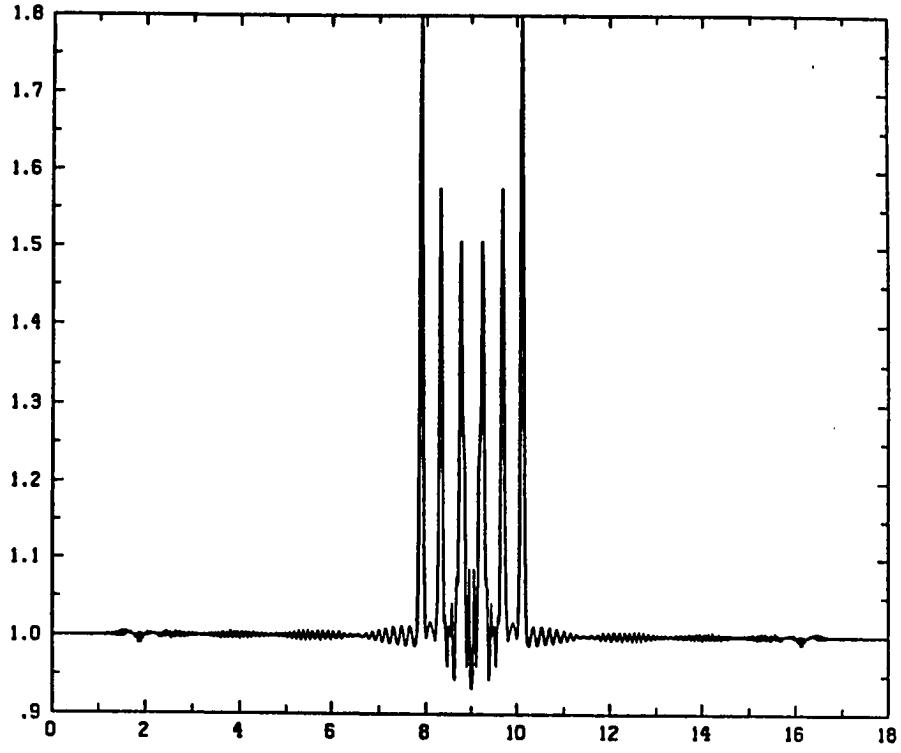

Fig. 3.3.6

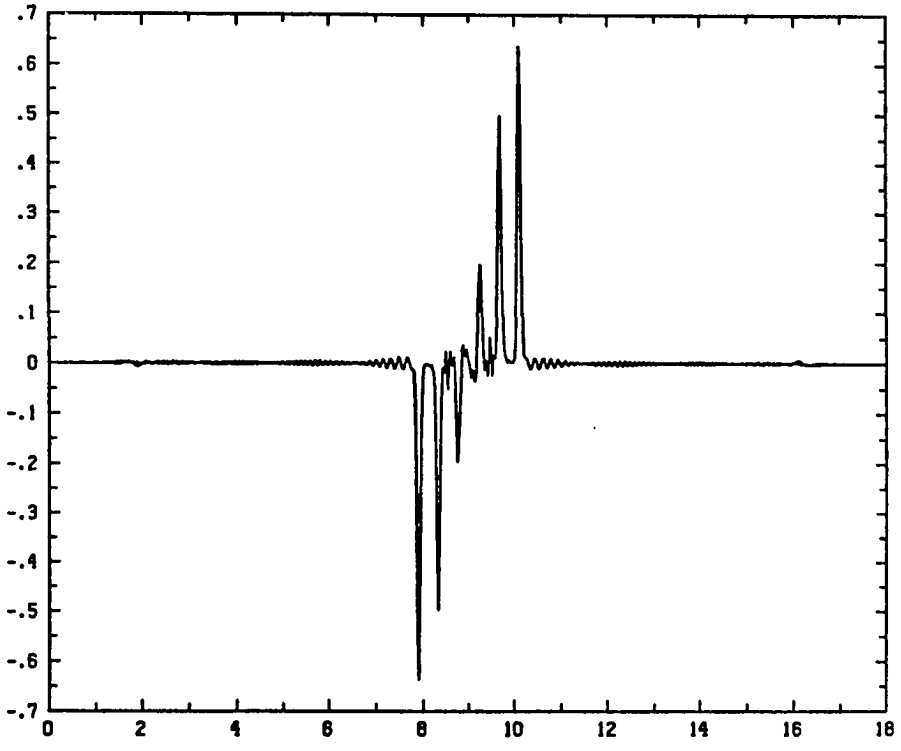

Fig. 3.3.7

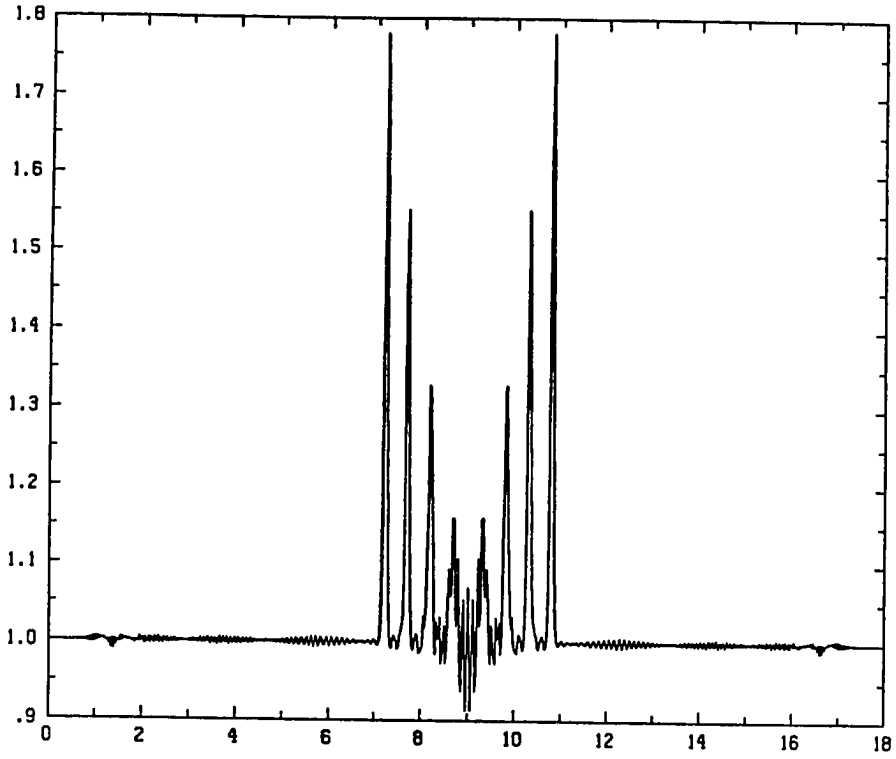

Fig. 3.3.8

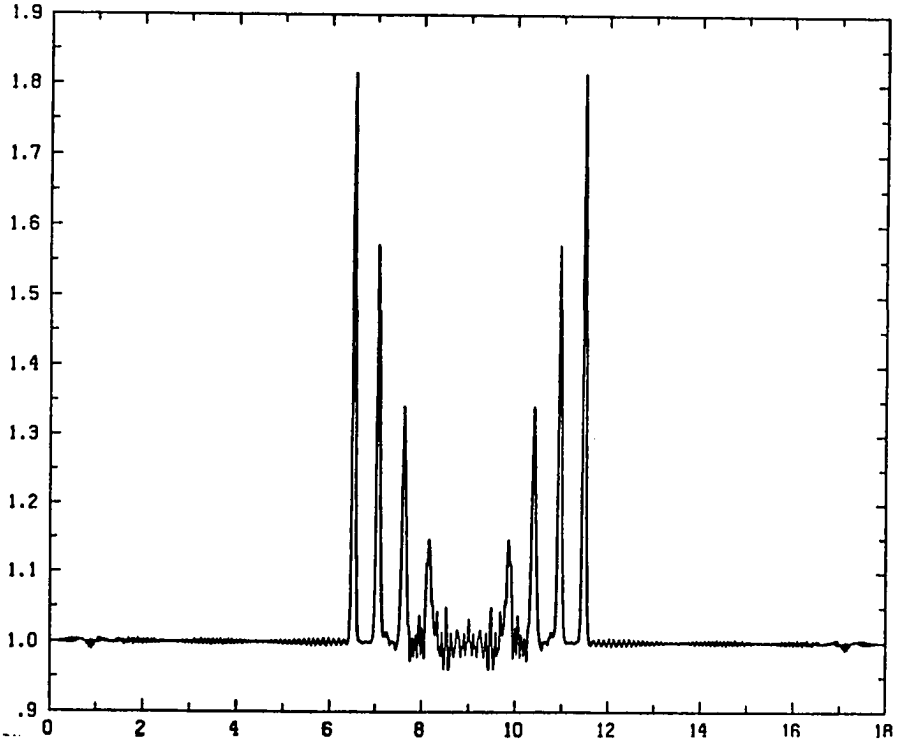

Fig. 3.3.9

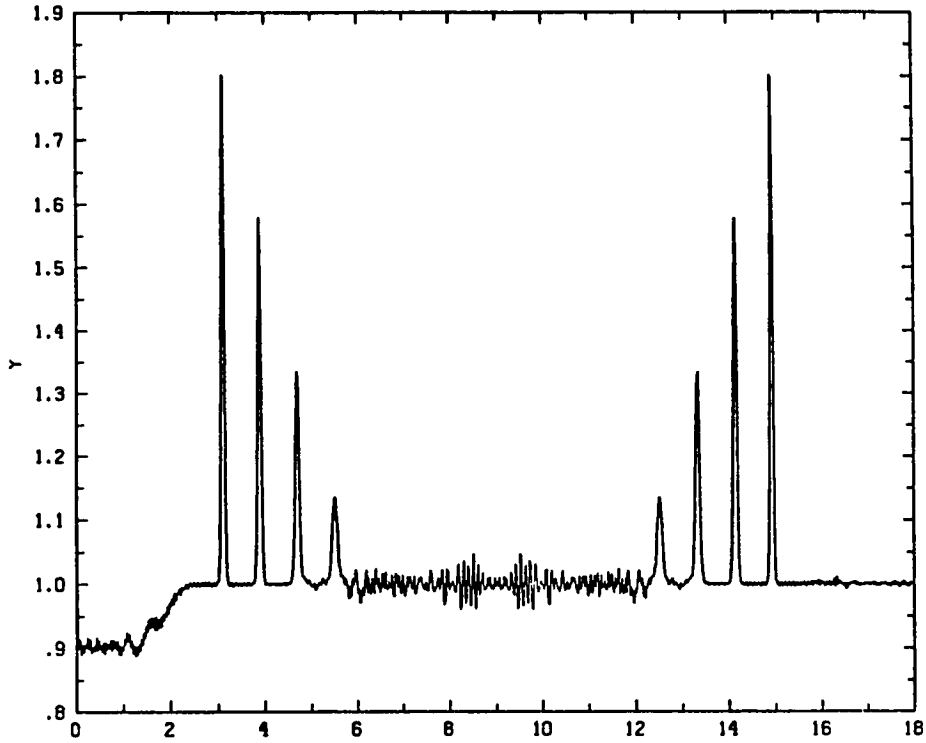

Fig. 3.3.10

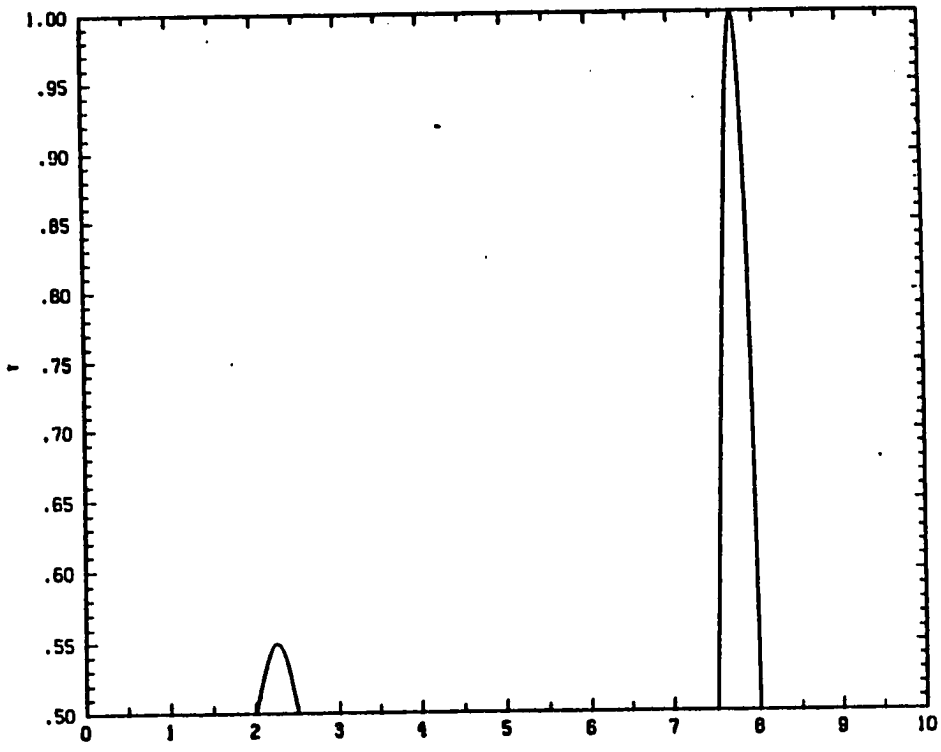

Fig. 3.4.1

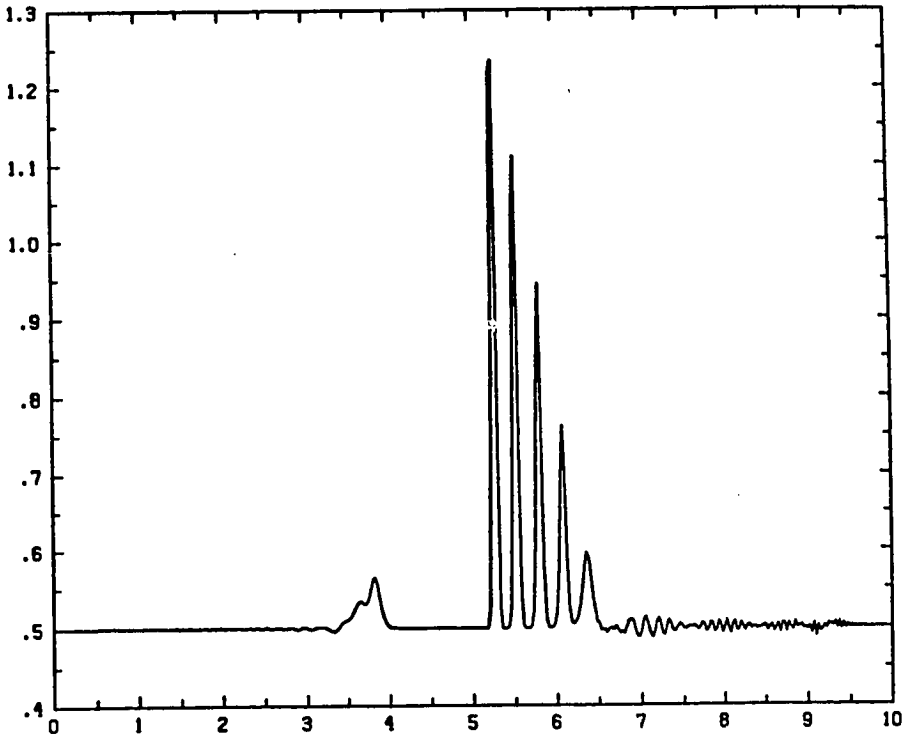

Fig. 3.4.2

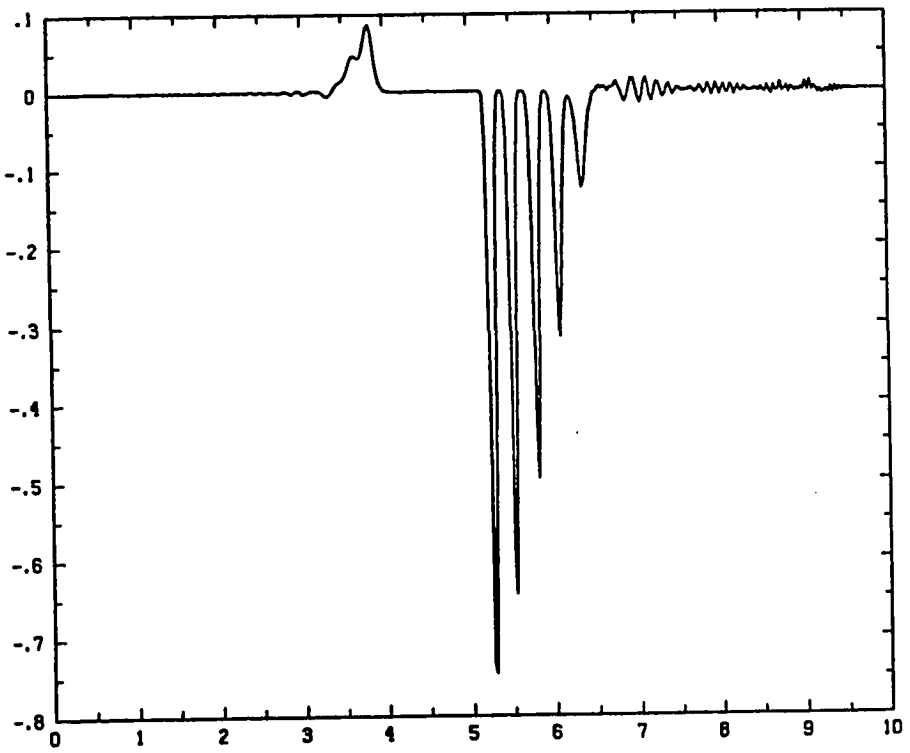

Fig. 3.4.3

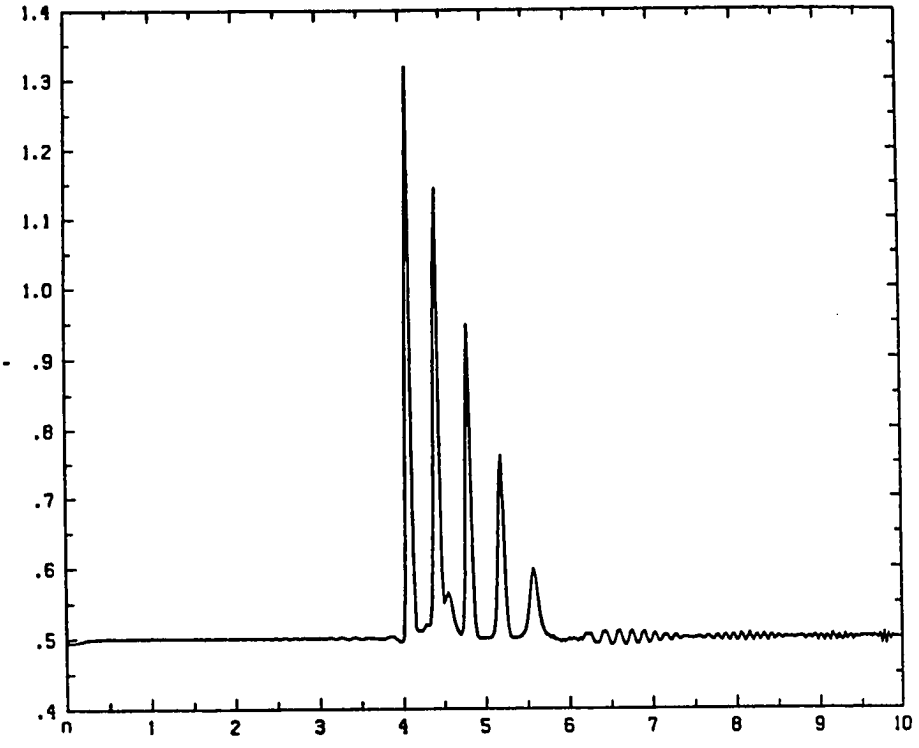

Fig. 3.4.4

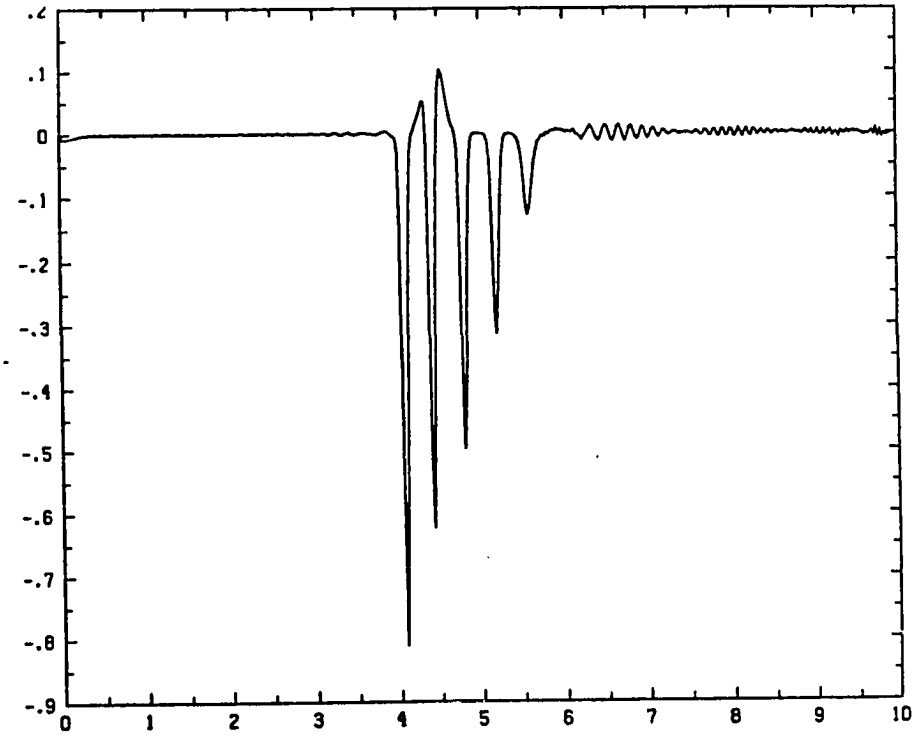

Fig. 3.4.5

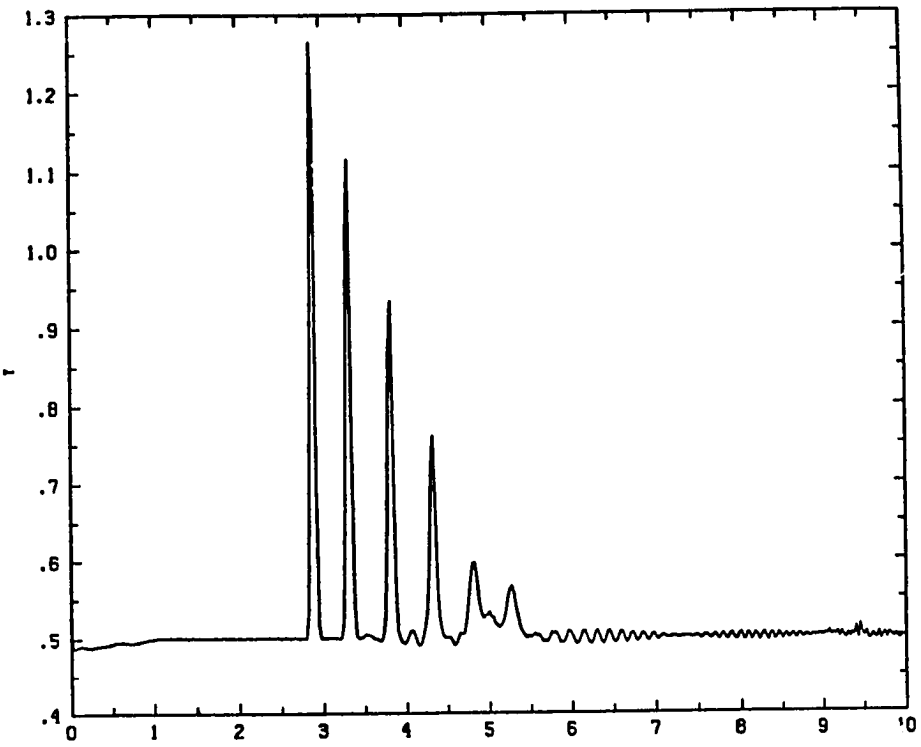

Fig. 3.4.6

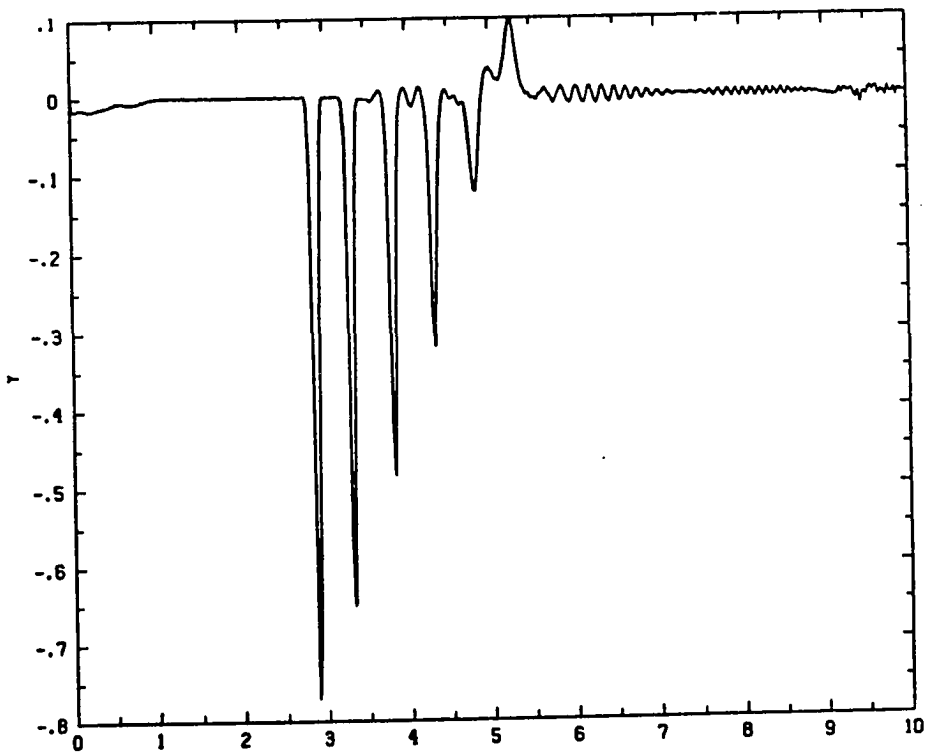

Fig. 3.4.7

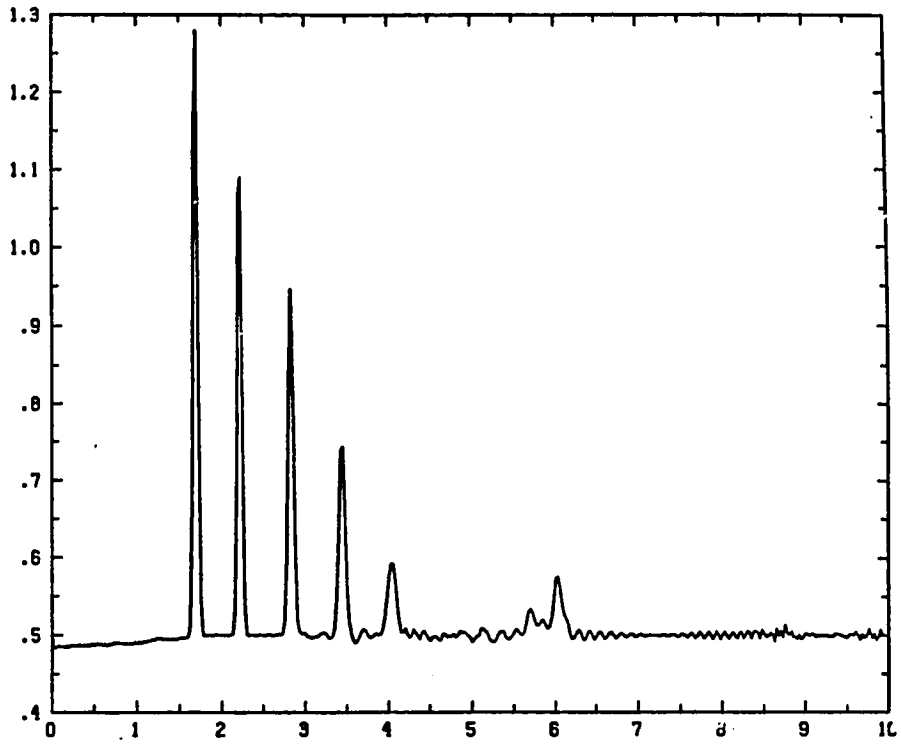

Fig. 3.4.8

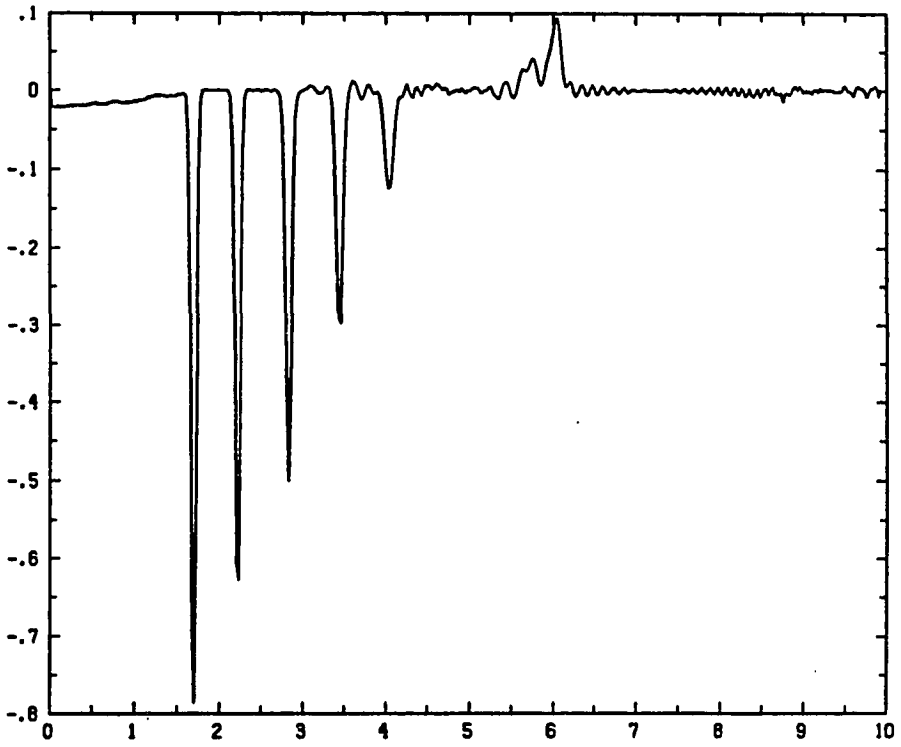

Fig. 3.4.9

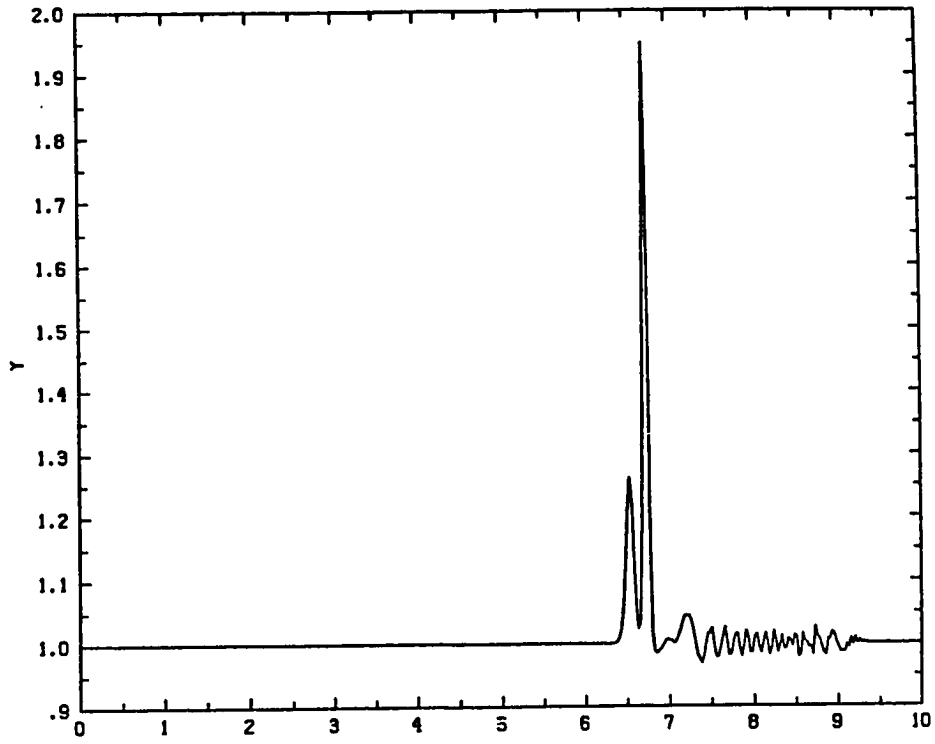

Fig. 3.5.1

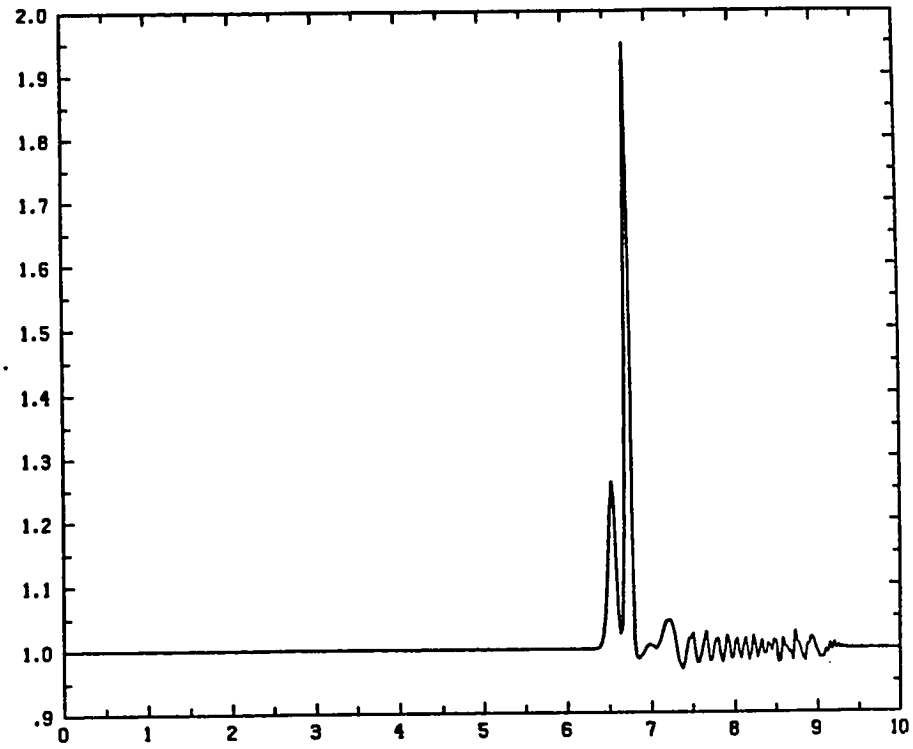

Fig. 3.5.2

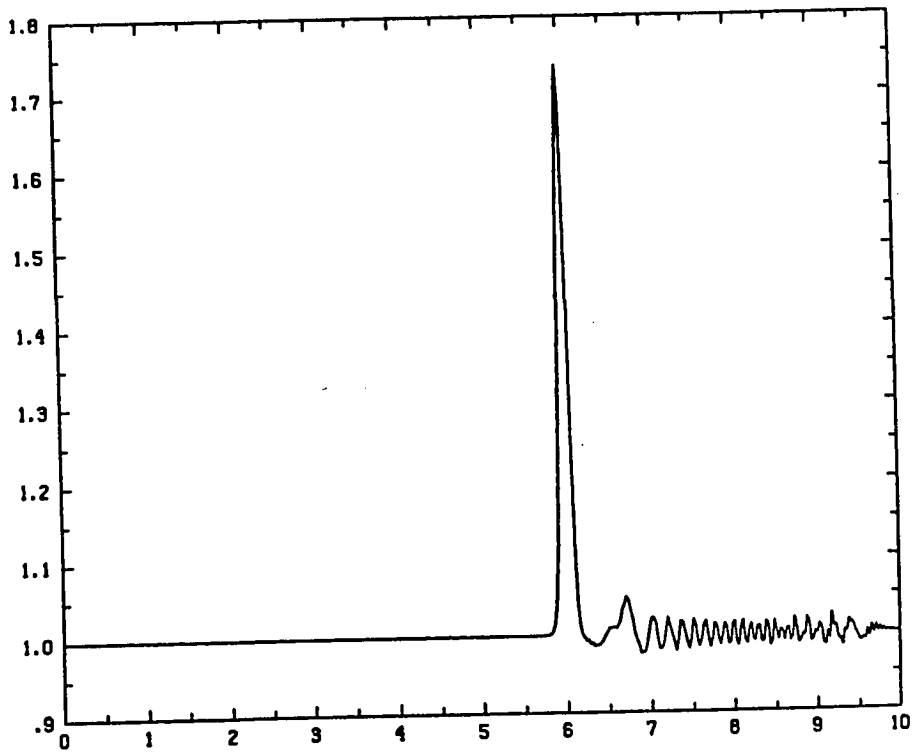

Fig.. 3.5.3

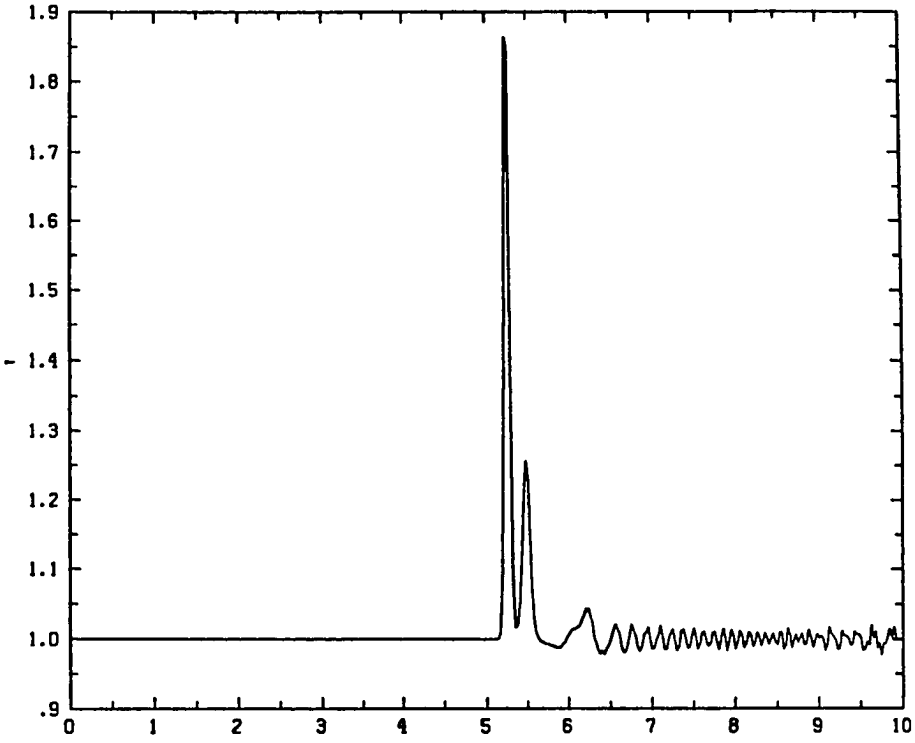

Fig. 3.5.4

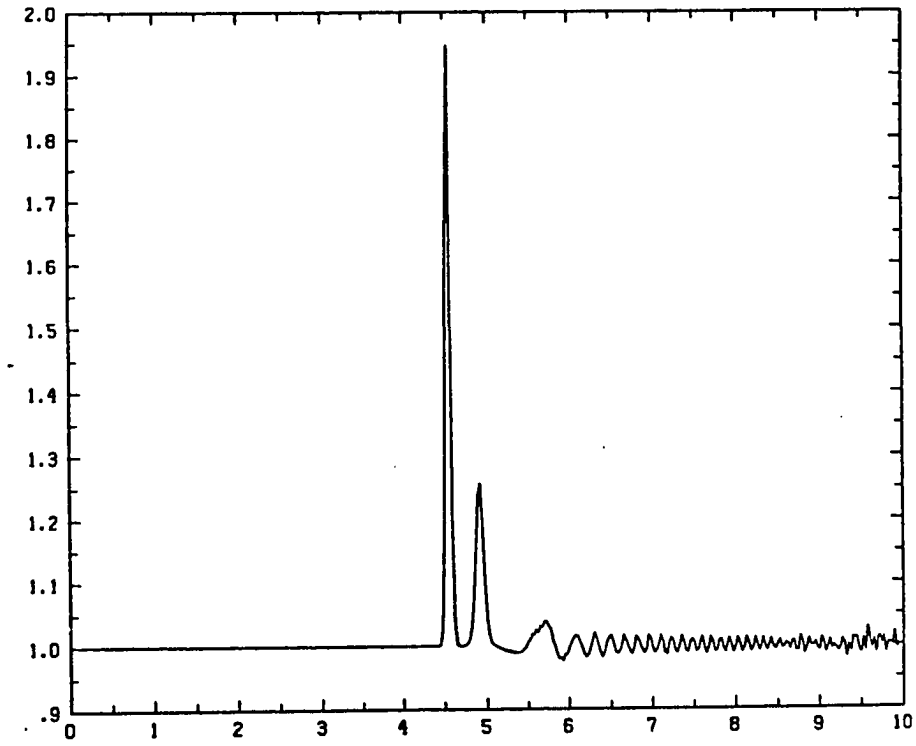

Fig. 3.5.5

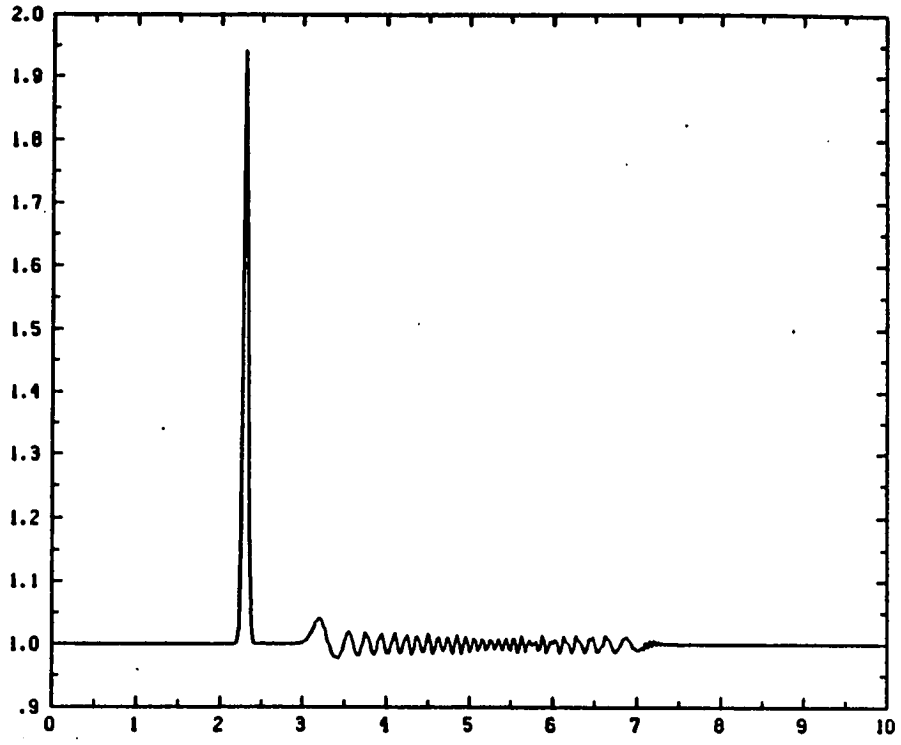

Fig. 4.1.1

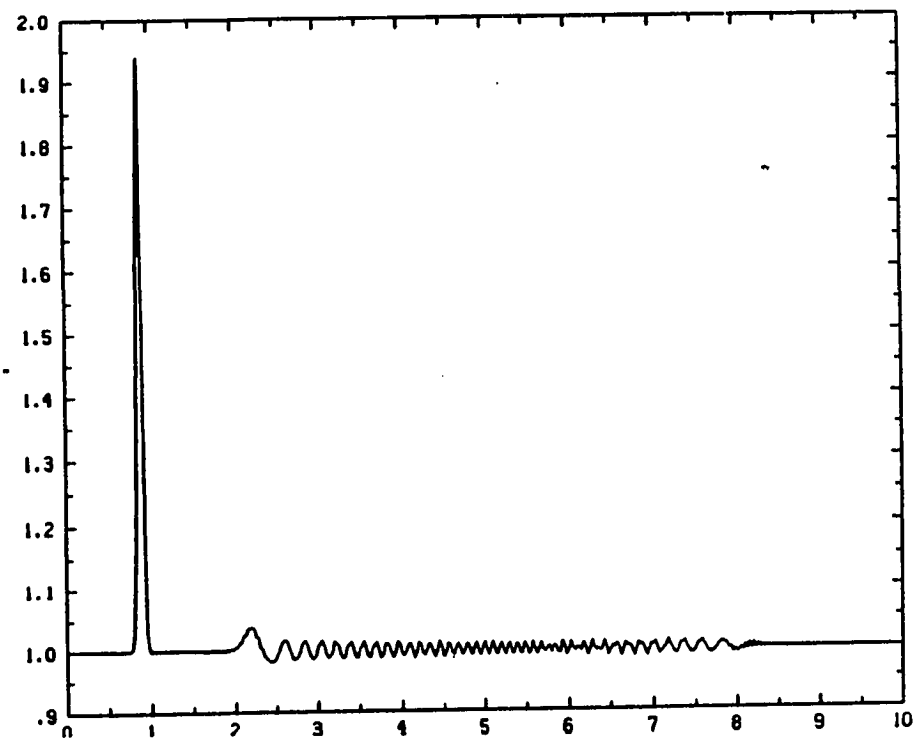

Fig. 4.1.2

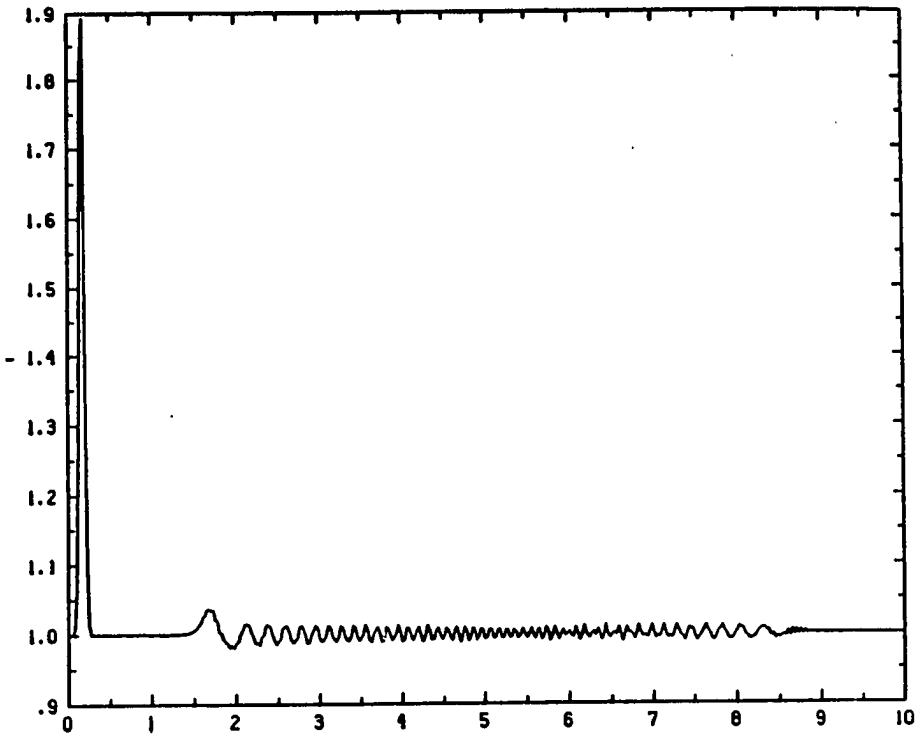

Fig. 4.1.3

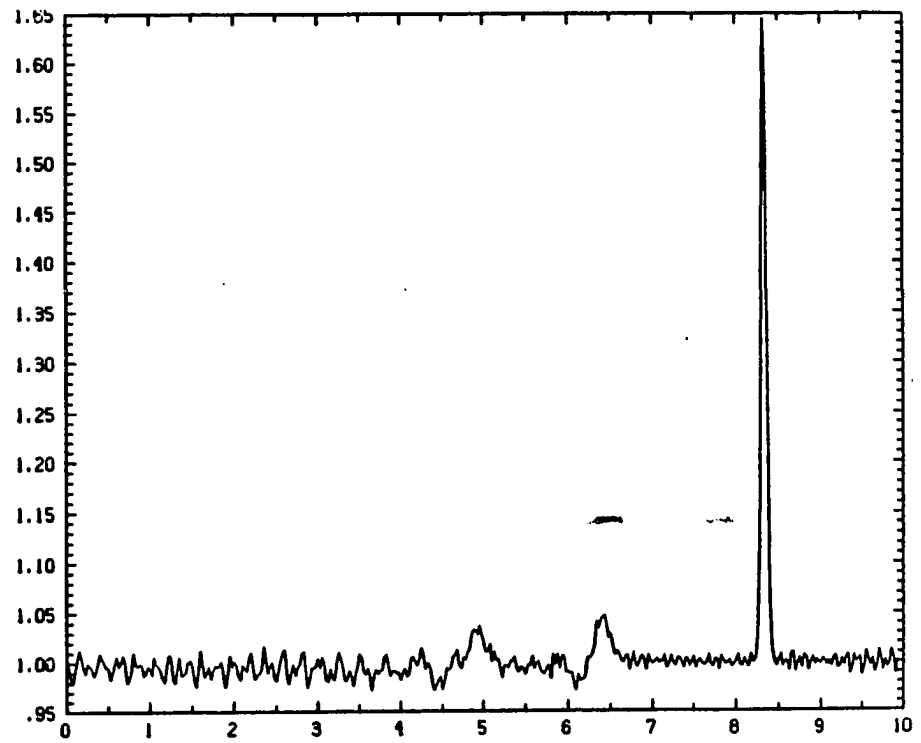

Fig. 4.1.4

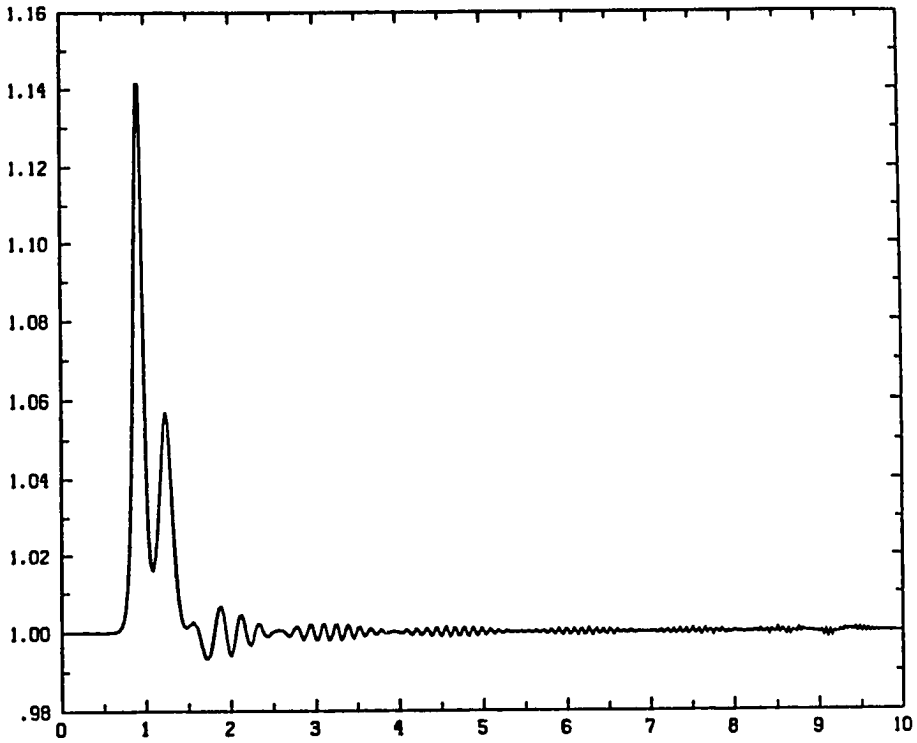

Fig. 4.2.1

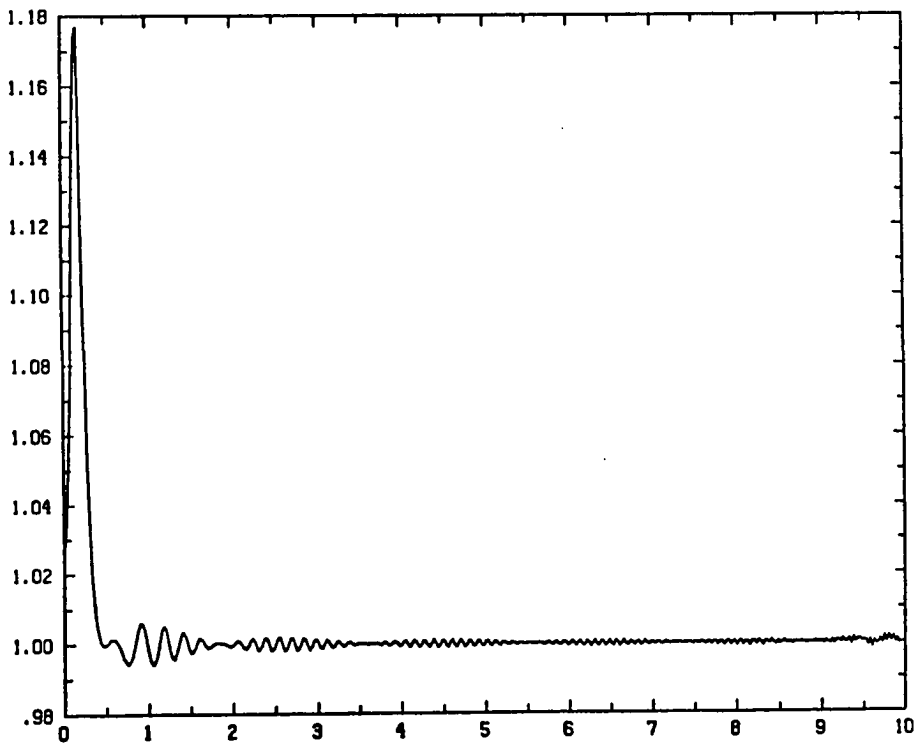

Fig. 4.2.2

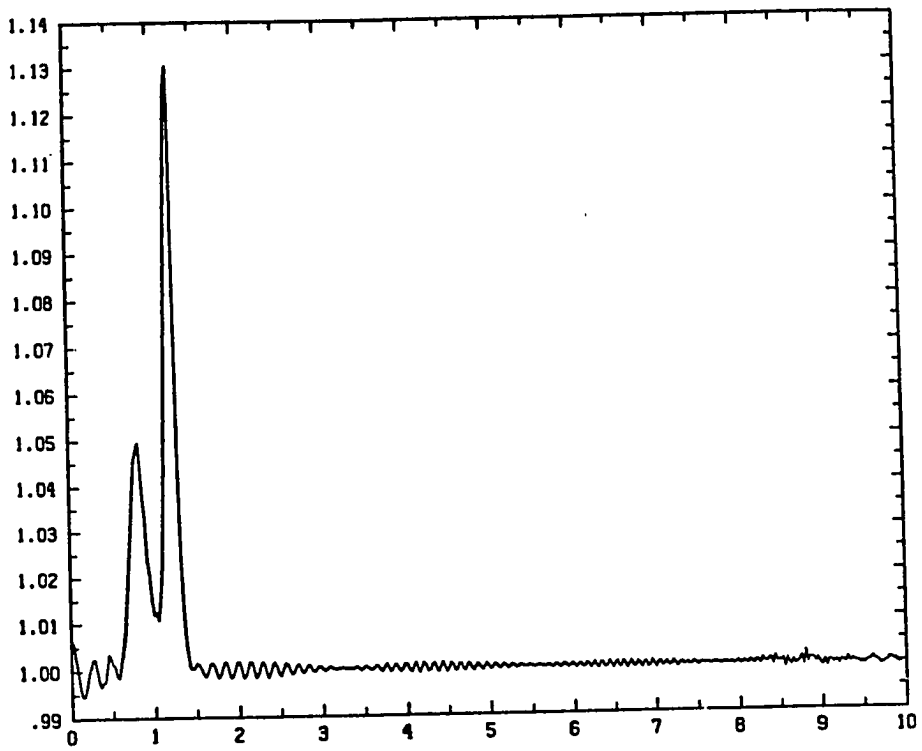

Fig. 4.2.3

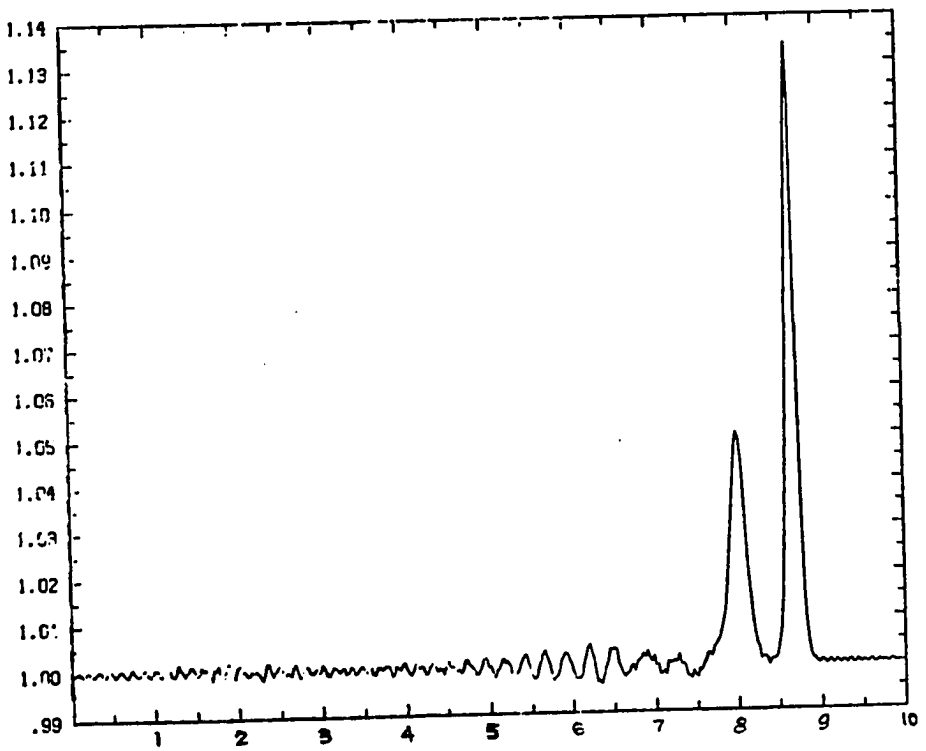

Fig. 4.2.4

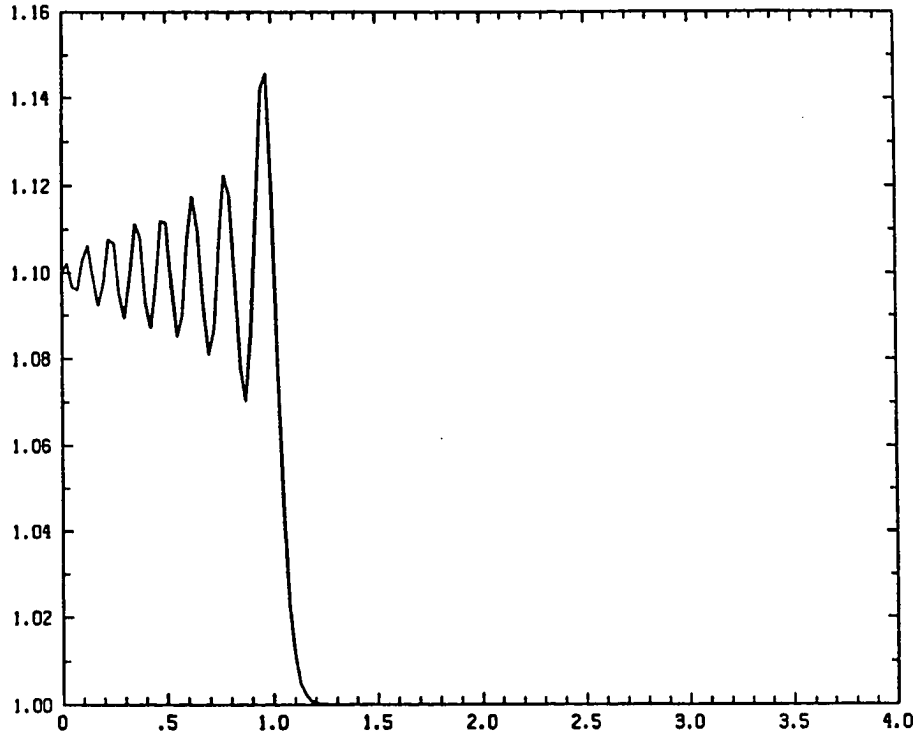

Fig. 5.1.1

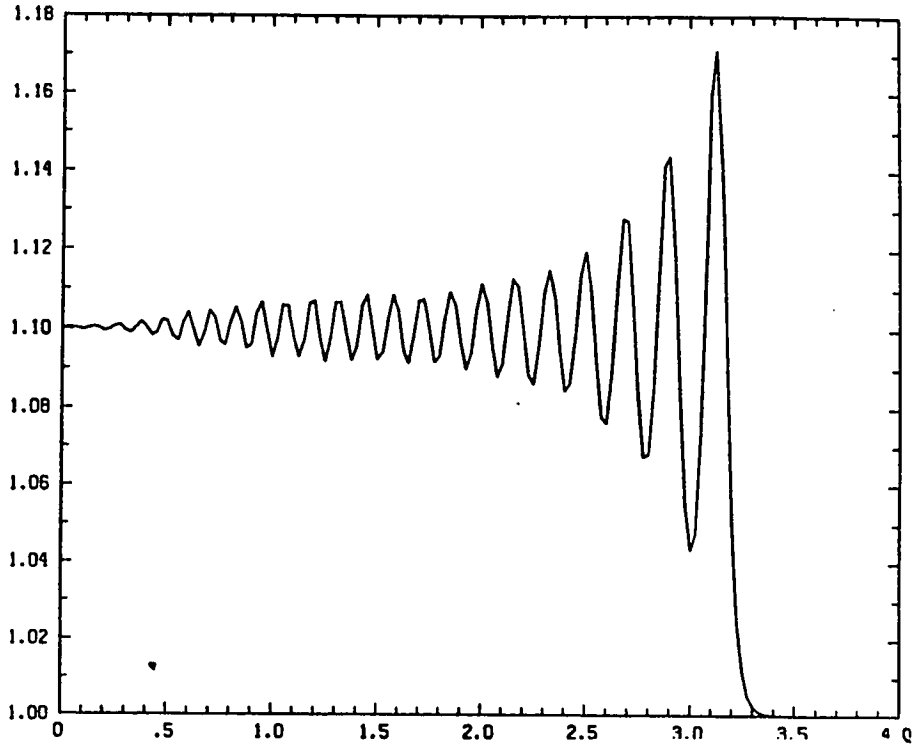

Fir. 5.1.2

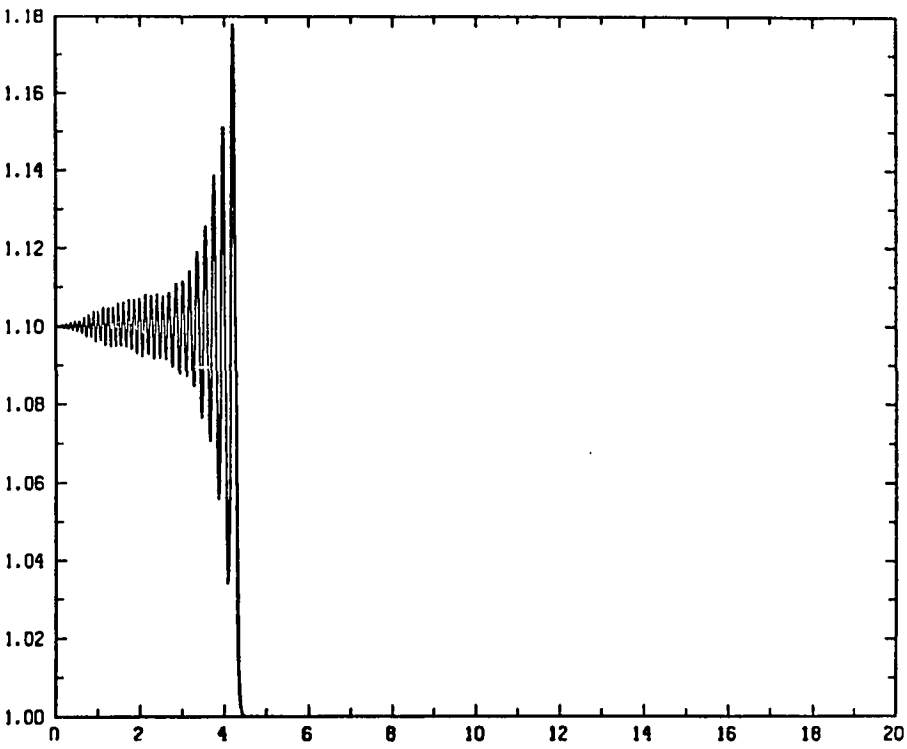

Fig. 5.1.3

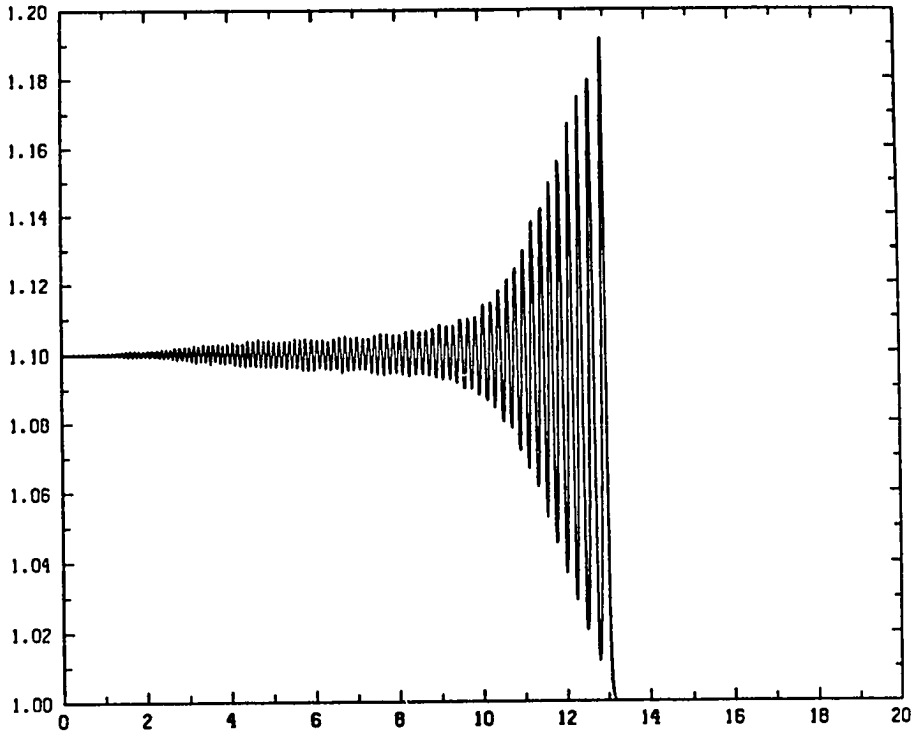

Fig. 5.1.4

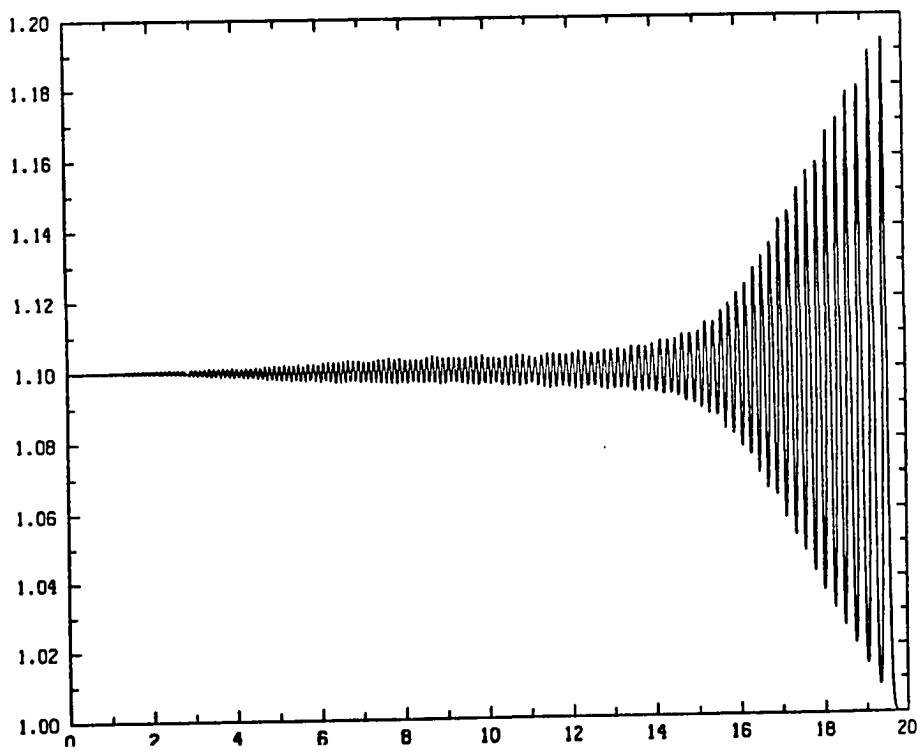

Fig. 5.1.5

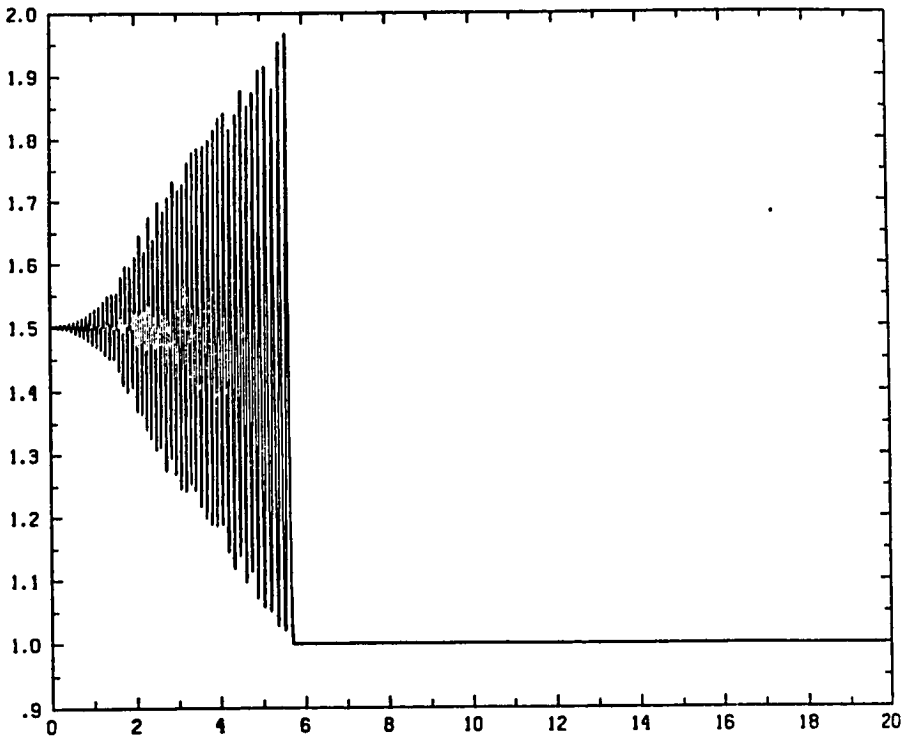

Fig. 5.2.1

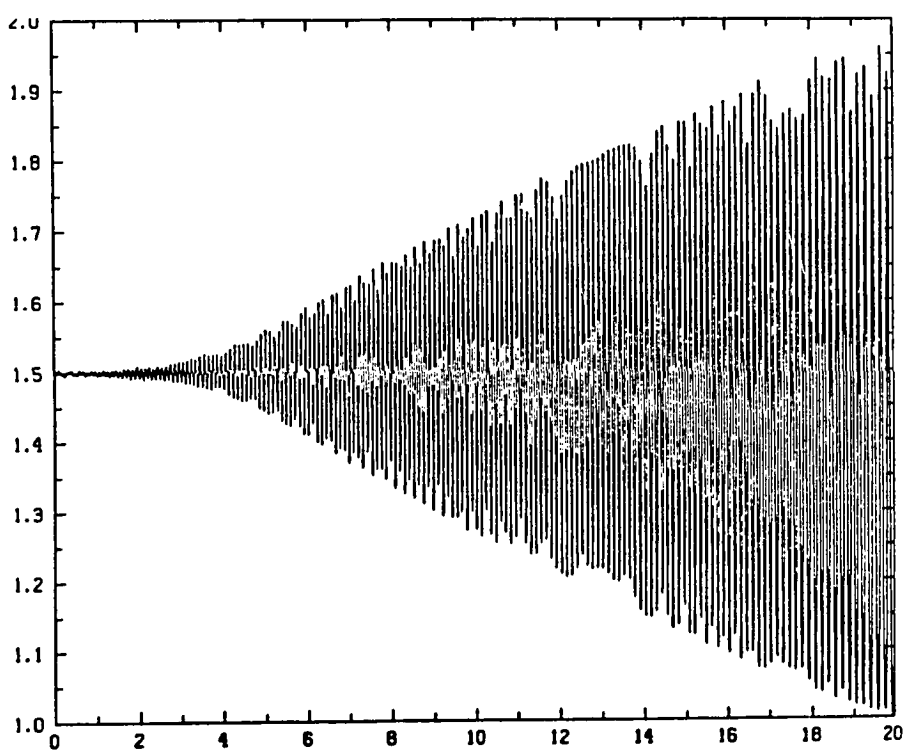

Fig. 5.2.2

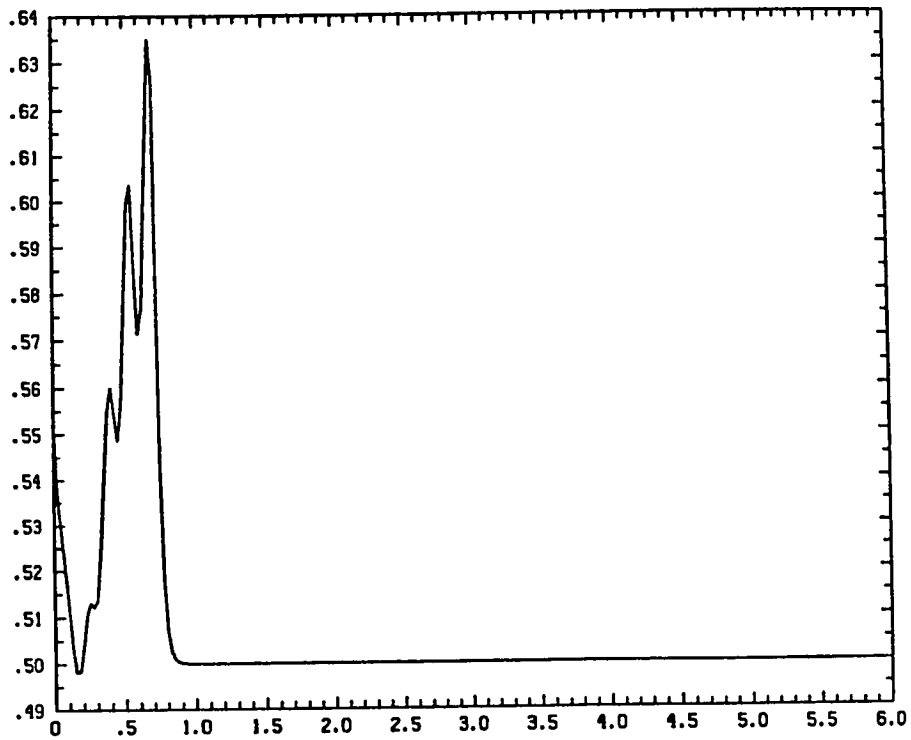

Fig. 5.3.1

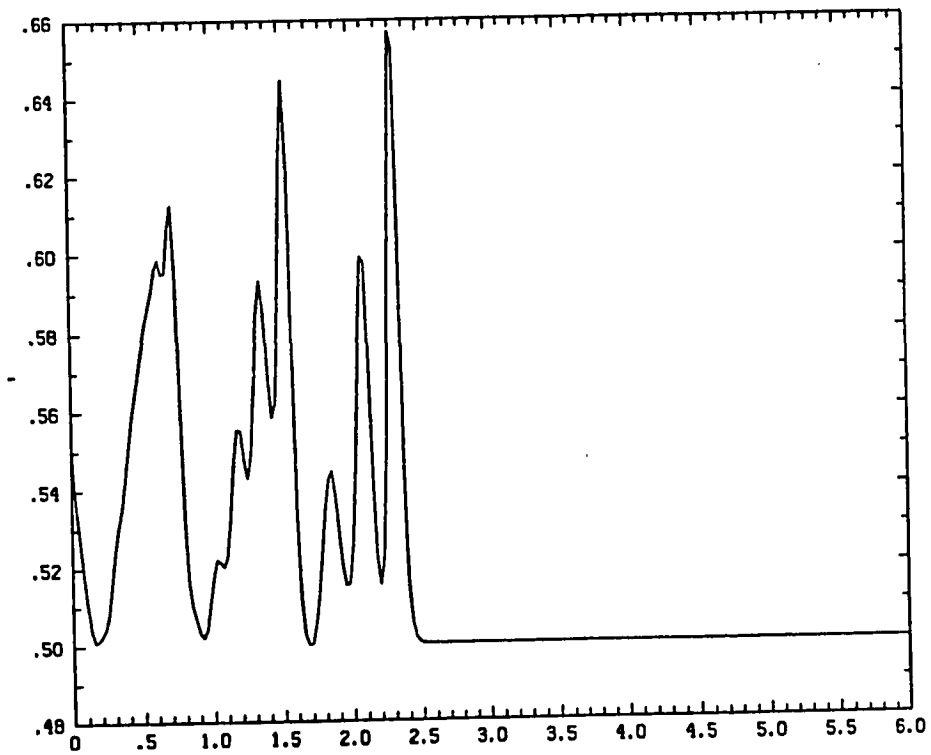

Fig. 5.3.2

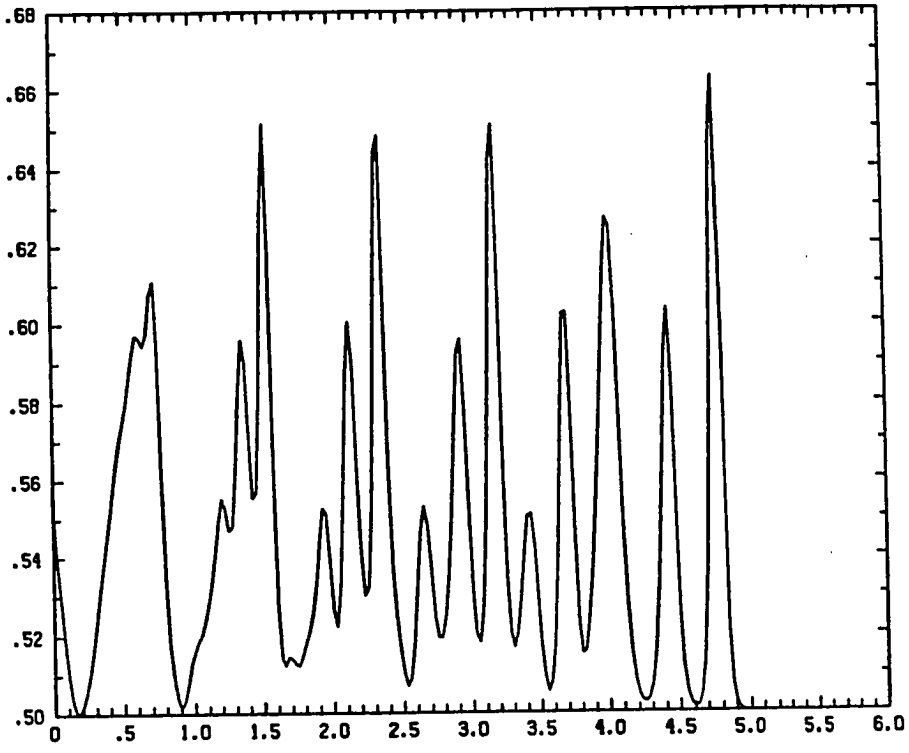

Fig. 5.3.3

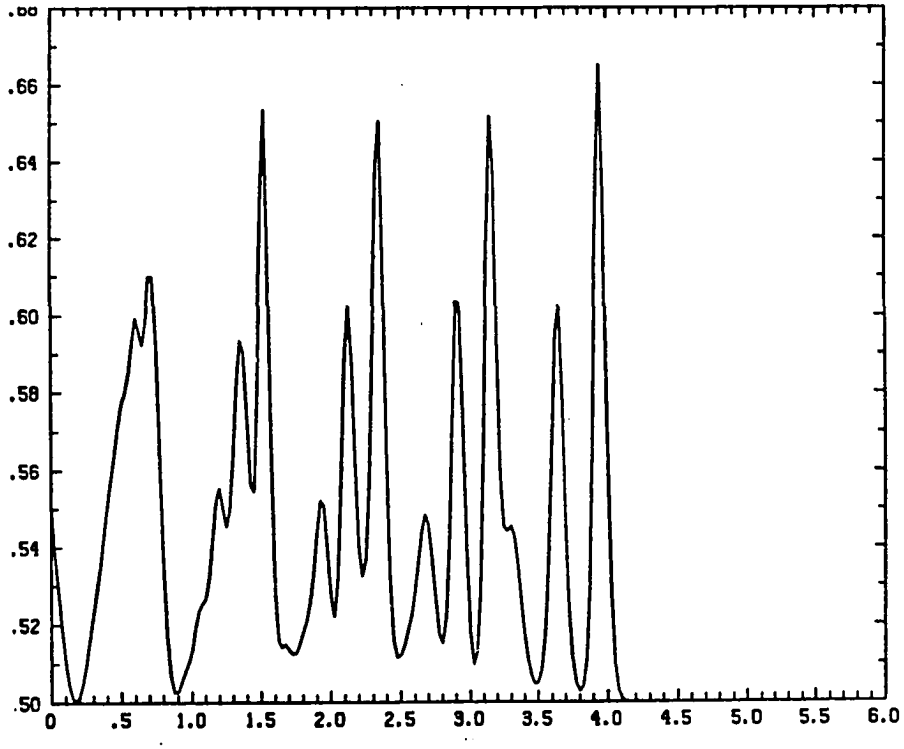

Fig. 5.3.4

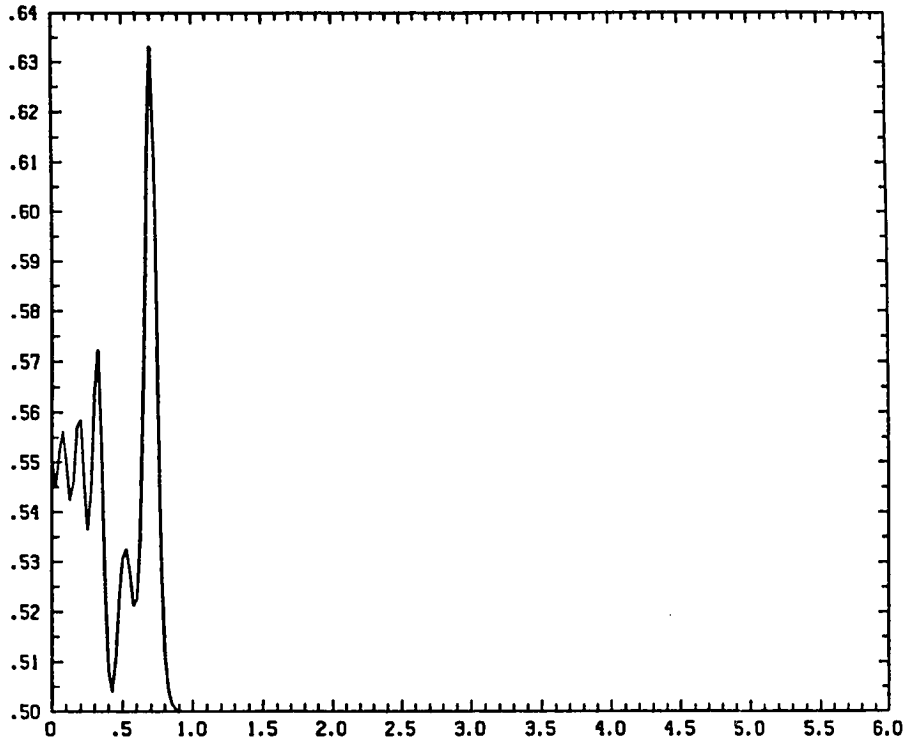

Fig. 5.4.1

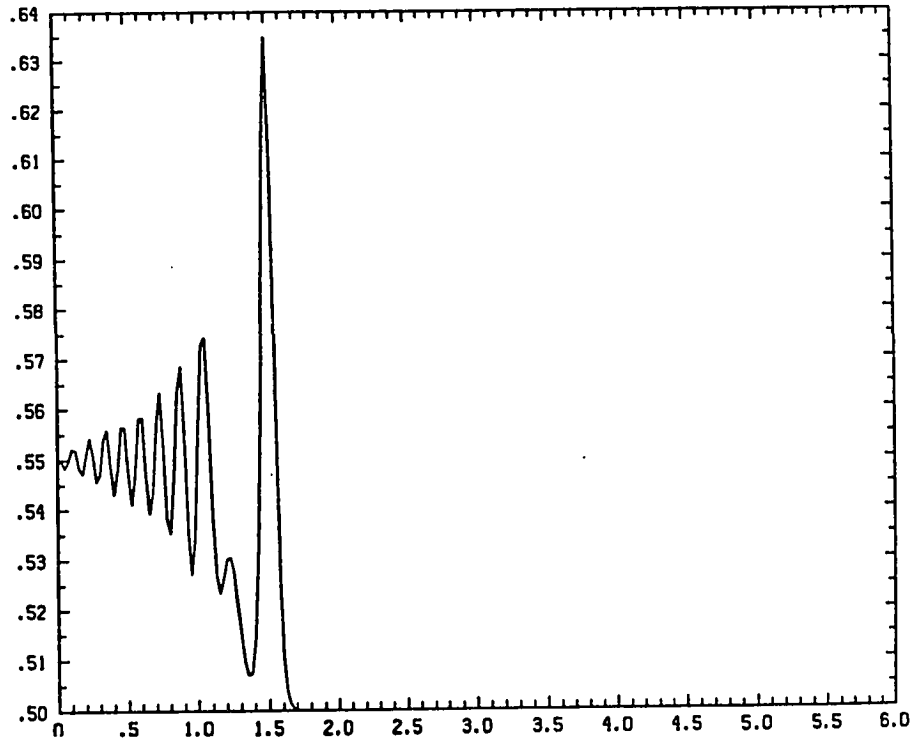

Fig. 5.4.2

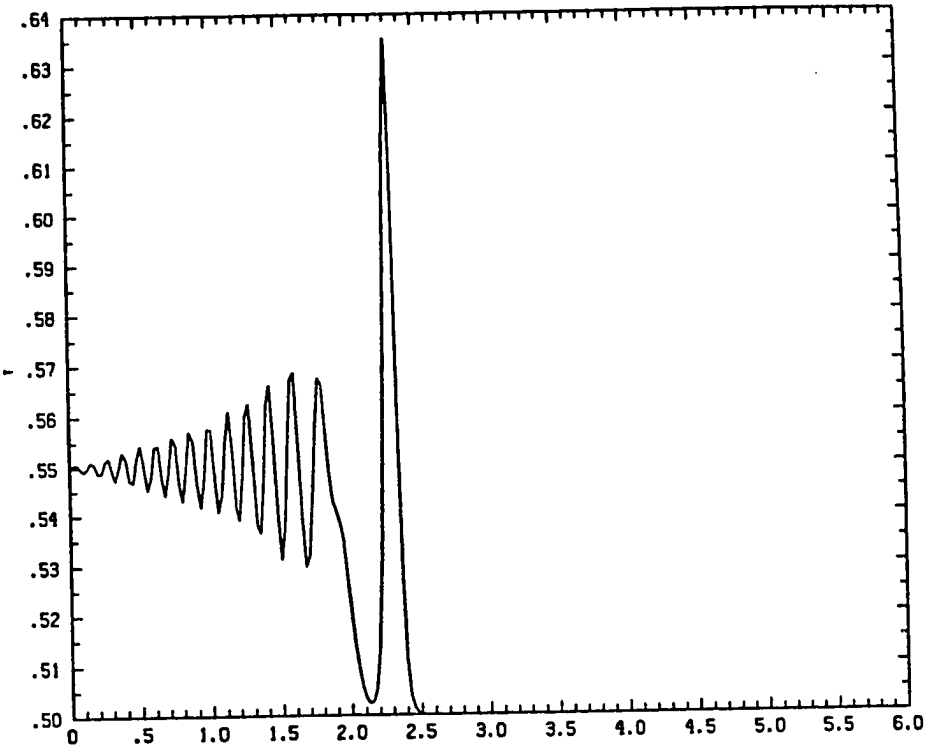

Fig. 5.4.3

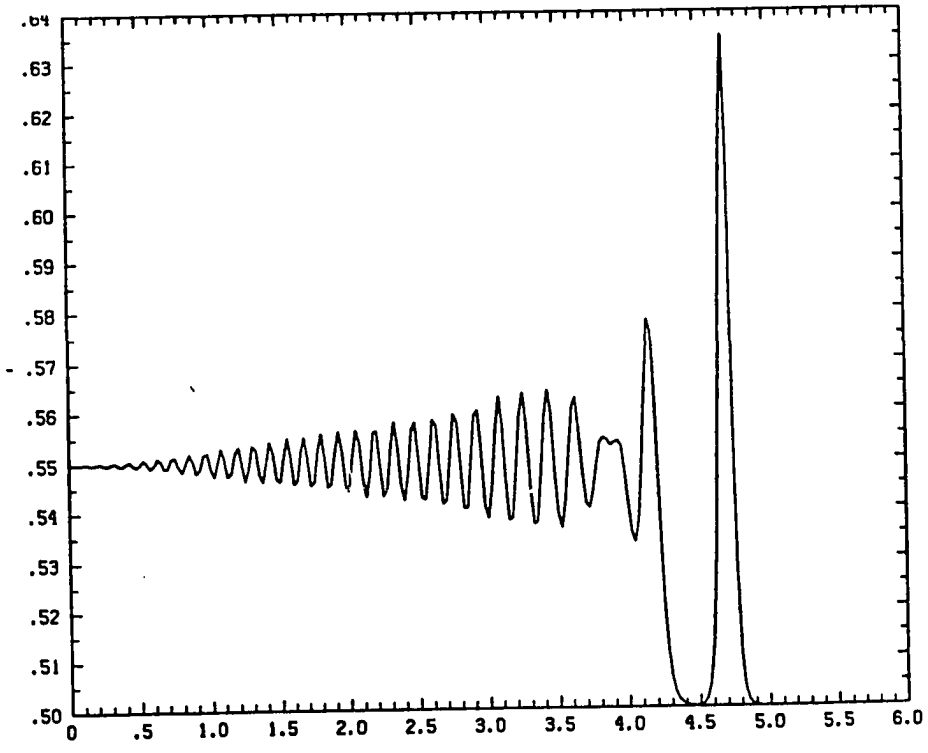

Fig. 5.4.4

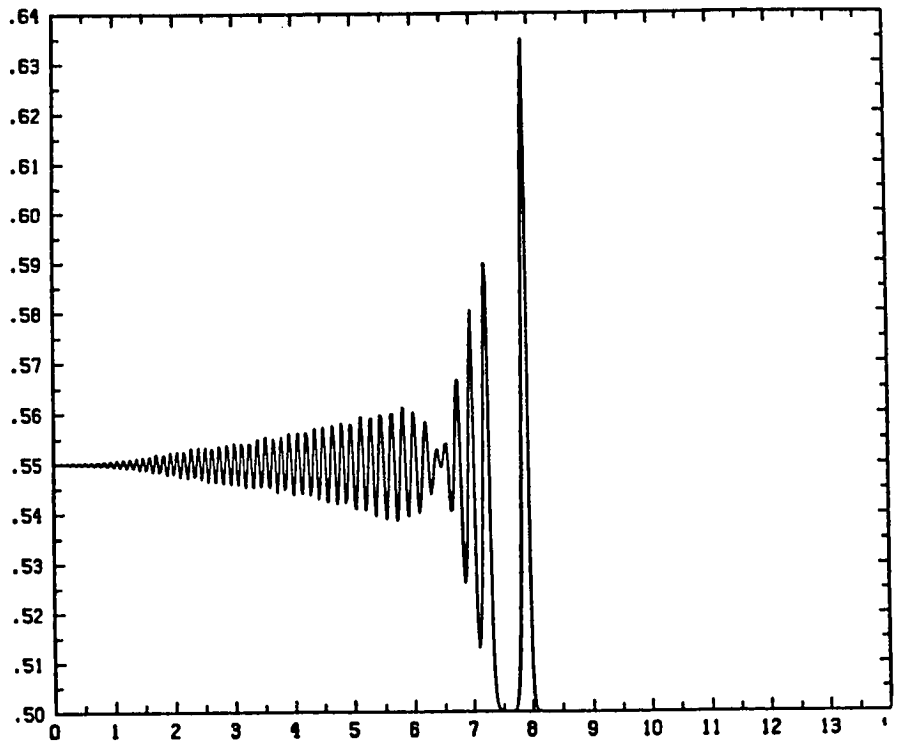

Fig. 5.4.5

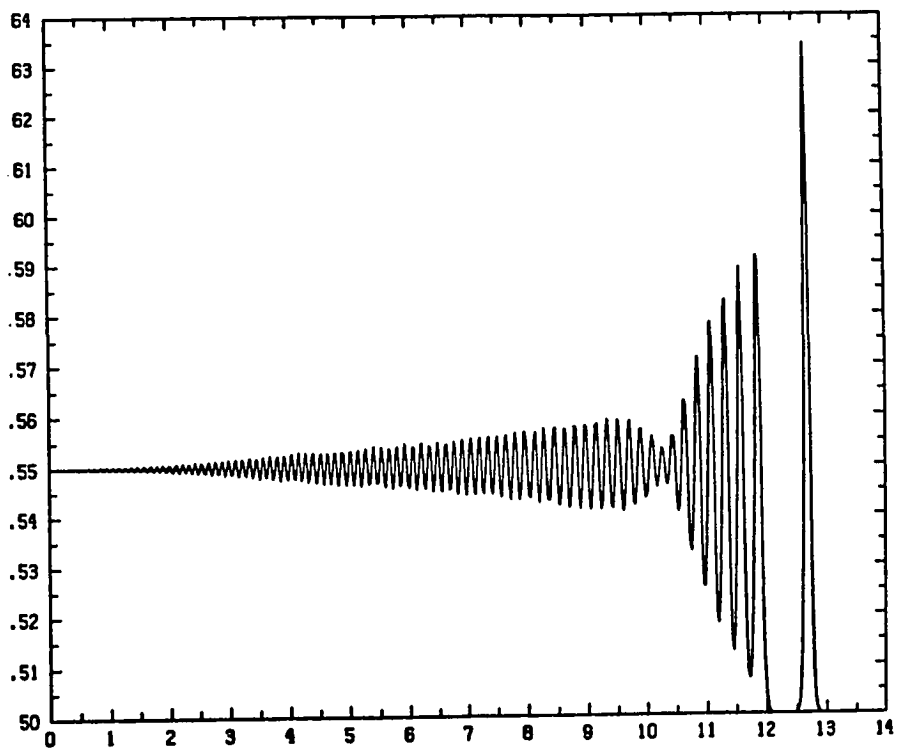

Fig. 5.4.6

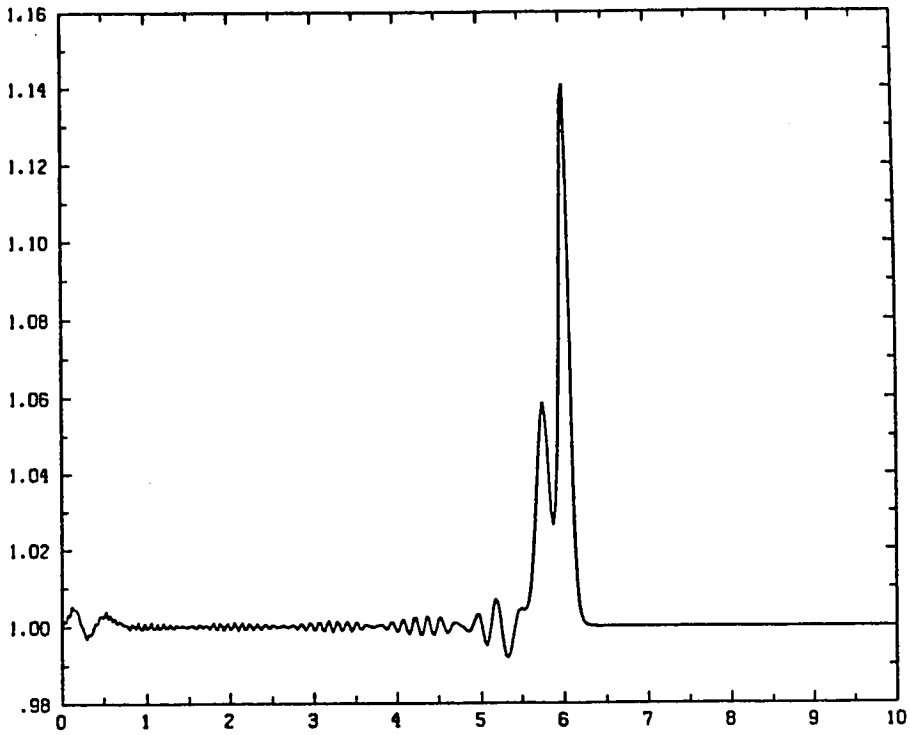

Fig. 6.1.1

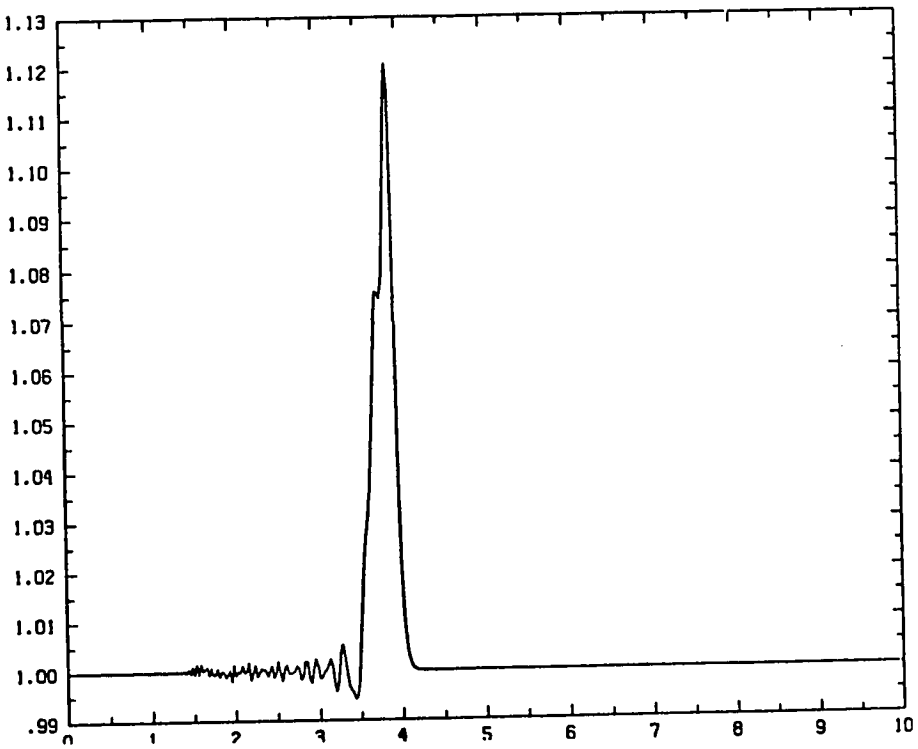

Fig. 6.1.2

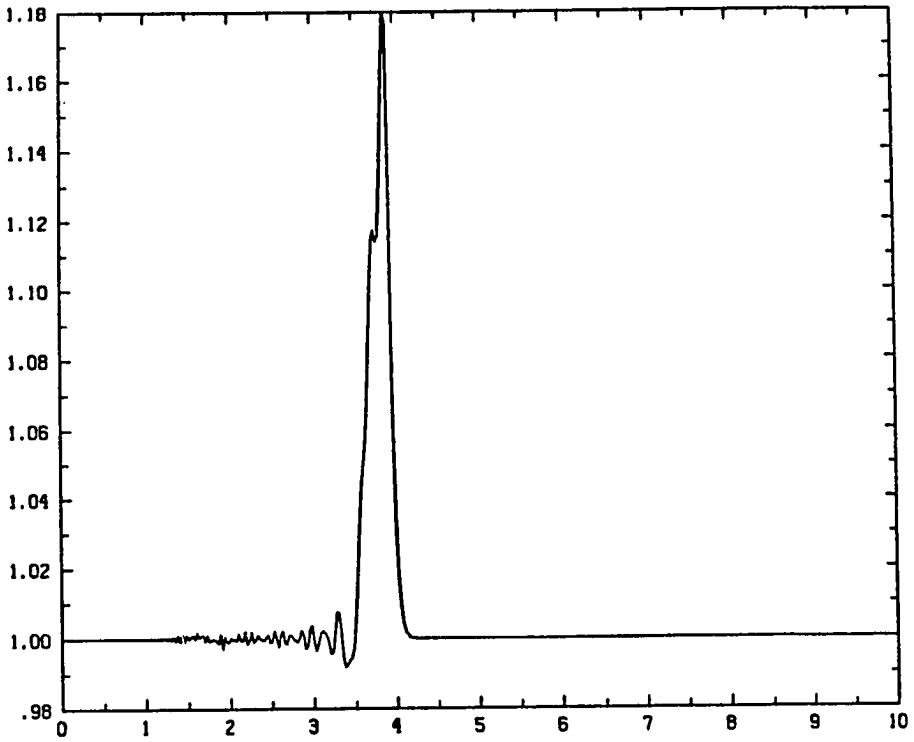

Fig. 6.2.1

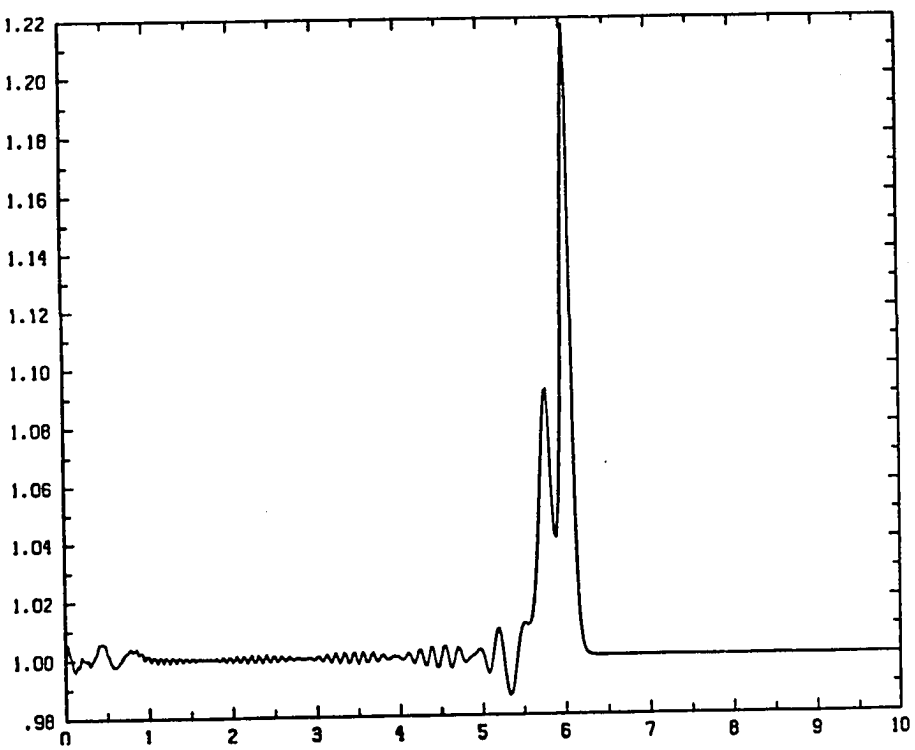

Fig. 6.2.2

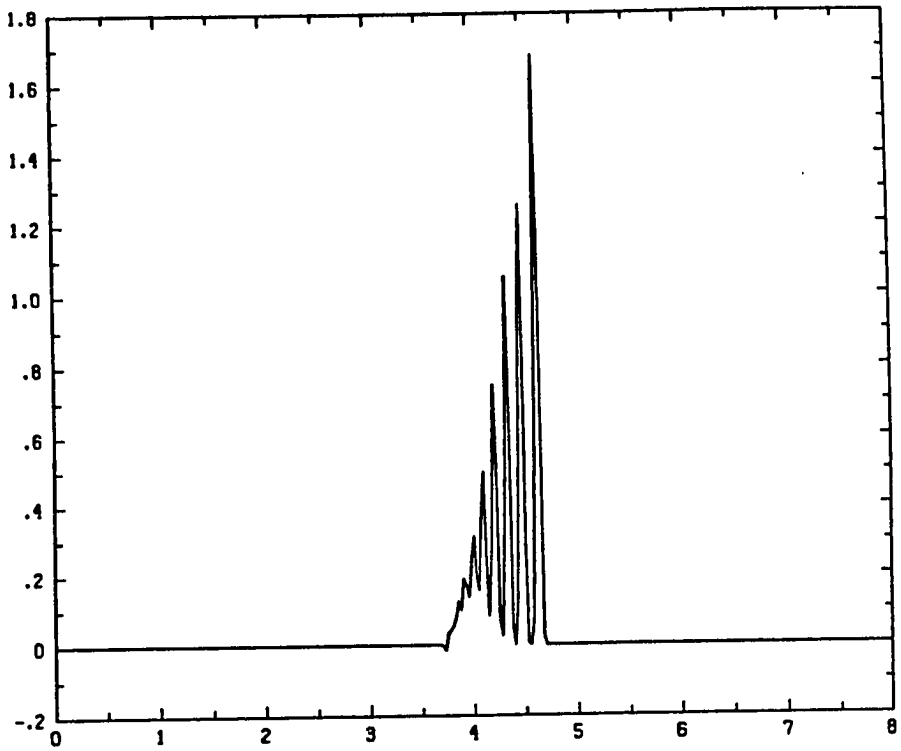

Fig. 7.1.1

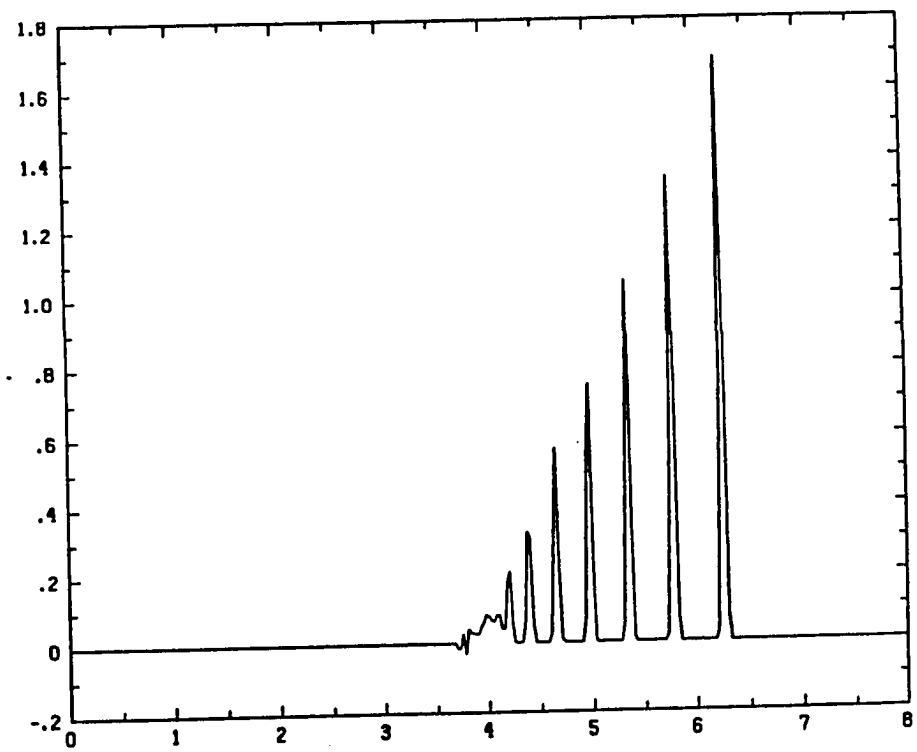

Fig. 7.1.2

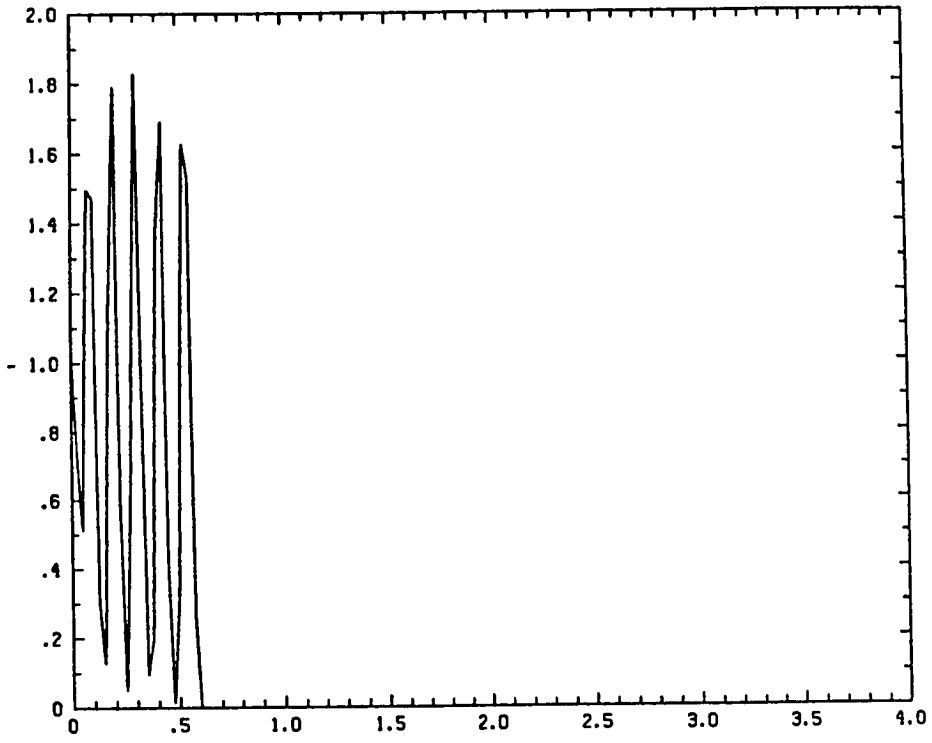

Fig. 7.2.1

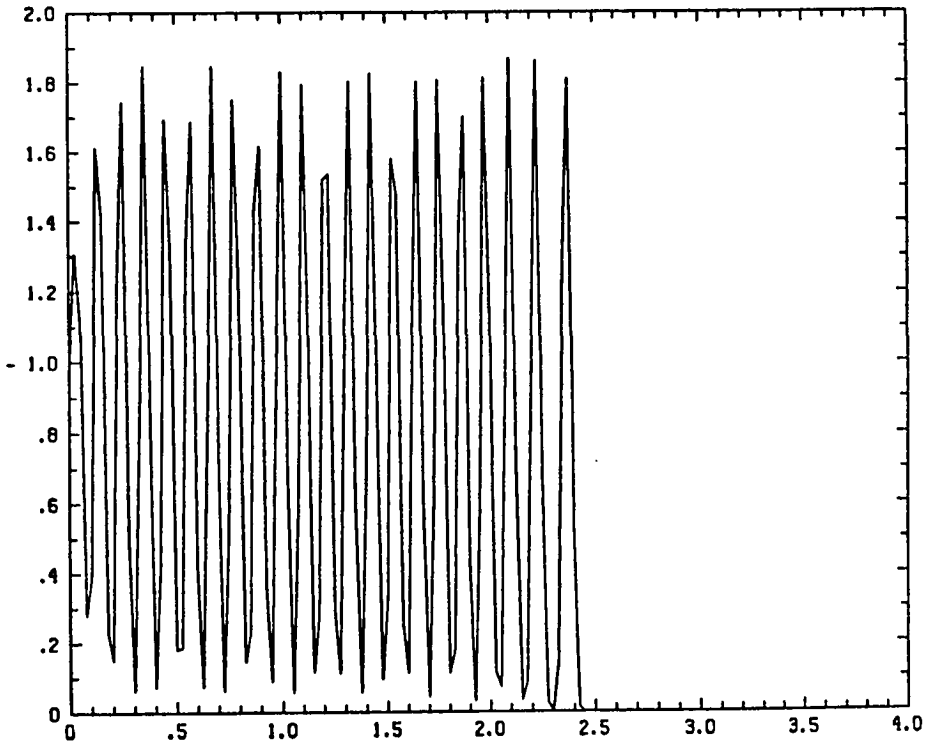

Fig. 7.2.2

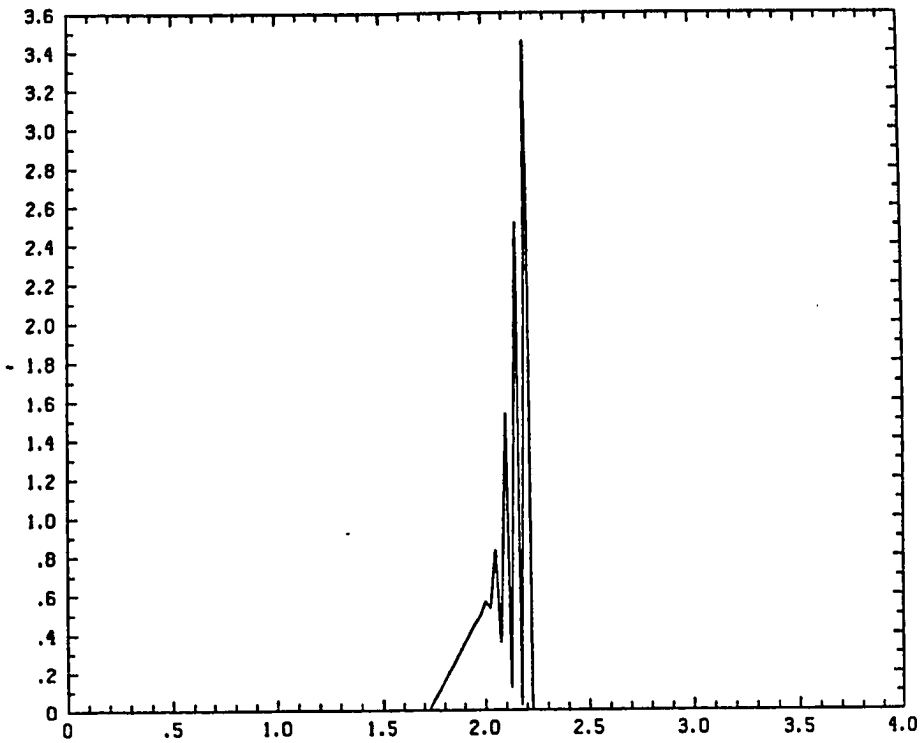

Fig. 7.3.1

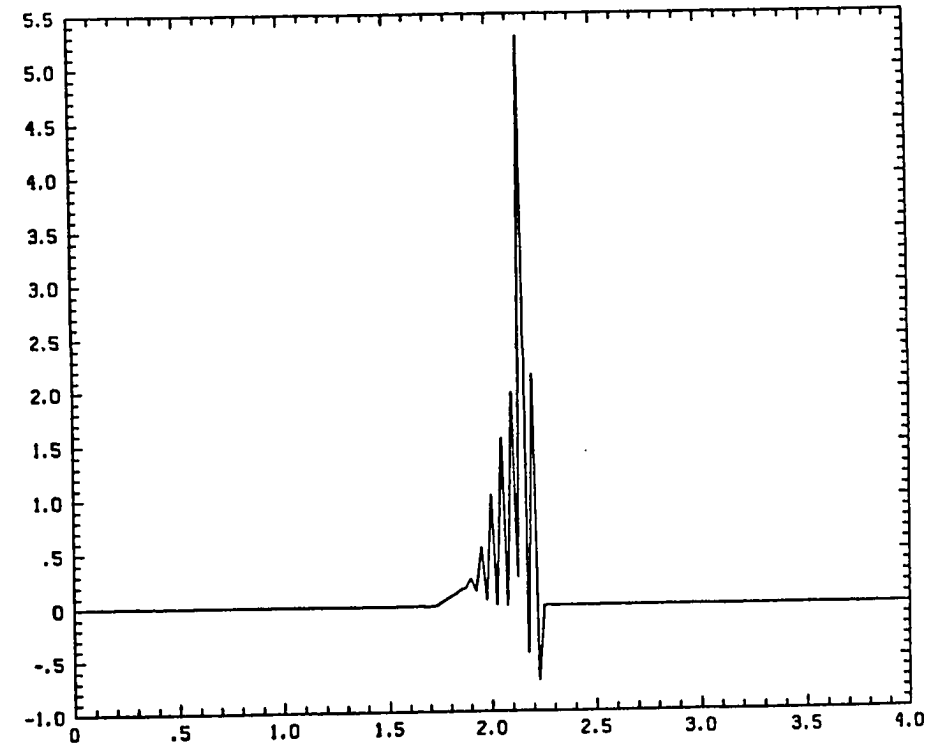

Fig. 7.3.2

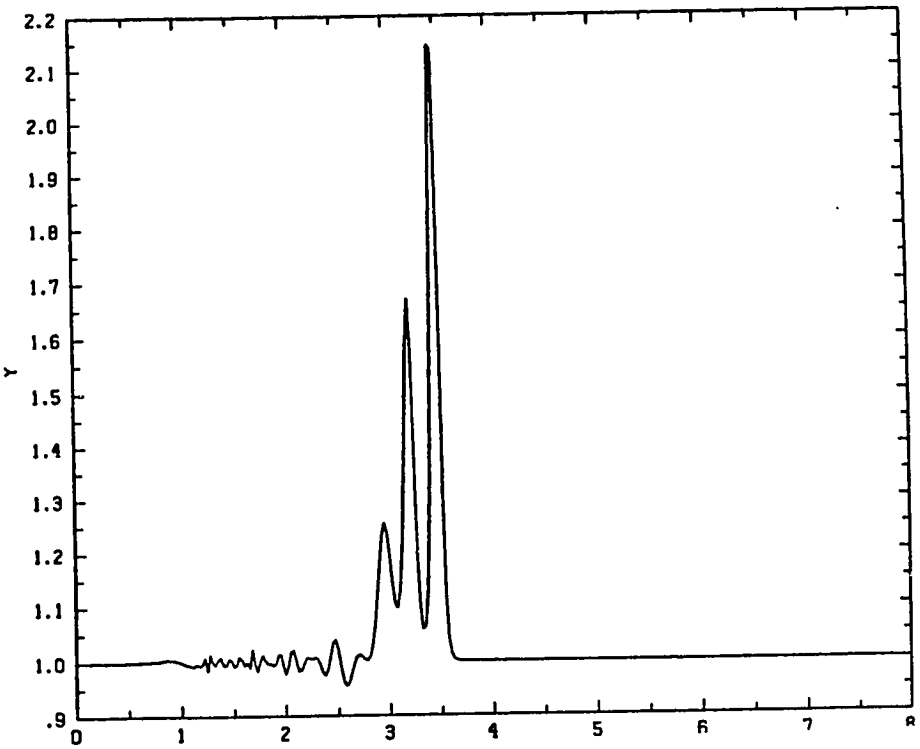

Fig. 7.4.1

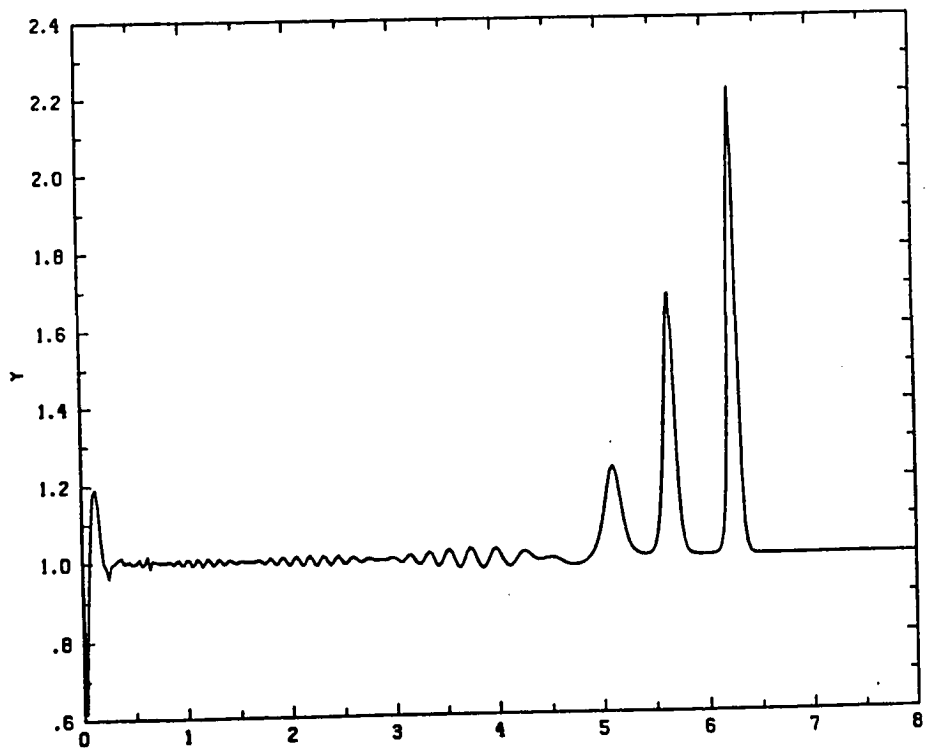

Fig. 7.4.2

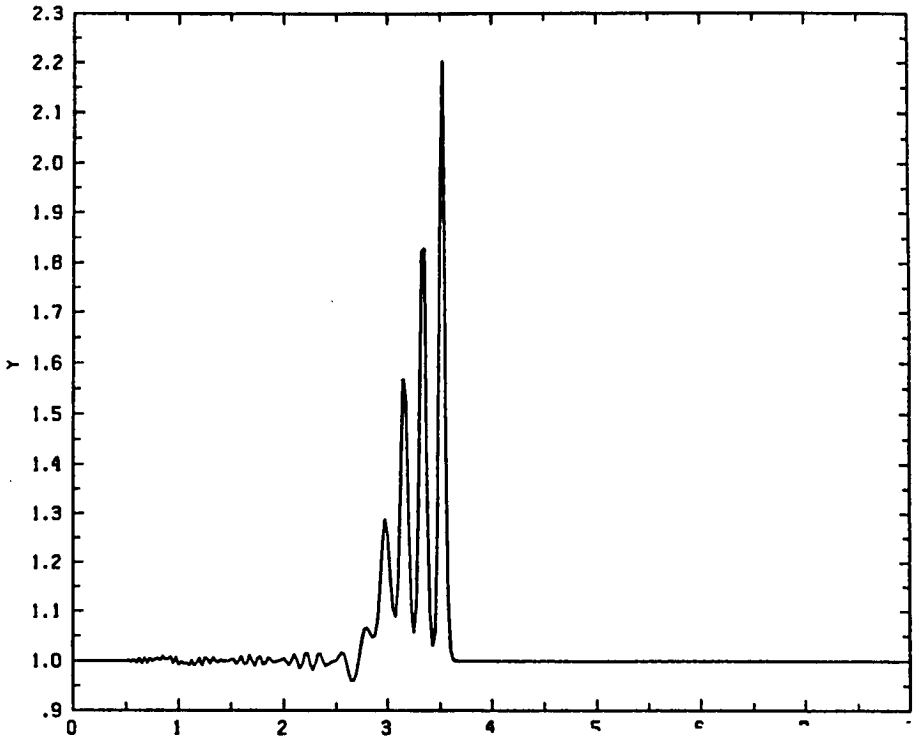

Fig. 7.5.1

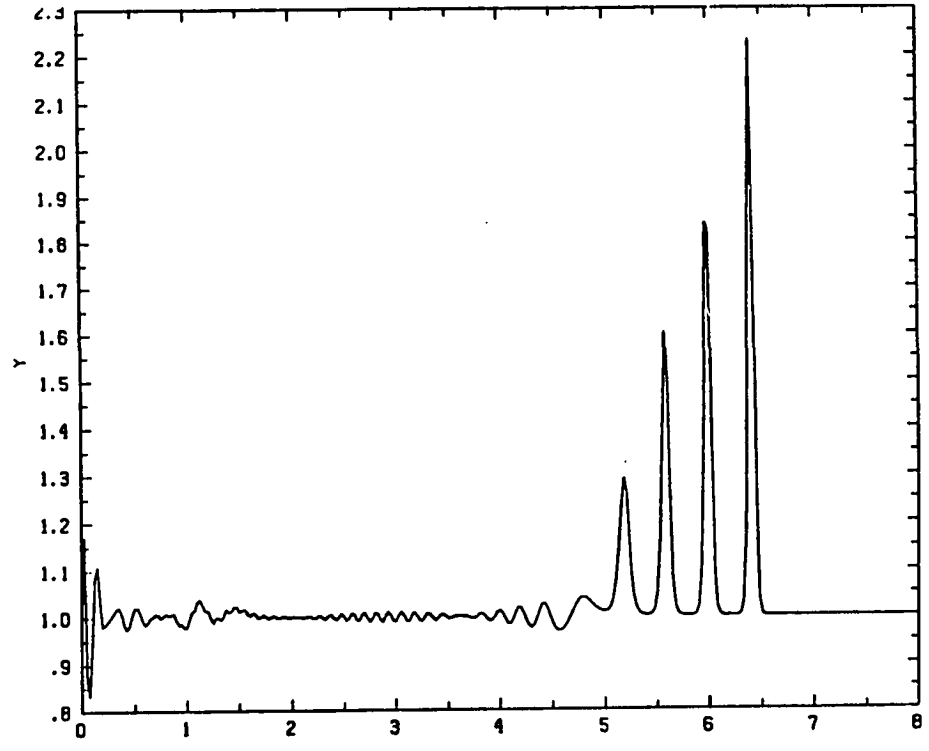

Fig. 7.5.2

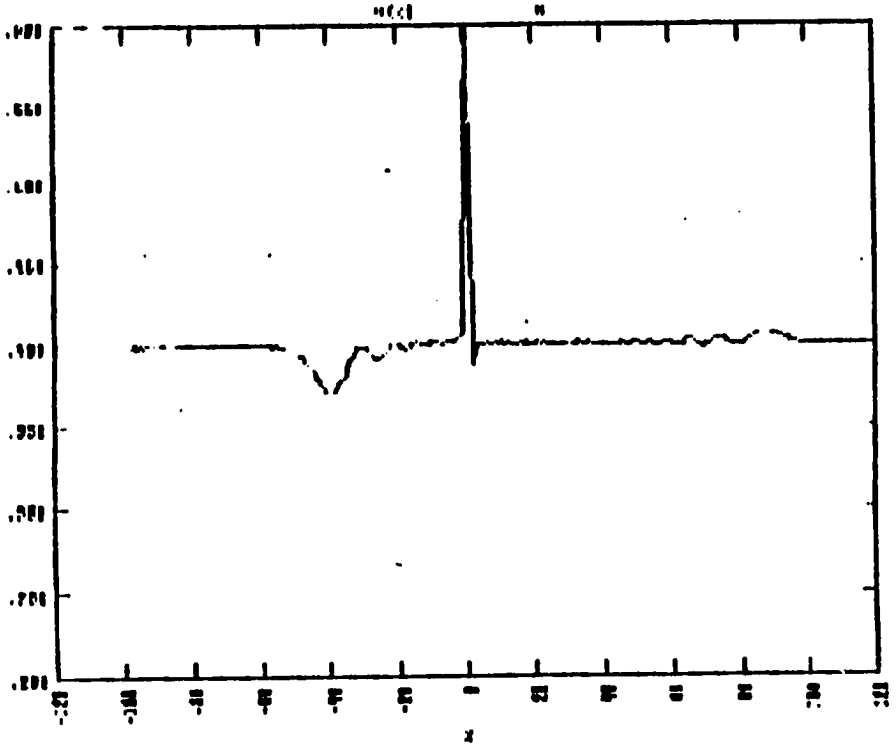

Fig. 8.1.1

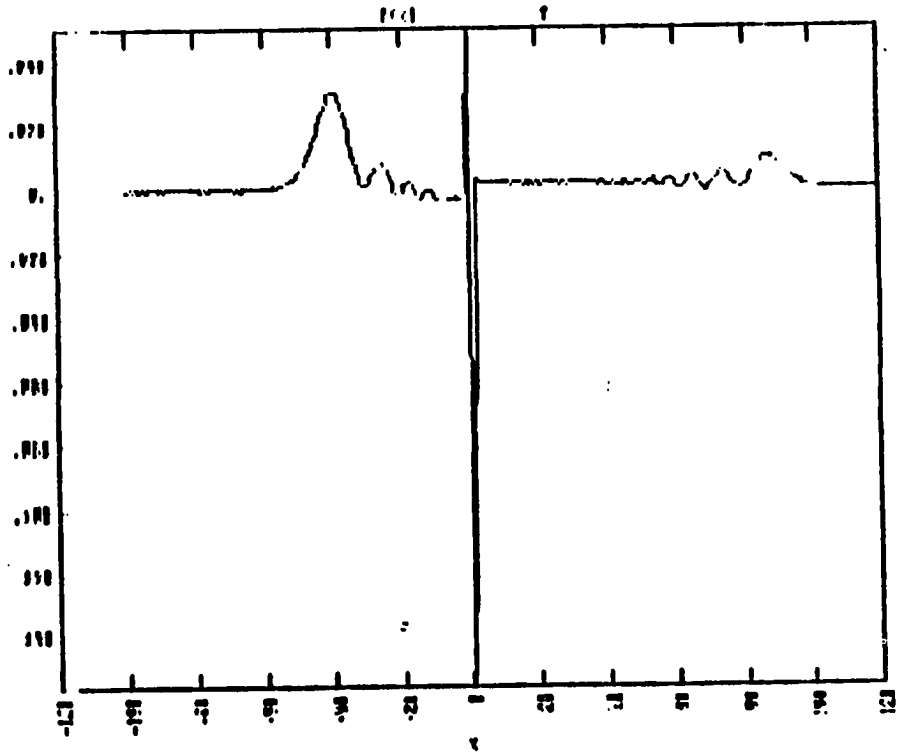

Fig. 8.1.2

References

1. Russell, J. S., Report on waves, Rep. 14th Meet. Brit. Assoc. Adv. Sci. York, 1844, pp. 311-390.

2. Boussinesq, J., Théorie de l'intumescence liquide appelée onde solitaire ou de translation, se propageant dans un canal rectangulaire, Compte Rendus Acad. Sci. Paris, 72, 1871, pp. 755-759.

3. Rayleigh, Lord, On waves, Phil. Mag. (5) 1, 1896, pp. 257-279; Sci. papers, vol. I, pp. 251-271. Cambridge University Press.

4. Korteweg, D. J. and de Vries, G., On the change of form of long waves advancing in a rectangular canal, and on a new type of long stationary waves, Phil. Mag. (5) 39, 1895, pp. 423-443.

5. Zabusky, N. J.and Kruskal, M. D., Interaction of "solitons" in a collisionless plasma and the recurrence of initial states. Phys. Rev. Lett. 15, 1965, pp. 240-243.

6. Gardner, C. S.,Green, J. M., Kruskal, M. D. and Miura, R. M., Method for solving the Korteweg - de Vries equation, Rev. Lett. 19, 1967, pp. 1095-1097.

7. Lax, P. D., Integrals of nonlinear equations of evolution and solitary waves, Comm. Pure Appl. Math. 21, 1968, pp. 467-490.

8. Zabusky, N. J., A synergetic approach to problems of nonlinear dispersive wave propagation and interaction, In Nonlinear Partial Differential Equations, ed. W.F. Ames, 1967, pp. 223-258. New York: Academic Press.

9. Davey,A., The propagation of a waek nonlinear wave, J. Fluid Mech. 53, 1972, pp. 769-781.

10. Klein, O, Elektrodynamik und Wellenmechanik vom Standpunkt des Korrespondenzprinzips, Zeit. für Phys. 41, 1927, pp. 407-442.

11. Gordon, W., Der Comptoneffekt der Schrödingerschen theorie, Zeit. für Phys. 40, 1926, pp. 117-133.

12. Deift, P., Tomei, C. and Trubowitz, E., Inverse scattering and the Boussinesq equation, Vol. XXXV, 1982, pp. 567-628.

13. Hirota, R., Exact N-soliton solutions of the wave equation oflong waves in shallow-water and in nonlinear lattices, J. Math. Phys. 14, No.7, 1973, pp. 810-814.

14. Toda, M., Wave propagation in anharmonic lattices. J. Phys.Soc. Japan 23, 1967b, pp. 501-506.

Grindlay, J. and Opie, A. H., The nonlinear and dispersive elastic solid: standing waves. J. Phys. C: Solid State Phys.10, 1977, pp. 947-954.

15. Davis, R. E. and Acrivos, A., Solitary internal waves in deep water. J. Fluid Mech. 29, 1967, pp. 593-607.

Benjamin, T. B., Internal waves of permanent form in fluids of great depth. J. Fluid Mech. 29, 1967, pp. 559-592.

Ono, H., Algebraic solitary waves in stratified fluids. J. Phys. Soc. Japan 39, 1975, pp. 1082-1091.

Titchmarsh, E. C., Introduction to the Theory of Fourier Integrals. 1948, 2nd edn. Oxford University Press.

16. Kadomtsev, B. B. and Petviashvili, V. I., On the stability of solitary waves in weakly dispersing media. Dokl. Akad. Nauk. SSSR 192, 1970, pp.753-756; or Sov. Phys. Dokl. 15, 1970, pp. 539-541.

17. Phyica 18D 1986. Solitons and Coherent Structures. Proceedings of the Conference on Solitons and Coherent Structures held at Santa Barbara, CA 93106, USA, Janurary 11-16, 1985. North - Holland, Amsterdam.

18. Sagdeev,R. Z., Review of Plasma physics, Vol. 4, 1966.

19. Washimi,H. and Taniuti,T., Propagation of ion-acoustic solitary wave of small amplitude, Phys. Rev. Lett. 17, 1966, p. 996.

20. Sakanaka, P. H., Formation and interaction of ion-acoustic solitary waves in a collisionless warm plasma, Phys. of Fluids 15, 1972, pp. 304-310.

21. Ikezi, H., Taylor, R. J. and Baker, D. R., Formation and interaction of ion-acoustic solitons, Phys. Rev. Lett. 25, 1970, p. 11.

22. Wu, D. M. and Wu, T. Y., Three dimensional nonlinear long waves due to moving surface pressure, Proceedings of

Fourteenth Symposium on Naval Hydrodynamics, Nat. Acad. Press, Washington, D.C., 1982, pp. 103-125.

23. Chu, C. K., Xiang, L. W. and Baransky, Y., Solitary waves induced by boundary motion, Comm. Pure Appl. Math. 36, No. 4, 1983, pp.495-504.

24. Bona, J. L., Pritchard, W. G. and Scott, L. R., An evaluation of a model equation for water waves, Phil. Trans. R. Soc. Lond., A, 302, 1981, pp. 457-510.

25. Whitham, G. B.,Linear and Nonlinear Waves. John Wiley and Sons, Inc.. 1974. p. 461.

26. ibid., pp. 431-434.

27. Berezin, Y. A. and Karpman, V. I., Nonlinear evolution of distutbances in plasma and other dispersive media, Sov. Phys. JETP, 24, 1967, p. 1049.